Structural Maintenance of Chromosomes (SMC) localization on the *Bacillus subtilis* chromosome

Anita Minnen

Dissertation an der Fakultät für Biologie der Ludwig-Maximilians-Universität München

Dissertation zur Erlangung des Doktorgrades an der Fakultät für Biologie der Ludwig-Maximilians-Universität München

vorgelegt von

Anita Minnen
aus den Niederlanden.
München, den 04.04.2015

Erstgutachter: Prof. Dr. Thorsten Mascher
Zweitgutachter: Prof. Dr. Marc Bramkamp

Tag der Abgabe: 04.04.2015

Tag der mündlichen Prüfung: 11.05.2015

Eidesstattliche Erklärung

Ich versichere hiermit an Eides statt, dass die vorgelegte Dissertation von mir selbständig und ohne unerlaubte Hilfe angefertigt ist.

München, den............................ ....

<div align="right">(Unterschrift)</div>

Erklärung

Hiermit erkläre ich, dass die Dissertation nicht ganz oder in wesentlichen Teilen einer anderen Prüfungskommission vorgelegt worden ist und dass ich mich anderweitig einer Doktorprüfung ohne Erfolg **nicht** unterzogen habe.

München, den............................ ....

<div align="right">(Unterschrift)</div>

Table of contents

1. Summaries

1.1 Summary

Cell divisions are required for the survival of species on planet Earth. Before a cell can physically divide, it must first faithfully replicate and segregate its DNA. In addition to this challenge, to fit inside a cell or cell nucleus the DNA needs to be highly condensed and at the same time remain organized. Structural maintenance of chromosomes (SMC) complexes play crucial roles in these processes and are highly conserved through all domains of life. In eukaryotes, the SMC complexes cohesin, condensin and Smc5/6 play key roles in, amongst others, sister chromatid cohesion, chromosome condensation and DNA repair, respectively. Prokaryotes usually harbor only one type of Smc complex, either of the MukBEF or Smc-ScpAB type, which functions in chromosome segregation and organization. The precise mechanism of action of Smc complexes is thus far poorly understood.

SMC complexes share sequence homology with ATP binding cassette (ABC) transporters and are distinct because of their unique and highly conserved architecture. A single SMC protein folds back on itself at its hinge domain, a ~50 nm long antiparallel coiled-coil connects the hinge domain with the head domain. This head domain is formed by the N- and C- termini of SMC and contains a nucleotide binding domain (NBD). In the SMC complex two SMC proteins dimerize at the hinge domain, a kleisin subunit (ScpA) binds to both SMC proteins at or just above the head domains and additional subunits (ScpB) usually associate with the kleisin subunit.

In the prokaryotic model organism *Bacillus subtilis*, which harbors Smc-ScpAB, the Smc complex is recruited to the chromosome by ParB, a protein thought to be involved in origin separation, which binds to ten 16 bp *parS* sites on the chromosome. Smc is mostly found in the half of the chromosome around the origin of replication. To elucidate the role of the Smc complex in chromosome segregation it is pivotal to gain a deeper understanding of the specific chromosomal association of the Smc complex. In this work I used *B. subtilis* Smc-ScpAB to study the chromosomal association of the Smc complex into more detail by investigating Smc-ScpAB recruitment to the chromosome, Smc-ScpAB translocation over the chromosome and whether Smc-ScpAB is able to hold different genomic loci together.

My major findings include that Smc blocked in ATP hydrolysis, which has heads in an engaged state, is recruited mostly to ParB binding (loading) sites on the chromosome. This recruitment depends on ScpAB and ParB. When the hinge is in a monomeric state or absent, and ATP hydrolysis is blocked, recruitment to these sites is enriched and this is independent of ScpA. In addition, I elucidated that the minimal Smc complex recruited to ParB loading sites consists of the Smc heads with approximately one-third of its head-proximal coiled-coil in an ATP hydrolysis blocked state. A full ATP hydrolysis cycle is necessary for wild-type distribution on the chromosome. Furthermore, I found indications that the Smc complex loads onto the chromosome at ParB loading sites and then translocates over large distances (Mbs) from there. Taken together, these results suggest a model in which a dimer of Smc associates with ScpAB which promotes head engagement and induces a state that interacts at the ParB loading sites, presumably by interacting

with ParB in the head-proximal one-third of the coiled-coils. After ATP-hydrolysis, the Smc complex translocates away from its initial loading sites and executes its pivotal roles in chromosome segregation and organization. It can now be easily tested whether this basic mechanism of SMC recruitment is conserved between prokaryotes and eukaryotes. Therefore, this work could lay part of the foundation in understanding the molecular mechanisms of SMC functioning in life.

1.2 Zusammenfasung

Zellteilung ist für die Existenz aller Lebewesen auf unserem Planeten essentiell. Bevor sich eine Zelle teilen kann, muss ihre DNA exakt repliziert und segregiert werden. Dafür muss die DNA stark kondensiert vorliegen, aber gleichzeitig organisiert bleiben, um in eine Zelle, oder den Zellkern, zu passen. „Structural maintenance of chromosomes" (SMC) Komplexe spielen bei den oben genannten Prozessen eine ausschlaggebende Rolle und sind in allen Domänen der Lebewesen sehr konserviert. In Eukaryoten haben, unter anderem, die SMC Komplexe Cohesin, Condensin und Smc5/6, eine Funktion im Zusammenhalt von Schwesterchromatiden, der Chromosom-Kondensation und DNA Reparatur. Prokaryoten besitzen im Normalfall nur eine Art der SMC Komplexe, entweder den MukBEF oder Smc-ScpAB Komplex, welche beide Funktionen in der Chromosomensegregation und -organisation haben. Der genaue Mechanismus über die Funktion der SMC Komplexe ist bis heute nur geringfügig bekannt.

SMC Komplexe haben Sequenz-Homologien zu ATP-Bindungskassetten (engl. „ABC") Transportern und sind vor allem aufgrund ihrer einzigartigen und hochkonservierten Proteinarchitektur bekannt. Dabei faltet sich ein SMC Monomer auf sich selbst zurück, wodurch die N- und C-Termini des Proteins eine ATP-bindende „Head" Domäne bilden. Ein ~50 nm langes antiparalleles Coiled-Coil verbindet dabei die Head Domäne mit der so genannten „Hinge" Domäne, die durch die Rückfaltung des SMC Proteins entsteht. Im SMC Komplex dimerisieren zwei SMC Proteinmonomere über die Hinge Domäne, ein Protein der Kleisin Familie (ScpA) verbindet die zwei SMC Proteine über die Head Domäne und ein drittes Protein (ScpB) bindet an das Kleisin Protein.

In dem prokaryotischen Modellorganismus *Bacillus subtilis*, welcher den Smc-ScpAB Komplex besitzt, wird der Smc Komplex durch das ParB Protein zum Chromosom rekrutiert, ein Protein, das wahrscheinlich in der Trennung der Replikationsursprünge involviert ist und an 16 bp *parS* Sequenzen ans Chromosom bindet. Smc befindet sich hauptsächlich auf der Hälfte des Chromosoms, die den Replikationsursprung umgibt. Um die Rolle des Smc Komplexes in der Segregation von Chromosomen zu verstehen, ist es ausschlaggebend ein tieferes Verständnis über die spezifische Interaktion des Komplexes mit dem Chromosom zu erlangen. In dieser Arbeit habe ich *B. subtilis* Smc genutzt, um diese Interaktion im Detail zu analysieren, in dem die Rekrutierung von Smc zum Chromosom und die Translokation von Smc über das Chromosom betrachtet wurden und des Weiteren ob verschiedene genomische Loci durch Smc zusammengehalten werden können.

Eines meiner Hauptergebnisse zeigt, dass bei Blockierung der ATP Hydrolyse von Smc, dadurch werden die beiden Head Domänen des Smc Proteindimers zusammengehalten, der Komplex fast ausschließlich an die ParB Bindungsstellen am Chromosom rekrutiert wird. Diese Rekrutierung hängt von ScpAB und ParB ab. Wenn die Hinge in einem monomerischen Zustand oder abwesend ist und die ATP Hydrolyse blockiert ist, ist diese Rekrutierung erhöht, dies ist unabhängig von ScpA. Außerdem habe ich herausgefunden, dass der minimale Smc Komplex der zu ParB Ladungsstellen rekrutiert wird, die Smc Head Domänen mit circa einem Drittel der Coiled-Coils in einem ATP Hydrolyse blockierten Zustand

enthält. Für die Wildtyp Verteilung auf dem Chromosom ist ein voller Zyklus der ATP Hydrolyse notwendig. Des Weiteren habe ich Hinweise dafür gefunden, dass Smc an ParB Ladungsstellen auf das Chromosom geladen wird und dann über weitreichende Distanzen (Mbs) auf dem Chromosom transloziert. Zusammengefasst weisen diese Daten auf ein Modell hin in dem ein Smc Dimer mit ScpAB interagiert um die Smc Head Domänen zusammenzubringen. Dies erzeugt einen Zustand, der nun mit den ParB Ladungsstellen interagieren kann, vermutlich über eine Interaktion mit ParB im Head-näheren Drittel der Smc Coiled-Coils. Nach der ATP Hydrolyse transloziert Smc von der Ladungsstelle weg und führt seine zentrale Rolle in der Chromosomensegregation und -organisation durch. Mit dieser Arbeit kann nun leicht erforscht werden, ob der grundlegende Mechanismus der SMC Rekrutierung auf das Chromosom zwischen Prokaryoten und Eukaryoten konserviert ist. Deswegen könnte diese Arbeit die Grundlage für das Verständnis des molekularen Mechanismus der SMC Funktion im Leben formen.

2. Introduction

To survive on planet Earth cells need to divide to produce offspring. The process of cell division is complicated and regulated on multiple levels. In general, the DNA inside a cell needs to be fully replicated and faithfully segregated, after which the cell needs to divide into two cells. The different domains of life have different ways of dealing with this challenge. This introduction focuses primarily on bacterial chromosome segregation, as the main topic of this thesis is the study of localization of Structural Maintenance of Chromosomes (SMC) complexes in the bacterial species *Bacillus subtilis*. However, eukaryotic chromosome segregation will also be briefly introduced. SMC complexes are highly conserved complexes that play major roles in chromosome organization and segregation, therefore chromosome organization will be succinctly discussed. Because of their conservation, SMC biology will be described for eukaryotes and bacteria.

2.1 Chromosome organization

DNA, the carrier of genetic information, is organized in chromosomes. The size of these chromosomes, when stretched out, are multiple orders of magnitudes larger than the confines of a cell or cell nucleus. To fit inside a cell or nucleus the chromosomes need to be tightly packed and need to remain organized, a challenging task considering the tangly nature of DNA double helices. Eukaryotes and prokaryotes have different ways of handling this challenge. In eukaryotes DNA wraps around histone proteins that form nucleosomes, these nucleosomes are packed together which increases the DNA compaction. Other proteins help in further compacting the DNA during various stages of the cell cycle (Teif & Bohinc, 2011). This compacted DNA has a specific organization with specific domains. Among these are for example large chromosome territories of Mb scale and topologically associating domains of sub-Mb scale. Loci within these domains tend to interact within their domain but rarely outside of their domain, indicating that chromosomes in eukaryotes contain higher order structures (Dekker et al., 2013).

Prokaryotes have several means of compacting and organizing their DNA: 1) by introducing negative supercoiling, i.e. underwinding of the DNA helix which induces local DNA folding into super helices also referred to as plectonemes; 2) by macromolecular crowding, by which the packed environment of a cell contributes to excluded volume effects in the DNA which favor compact molecular conformations; 3) by nucleoid associated proteins which are small abundant proteins that can bend or bridge DNA. Several studies have demonstrated the existence of macrodomains of Mb scale within a bacterial chromosome. Interactions between DNA loci often take place within macrodomains but not between macrodomains, as was observed for the large chromosome territories and topologically associating domains in eukaryotes. It is thought that formation of loops of DNA might be one way to produce these macrodomains in prokaryotes. (Thanbichler & Shapiro, 2006; Rimsky & Travers, 2011; Teif & Bohinc, 2011; Gruber, 2014).

2.2 Bacterial chromosomes

2.2.1 Bacterial chromosome replication

Most bacterial genomes comprise a single circular chromosome of 2-8 megabase in size. Replication of a bacterial chromosome is initiated at a single origin of replication (*oriC*) from where two replication machineries (also referred to as replication forks) proceed in opposite direction towards the terminus of replication where the replication forks meet (Fig. 1A). The speed of these replication forks is approximately 1000 base pairs/second, which means that duplication of a typical bacterial chromosome of four megabases takes around 33 minutes (Thanbichler, 2010; Wang et al., 2013).

The doubling time of many bacterial species such as *B. subtilis*, *Escherichia coli* and *Streptococcus pneumoniae* is shorter than the duration of this replication time (or S-phase). To achieve this fast growth, replication is initiated from the new *oriC* before the completion of the previous round of replication. This results in daughter cells that inherit partially replicated chromosomes (Cooper & Helmstetter, 1968; Niki & Hiraga, 1998; Nielsen et al., 2007).
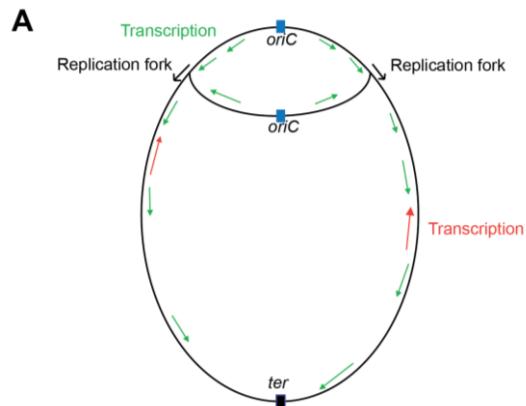
Figure 1. Chromosome segregation in prokaryotes and eukaryotes
A.A bacterial chromosome with two replication forks (black) and transcription with the majority of genes laying in the direction of *oriC* to terminus (green), and occasionally into the direction of terminus to *oriC* (red) are depicted.
B.Overview of eukaryotic chromosome segregation in mitosis. Sister chromatid cohesion is established during DNA replication by cohesin rings that hold the two sisters together. Kinetochores attach to centromeres, microtubules connect to these kinetochores. After cleavage of the cohesin kleisin subunit the forces of the mitotic spindle transmitted via the microtubules allow sister chromatids to segregate to opposite cell poles. Taken from (Duro & Marston, 2015).
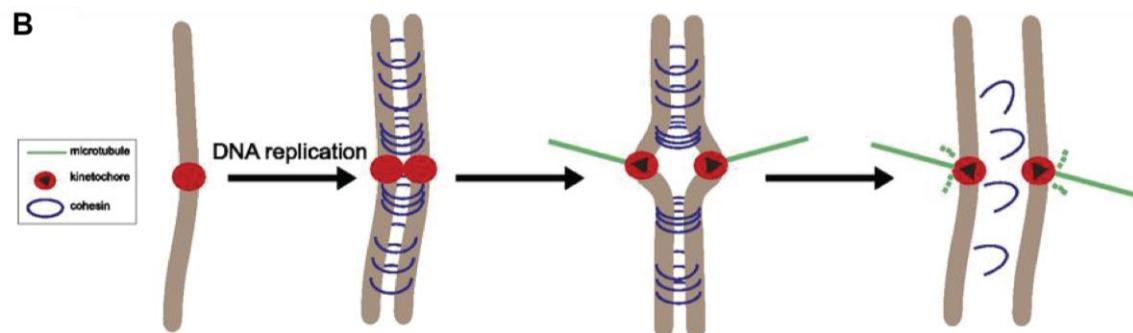
2.2.2 Bacterial chromosome segregation

Soon after the *oriC* is replicated, the replication origins move towards opposite cell poles (Webb et al., 1997; Niki & Hiraga, 1998). Subsequently, the remainder of the chromosome needs to be separated. Thus far,

few conserved proteins are known to be implicated in bacterial chromosome segregation. In addition, several processes have been postulated to (help) drive faithful bacterial chromosome segregation. The conserved proteins and postulated processes will be outlined below.

2.2.2.1 The ParABS system

The name of *par* loci is derived from the partitioning defects mutants in *par* loci have on (low copy) plasmids. The *par* loci present on plasmids are usually responsible for segregation of the same plasmid. *par* loci can be distinguished into three types; Type I encodes for a deviant Walker-type ATPase, Type II encodes for an actin-like ATPase and Type III encodes for a tubulin-like GTPase. All three types of *par* loci types play roles in plasmid segregation whereas Type I is also encoded on most bacterial species on the chromosome. It is known that chromosomally encoded *par* loci have a role in chromosome segregation (Ebersbach & Gerdes, 2005; Gerdes et al., 2010).

The Type I *par* locus encodes for ParA (the Walker or P-loop–type ATPase), a DNA binding protein named ParB and a centromere-like sequence *parS*. ParA binds non-specific DNA cooperatively in an ATP-bound dimer state. Binding of multiple dimers on the DNA leads to the formation of ParA filaments on the DNA. ParA disengages from the DNA upon ATP hydrolysis. The *parS* sites are usually found in close proximity to the *oriC* and they are specifically bound by ParB. ParB was shown to stimulate the ParA ATPase rate and thereby influences the turnover rate of nucleoid bound ParA. It was shown for some species that ParA interacts with ParB and that they have direct implications on chromosome segregation. For example, in *Vibrio cholerae* ParA structures extend from the new cell pole towards the old cell pole during the cell cycle. Upon *oriC*/ParB segregation, ParB follows the retracting ParA structures which suggests that ParB interacts with ParA to move the *oriC* to the opposite cell pole (Fogel & Waldor, 2006; Toro et al., 2008; Gerdes et al., 2010; Ptacin et al., 2010). A more recent study in *Caulobacter crescentus* suggests that ParA and ParB act in a DNA-relay mechanism. This model is based on the proposal that chromosomes have elastic properties. ParA-ATP dimers bound to DNA interact with ParB bound to *parS* sites, because the chromosome has elastic properties, ParB gets moved to the direction where most ParA is bound to the chromosome. ParA is not bound uniformly on the *C. crescentus* chromosome and therefore this DNA-relay mechanism may promote chromosome segregation (Lim et al., 2014).

The ParABS system of *B. subtilis* has been studied in detail. Its ParB analogue, Spo0J, contains a Helix-Turn-Helix-motif that allows specific binding to ten 16 bp palindromic *parS* sites in the *B. subtilis* chromosome, eight of which are in the 20% *oriC*-proximal region of the genome (Ebersbach & Gerdes, 2005; Breier & Grossman, 2007). ParB binds as a dimer and spreads from the *parS* site onto several kb around this site, thereby generating large nucleoprotein complexes in the vicinity of *oriC* (Murray et al., 2006). A *parB* deletion strain shows an increase in the fraction of anucleated cells and cells that are elongated. In general those cells have abnormal nucleoid morphology. In addition, cells lacking ParB show origins that are closer together than in wild-type cells (Ireton et al., 1994; Autret et al., 2001; Lee et al., 2003; Ebersbach & Gerdes, 2005). Although ParB seems to play a role in origin segregation, ParA does

7

not seem to play a major role in origin or chromosome segregation during vegetative growth since a *parA* deletion does not result in aberrant cell or nucleoid shapes or an increase in the fraction of anucleated cells. In *B. subtilis,* it seems that the ParABS plays a more important role in chromosome segregation during sporulation (Ireton et al., 1994).

Recently, it was demonstrated that *B. subtilis* ParB is capable of condensing and bridging DNA *in vitro* (Graham et al., 2014; Taylor et al., 2015). ParB mutants described for having defects in spreading (G77S and R80A) (Autret et al., 2001; Breier & Grossman, 2007; Graham et al., 2014) were studied. ParB(R80A) is capable of binding *parS* sites *in vitro* but does not compact DNA. ParB(G77S) is also capable of binding *parS* sites *in vitro*, however the pattern of the gel-shift is quite distinct from wild type. For wild type two bands appear in the gel shift with increasing concentrations of protein relative to the *parS* DNA, for ParB(G77S) only the upper band was observed. This suggests that ParB(G77S) has a different binding mode than wild type to *parS* DNA. ParB(G77S) is also capable of compacting DNA. The authors suggest that the spreading of ParB does not occur in one-dimensional filaments along the DNA but rather by interaction of dimers of ParB that are separated on the DNA and thereby form DNA loops (Graham et al., 2014). The mutants seem to be impaired in either DNA bridging (ParB(R80A)) or interacting with neighbors on the DNA (ParB(G77S)) (Graham et al., 2014). It appears that the spreading and DNA bridging activity of ParB plays a role in organization of the chromosome and are thereby involved in chromosome segregation, particularly because of the interaction with Smc complexes (see Chapter 2.4).

2.2.2.2 Postulated processes involved in segregation of chromosomes

After faithful separation of the *oriC* regions of chromosomes, the remainder of the chromosome needs to segregate. Little is known about the segregation of regions of the chromosome between the origin and terminus of replication. However, a few processes have been postulated that may help in segregation of these regions.

2.2.2.2.1 Lengthwise chromosomal condensation directly followed upon replication

This model suggests that compaction of adjacent DNA (which makes condensed structures) promotes newly replicated sister chromosomes to segregate (Yan et al, 1999; Marko, 2009; Wang et al., 2013). Data that supports this model includes observations where replicated sister loci segregate sequentially and that these loci colocalize with adjacent genetic loci (Viollier et al., 2004; Wiggins at al., 2010). This suggests that segregation and condensation function in a coupled fashion. Mathematical modelling of two flexible polymer rings gives additional support for the model; if catenated rings are compacted orderly and are locally controlled along their lengths, this is sufficient to eliminate entanglements between them, provided that a mechanism is present to decatenate the rings (Marko, 2009; Wang et al., 2013).

2.2.2.2.2 Transcription

The direction of transcription of the majority of genes in many bacteria is oriented from *oriC* to terminus (Fig. 1A), especially for highly transcribed genes. Thus, in most cases transcription and genome replication take place in the same direction, presumably this orientation evolved to avoid head on collisions between the replication and transcription machineries (Brewer, 1986; McGlynn et al., 2012). Transcription has been suggested to be involved in chromosome segregation in *B. subtilis* and *S. pneumoniae.* (Dworkin & Losick, 2002; Kjos & Veening, 2014). It was observed by fluorescence microscopy for *B. subtilis* and *S. pneumoniae* that inhibition of the transcription machinery, by drugs or introducing inhibitory mutations in the transcription machinery, resulted in chromosome segregation defects (Dworkin & Losick, 2002; Kjos & Veening, 2014). Similar experiments in *E. coli* did not show an effect of the transcription machinery on chromosome segregation (Wang & Sherratt, 2010). It needs to be noted that many cellular processes may be affected by inhibiting the transcription machinery, therefore the observed defects in chromosome segregation may be of an indirect nature rather than a direct consequence of reduced transcription.

It was also suggested that the process of transertion (coupled transcription, translation and insertion of a native polypeptide into the membrane) could play a role in chromosome segregation (Woldringh, 2002; Toro & Shapiro, 2010). However, direct evidence to confirm this hypothesis is currently lacking.

2.2.2.3 FtsK

At the final stage of chromosome segregation the terminus region needs to be faithfully segregated. This is particularly challenging because the chromosomes can be catenated or, due to homologous recombination, may consist of chromosome dimers. A widely conserved protein that plays a crucial role in terminus segregation is the DNA translocase protein FtsK which is associated with the divisome. FtsK translocates DNA towards a *dif* site located near the terminus, it is directed by FtsK orienting polar sequences (KOPS) that are oriented towards the *dif* site. FtsK can bring two sister chromosomes together at this *dif* site. FtsK recruits and activates XerCD recombinases at the *dif* site, these recombinases resolve chromosome dimers. DNA is pumped into the two daughter cells by FtsK. In addition, FtsK recruits DNA recombinases, such as topoisomerase IV, to resolve the chromosome catenanes (Espeli et al., 2003; Sherratt et al., 2004; Stouf et al., 2013; Besprozvannaya & Burton, 2014).

In *B. subtilis* CodV and RipX are XerC and XerD orthologues, respectively. SpoIIIE and SftA share substantial sequence identity with FtsK and were shown to have an impact on chromosome segregation in *B. subtilis* (Kaimer et al., 2009; Kaimer et al., 2011).

2.3 Eukaryotic chromosome segregation

Eukaryotic chromosome segregation is most widely studied in budding yeast, fission yeast, *Xenopus laevis* egg extracts, worms, flies and mammalian tissue culture cells. Although chromosome segregation is well conserved between these organisms, differences do exist. Therefore, eukaryotic chromosome segregation will be described in a general fashion.

A eukaryotic cell cycle consists of four main phases; S-phase, G2, mitosis and G1. During S-phase, DNA replication is initiated from multiple origins per chromosome and multiple DNA replication forks replicate the DNA until all chromosomes are fully duplicated (Akiyoshi & Gull, 2013). The two sister chromosomes are held together by a complex called cohesin (Fig. 1C). Cells go through the G2 phase and subsequently enter mitosis. During mitosis the DNA is condensed, kinetochores (a macromolecular protein complex) attach to the centromeres of the chromosomes on one side and connect to the microtubule polymers (made of tubulin) from the mitotic spindle on the other side (Fig. 1C). Once the mitotic spindle is properly attached to the chromosomes, the spindle checkpoint can be passed which triggers a protease called separase to cleave the cohesin complex at anaphase (a subphase of mitosis) onset. This releases the sister chromosomes from each other and facilitates segregation of the sisters to opposite sides of the cell nucleus (Fig. 1C). Next, the cell divides into two daughter cells and enters the G1 phase (Yanagida, 2005; Akiyoshi & Gull, 2013; Duro & Marston, 2015).

2.4 Structural Maintenance of Chromosomes (SMC) complexes

SMC complexes are highly conserved throughout all domains of life. In eukaryotes these complexes are involved in very pivotal processes during the cell cycle such as sister chromatid cohesion, chromosome organization and DNA repair. In bacteria these complexes function in chromosome segregation and DNA repair. Defects in these complexes have been associated with several diseases in humans such as, microcephaly (size reduction of the frontal brain lobe), Cornelia de Lange syndrome (which symptoms include low body weight and body length, small head size, developmental delays and behavioral issues) and Roberts syndrome (characterized by prenatal growth retardation, limb malformations and craniofacial abnormalities). SMC complexes have a unique and highly conserved structure, which indicates a conserved biochemical mechanism throughout the domains of life. Understanding the mechanism of action of SMC complexes is currently a 'hot topic' in science, and although we understand much more than decades ago, the precise ways of how SMC complexes complete their biological function in chromosome organization and maintenance remain unclear. Below I dissect the structure and function of different SMC complexes. The family of SMC proteins will be denoted as 'SMC', prokaryotic Smc will be referred to as 'Smc'.

2.4.1 The composition of SMC complexes

SMC complexes are distinct because of their unique structure. They are comprised of two SMC proteins, a kleisin subunit and one or more additional subunits (Fig. 2A). In eukaryotes, the two SMC proteins form a heterodimer whereas in bacteria they make a homodimer.

2.4.1.1 SMC proteins

An SMC protein has a very special fold; it folds back on itself in the middle and thereby forms a globular 'hinge' domain. This is followed on both sides with a long α-helix, which together form one antiparallel coiled-coil. The N- and C-termini form a so called 'head' or nucleotide binding domain (NBD) domain that

contains an ATP binding cassette (ABC) ATPase domain (Fig. 2B). One SMC protein forms a long rod shaped structure of approximately 50 nm in length. Two SMC proteins dimerize at the hinge domain, the two head domains of the dimer form a functional ABC-type ATPase (Nasmyth & Haering, 2005; Nolivos & Sherratt, 2014).
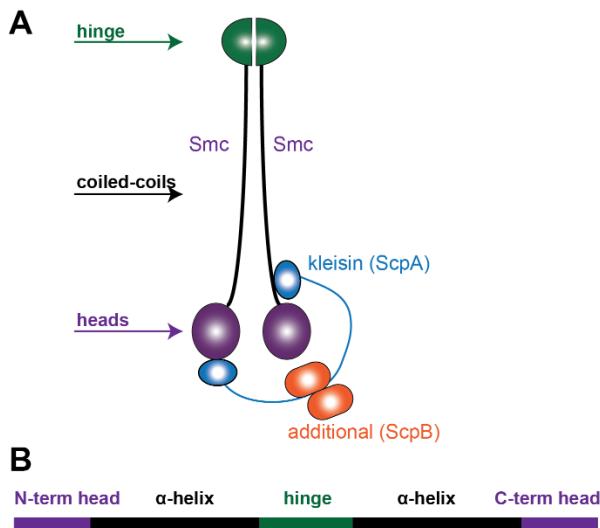
Figure 2. The architecture of SMC complexes
A.Schematic overview of the architecture of a typical SMC complex, in *B. subtilis* the kleisin is ScpA, the additional subunit ScpB.
B.Schematic overview of the different domains in an unfolded SMC protein

2.4.1.2 The kleisin subunit

The name of the kleisin subunit comes from the Greek word for closure: kleisimo (Schleiffer *et al.*, 2003). Kleisins are conserved throughout all domains of life and are divided into different subfamilies depending on their sequence similarity and the SMC complex they belong to, thus far five subfamilies have been described, α ,β ,γ, δ and prokaryotic kleisins (Schleiffer et al., 2003; Nasmyth & Haering, 2005).

In general, kleisin subunits consist of two globular domains at the N- and C-termini with a presumably unstructured linker region in-between (Schleiffer et al., 2003). The kleisin subunit associates asymmetrically with the SMC dimer. It binds with its C-terminal end to the bottom of the head domain (also called cap) (Fig. 2A) of one SMC protein and with its N-terminal domain to a region just above the head domain (referred to as neck) of the other SMC protein (Fig. 2A) in *B. subtilis* Smc-ScpAB and *Saccharomyces cerevisiae* cohesin (Gruber et al., 2003; Haering et al., 2004; Bürmann et al., 2013; Gligoris et al., 2014). This forms a closed ring consisting of the SMC dimer and kleisin (hence the name kleisin) (Fig. 2A) (Gruber et al., 2003).

2.4.1.3 The additional subunits

The additional subunits of the SMC complex are comprised of different structures and are less well conserved than the other subunits of the complex, although as far as is known today every SMC complex contains at least one additional subunit. In eukaryotic SMC complexes several additional subunits are

present whereas prokaryotes usually contain only one additional subunit which binds to the kleisin subunit (Fig. 2A) (Nasmyth & Haering, 2005; Nolivos & Sherratt, 2014). It has been suggested for a bacterial Smc complex that binding of the additional subunit to the kleisin subunit induces a conformational change in the sub-complex (consisting of the additional subunit and kleisin subunit) and that this induces ATPase activity in the Smc complex (Kamada et al., 2013). In eukaryotes, the additional subunits are also implicated in regulating the different functions of the SMC complexes at various stages during the cell cycle (Jeppsson et al., 2014a).

2.4.2 Similarities with ABC transporters

SMC complexes share similarities with ABC transporters because of their NBDs. ABC transporters are a superfamily of membrane proteins that use the energy of ATP hydrolysis to transport a substrate across a membrane. A typical ABC transporter contains two NBDs where, as is the case for SMC complexes, ATP can bind and hydrolyze upon dimerization of the two NBDs. Magnesium ions are needed for catalysis of this reaction. At the sequence level the NBDs of ABC transporters are characterized by seven highly conserved motifs: 1) the A-loop, 2) the Walker A motif (GXXGXGK(S/T), 3) the Walker B motif ($\phi\phi\phi$DE, where ϕ is a hydrophobic amino acid), 4) the D-loop (SALD), 5) the H-loop, 6) the Q-loop and 7) the ABC signature motif or C-motif (LSGGQ). The ABC signature motif defines the ABC superfamily of transporters (Fig. 3AB) (Locher, 2009; Rees et al., 2009; ter Beek et al., 2014).
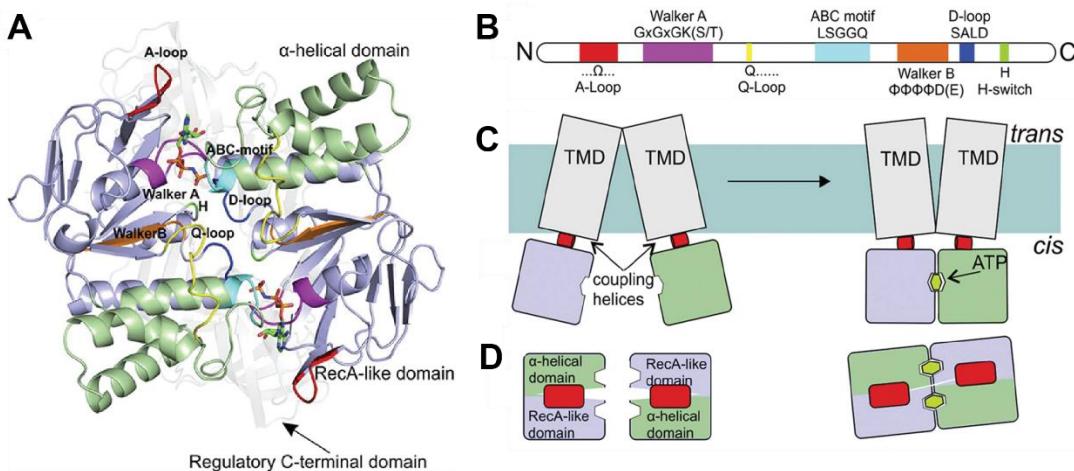
Figure 3. Structural overview of ABC transporters
A. Structure of the NBDs of a MalK dimer, part of the maltose transporter MalEFGK$_2$ (PDB 3RLF). The different conserved domains and motifs are colored: red, A-loop; magenta, Walker A; orange, Walker B; blue, D-loop; green, H-loop; cyan, ABC motif; yellow, Q-loop. In sticks is the ATP analogue AMP-PNP.
B. An overview of the different sequence motifs in the NBD is depicted.
C. Schematic overview of a conformational change in the overall structure of an ABC transporter. A side view in which only one ATP molecule is visible is shown. The NBDs are blue and green. A coupling helix (red) connects the NBD with the TMD. Upon ATP binding and hydrolysis a conformational change is induced from the NBD to the TMD via the coupling helices.
D. A top view of the NBD is shown in which the two molecules of ATP are visible.
   Taken from (Ter Beek et al., 2014).

In ABC transporters each NBD is connected to a transmembrane domain (TMD) via a coupling helix (Fig. 3C). These two NBDs can either be in a disengaged or engaged state. Each NBD can bind one ATP, upon ATP binding to the two NBDs these NBDs can engage by which a conformational change takes place (Fig. 3CD). Via the coupling helix the TMD changes conformation upon engagement of the NBDs. This allows the cargo to move through the transporter to the other side of the membrane. The hydrolysis of ATP destabilizes the engaged NBDs making them return to the original disengaged state (Fig. 3C). Several intermediate conformational changes in ABC transporters have been observed during the ATP binding and hydrolysis cycle (Locher, 2009; Rees et al., 2009; ter Beek et al., 2014).

In the SMC head domain, all the above mentioned motifs are present except for a clear A-loop (Löwe et al., 2001). The different domains have different roles during the ATP hydrolysis cycle. For example, the Walker A motif binds the β- and γ-phosphate of ATP. A magnesium ion is coordinated by the aspartate residue of the Walker B motif and the glutamate residue of the Walker B motif is thought to polarize the 'attacking' water molecule in the ATP hydrolysis reaction. The ABC signature motif guides the γ-phosphate of ATP (Fig. 3A). ATP binds to the ABC signature motif in one NBD and to the other motifs in the other NBD. It thereby promotes the two NBDs to engage (Locher, 2009; Rees et al., 2009; ter Beek et al., 2014). Mutations in the highly conserved lysine (K) of the Walker A motif prevents ATP binding similarly to mutations in the aspartate residue (D) of the Walker B (Rao et al., 1988; Hirano & Hirano, 1998; Hirano et al., 2001), prevention of ATP binding results in the two NBDs to remain undimerized (Fig. 4). Mutation of the serine (S) in the ABC signature motif does not affect ATP binding but prevents NBD dimerization (Jones & George, 1999; Hopfner et al., 2000; Hirano et al., 2001) (Fig. 4). When the glutamic acid (E) in the Walker B motif is mutated to a glutamine (Q) ATP can bind, the NBDs can dimerize but ATP hydrolysis is strongly reduced. Thereby the two NBDs remain in an engaged state for longer periods of time (Fig. 4) (Moody et al., 2002; Hirano & Hirano, 2004).
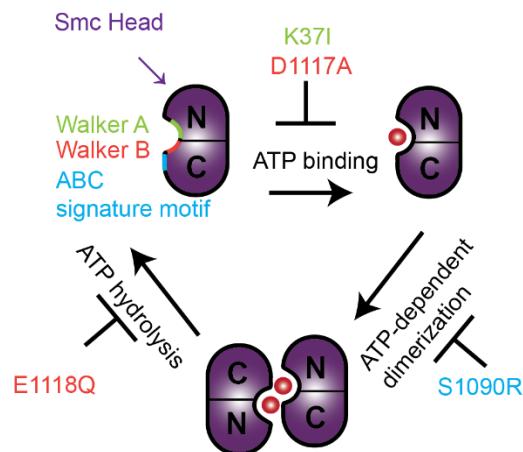

Figure 4. Overview of the ATP hydrolysis cycle in SMC
Shown is a NBD of SMC, indicated are the different steps in the ATP hydrolysis cycle. The corresponding inhibiting mutations in *B. subtilis* Smc are color coded for the motifs in the NBD in which they are present. Walker A is depicted in green, Walker B in red and the ABC signature motif in blue.

ATP hydrolysis is essential for SMC functioning, however the role of the ATP hydrolysis cycle for SMC complexes is largely unknown, both on a functional and structural level. Only very recently a role for ATP dependent head engagement in changing the conformation of the coiled-coil was described; ATP and DNA binding induced a conformational change from a rod shape (in which the two coiled-coils are aligned) to a more ring-like conformation (in which the two coiled-coils are separated) (Soh et al., 2014). The relatedness of SMC complexes to ABC transporters and this very recent data suggest that ATP hydrolysis induces a conformational change in the complex that is important for functioning.

2.4.3 Eukaryotic SMC complexes

Three eukaryotic SMC complexes are most widely studied, namely cohesin, condensin and the Smc5/6 complex. I will focus on these three complexes as representatives of eukaryotic SMCs.

2.4.3.1 Cohesin

Cohesin contains a heterodimer of Smc1 and Smc3 and an α-kleisin subunit Scc1 (Rec8 during meiosis). Additional subunits are Scc3, Pds5 and Wpl1 of which Scc3 and Pds5 bind to Scc1 and Wpl1 to Scc3 and Pds5 (Nasmyth & Haering, 2009; Jeppsson et al., 2014a). Cohesin in higher eukaryotes has been suggested to function in DNA double-strand break repair, chromosome condensation, spindle pole body integrity during mitosis, pairing of homologues chromosomes, non-homologous centromere coupling, mono-orientation of sister kinetochores during meiosis and regulation of gene expression (Mehta et al., 2013). However, cohesin is most famous for its crucial role in sister chromatid cohesion during mitosis (and meiosis). Cohesion between sister chromatids is established during S-phase, by which newly replicated sister chromatids are held together by cohesin rings. Eukaryotes presumably require sister chromatid cohesion to avoid the multiple replicated chromatids per cell to separate and intermix which would be detrimental for faithful chromatid segregation. It is also suggested that cohesion is needed to resist the spindle forces which are build up when the chromatids attach to microtubules and generate force from opposite cell poles (Marston, 2014). The spindle checkpoint senses the proper attachment of microtubules and allows activation of separase. Separase cleaves the kleisin subunit of cohesin, thereby sister chromatid cohesion is destroyed and anaphase proceeds (Marston, 2014). It is thought that cohesin can hold sister chromatids together by topologically embracing (trapping within the SMC ring) them. *Ex-vivo* experiments indicate that cohesin can hold two mini-chromosomes together when purified from yeast (Ivanov & Nasmyth, 2005, 2007; Haering et al., 2008). Together with the notion that the kleisin subunit needs to be cleaved before chromosomes can be segregated during mitosis (Uhlmann et al., 1999; Uhlmann et al., 2000) this is evidence that cohesin indeed topologically embraces sister chromosomes (Jeppsson et al., 2014a).

The suggested role of cohesin in gene expression in higher eukaryotes comes from more recent studies which indicate that cohesin maintains DNA loops between enhancer elements and promotors. It was proposed that cohesin can thereby inhibit and stimulate enhancer-promoter interactions by associating with

the transcriptional regulator CCCTC-binding factor (CTCF) or mediator complex, respectively (Hadjur et al., 2008; Wendt et al., 2008; Kagey et al., 2010; Jeppsson et al., 2014a). It is even suggested that with these interactions, which may be cell type specific, transcriptional programs are regulated (Kagey, Newman, & Bilodeau, 2010). In several eukaryotes it was implied that cohesin influences chromosome organization at selected loci such as tDNA and rDNA (Guacci et al., 1997; Gard et al., 2009; Dorsett & Merkenschlager, 2013). Novel methods based on chromosome conformation capture (3C) techniques elucidate genome-wide chromosomal interactions (Box 1) (Belton et al., 2012; Ferraiuolo et al., 2012). Constructing the genome-wide interaction maps in the presence and absence of functional cohesin (subunits) revealed that cohesin is necessary for the maintenance of large chromosome territories of Mb in scale and topologically associating domains of sub-Mb scales (Phillips-Cremins et al., 2013; Seitan et al., 2013; Sofueva et al., 2013; Mizuguchi et al., 2014; Zuin et al., 2014). Chromatin interaction analysis using paired end tag sequencing (ChIA-PET) is a ChIP derived 3C method to investigate genome-wide chromatin interactions and has as major advantage that the role of specific proteins can be studied directly (Box 2). This is in contrast with the classical 3C methods where comparisons between wild-type and mutant cells are necessary (Box 1 and 2) (Fullwood et al., 2009; Fullwood et al., 2010; Li et al., 2010). Using ChIA-PET, cohesin in embryonic stem cells was suggested to loop DNA through specific CTCF interaction sites into specific domains which is important for gene transcription (Dowen et al., 2014). Also, interactions that were tissue-specific for activated or repressed genes have been reported indicating a possible role for cohesin in tissue specific gene regulation (DeMare et al., 2013; Heidari et al., 2014).

Cohesin targeting to chromosomes is catalyzed by a complex of Scc2/Scc4 also called kollerin in yeast (Nasmyth, 2011). The exact molecular mechanism of the actual loading of cohesin is still under intense investigation but evidence thus far directs into a model in which the hinge opens to load DNA into the ring (Gruber et al., 2006) presumably driven by ATP hydrolysis (Arumugam et al., 2003; Weitzer et al., 2003). The assumed DNA exit gate is at the Smc3-kleisin interface (Chan et al., 2012; Buheitel & Stemmann, 2013), dissociation of cohesin from DNA is catalyzed by Wapl, Pds5 and several other subunits (Tanaka et al., 2001; Sutani et al., 2009; Rowland et al., 2009). Sororin can counteract the action of Wapl in humans (Rankin et al., 2005; Nishiyama et al., 2010). Cohesin can be protected from this dissociation by acetylation of Smc3 by Eco1, a member of the cohesin acetyl transferase family, which stabilizes the ring presumably by shutting the exit gate (Ben-Shahar et al., 2008). Separase opens the ring by proteolytic cleavage of the kleisin subunit by which cohesin is released from the chromatin at anaphase onset (Hauf et al., 1997; Uhlmann et al., 1999; Nasmyth, 2011).

In higher eukaryotes cohesin localizes mostly to the regions where cohesion's transcriptional function may be expected. However, centromere regions contain highly repetitive sequences and are therefore often omitted from ChIP-on-chip or ChIP-seq data. Different experiments do indicate that cohesin localizes to centromeres in higher eukaryotes (Jeppsson et al., 2014a). In flies, cohesin and Scc2 colocalize with RNA polymerase II (Misulovin et al., 2008). Human cohesin colocalizes with CTCF and the mediator complex (Parelho et al., 2008; Rubio & Reiss, 2008; Wendt et al., 2008; Kagey et al., 2010;). When CTCF is depleted,

cohesin's localization to sites other than the CTCF sites is not impaired. The depletion of CTCF does influence transcription, however sister chromatid cohesion remains functional (Wendt et al., 2008; Jeppsson et al., 2014a).

Box 1. Overview of chromosome conformation capture methods

a 3C: converting chromatin interactions into ligation products

Crosslinking of interacting loci   Fragmentation   Ligation   DNA purification

b Ligation product detection methods

3C	4C	5C	ChIA–PET	Hi-C
One-by-one All-by-all	One-by-all	Many-by-many	Many-by-many	All-by-all
			• DNA shearing • Immunoprecipitation	• Biotin labelling of ends • DNA shearing
PCR or sequencing	Inverse PCR sequencing	Multiplexed LMA sequencing	Sequencing	Sequencing

All chromosome conformation capture (3C) (panel a) techniques cross-link DNA (usually with formaldehyde) that is in close proximity, often mediated by a protein (complex). The DNA is subsequently fragmented by sonication or restriction digestion. Next, the DNA undergoes proximity ligation. This is a ligation step under dilute conditions, which favors ligation of DNA that is in close proximity to each other over random ligations. This is the crucial step in 3C experiments. The DNA is subsequently purified and the DNA ligations are quantified. The different 3C methods use different methods to analyze the amount and origin of the ligated DNA fragments (panel b). Classical 3C uses qPCR to quantify the ligated DNA fragments, this is a one to one approach. 4C (from circular 3C) uses inverse PCR by which genome-wide interactions can be detected for a single locus by microarrays or high throughput sequencing. 5C makes use of ligation mediated amplification (LMA) of primers specifically designed over ligation junctions, thereby many ligated DNA fragments can be detected by microarrays or high throughput sequencing. During a Hi-C experiment, the digested DNA is blunt ended by incorporating biotinylated nucleotides (represented by the star in the image), this allows specific purification of the ligated DNA fragments which can be analyzed directly by high throughput sequencing. Hi-C provides an all-by-all genome-wide overview of DNA interactions, the resolution of this overview depends on the sequencing depth. In ChIA-PET (Chromatin interaction analysis using paired end tag sequencing) the proximity ligation step is preceded by ChIP which facilitates a genome-wide overview of DNA interactions mediated by a protein of interest. ChIA-PET is explained in more detail in Box 2 (Chapter 4.3.2). Taken from (Dekker et al., 2013).

In yeast, cohesin localizes to sites of convergent transcription (Tanaka et al., 1999; Laloraya et al., 2000; Lengronne et al., 2004; Schmidt et al., 2009). Scc2, part of the cohesin loader, localizes to core centromeres and highly transcribed genes. This implies that cohesin is loaded at those sites and then translocates to the sites of convergent transcription (Lengronne et al., 2004; Schmidt et al., 2009; Jeppsson et al., 2014a). Cohesin was suggested to be able to translocate tens of kbs from a loading site (Hu et al., 2011). When

cohesin cannot hydrolyze ATP (but can bind ATP and engage heads) by mutating the glutamic acid (E) of the walker B motif into a glutamate (Q) cohesin is mainly found at the Scc2/Scc4 loading sites (Hu et al., 2011). Therefore the current model is that cohesin is loaded in a pre-hydrolysis state at the Scc2/Scc4 loading sites which are mostly found at centromeres and highly transcribed genes. Subsequently, ATP hydrolysis is needed to translocate away from those sides. The transcription machinery may help cohesin translocating (Lengronne et al., 2004; Hu et al., 2011). However, the model is mostly supported by work from budding yeast. In fission yeast, in contrast, ChIP data showed that removal of an Scc2 binding site did not change the levels of cohesin in nearby loci which is not consistent with the model (Schmidt et al., 2009). Alternatively, this may imply that cohesin is capable of translocating from loading sites further away (Jeppsson et al., 2014a). The reason for the difference of localization between organisms of higher and lower eukaryotes is thus far poorly understood.

2.4.3.2 Condensin

Condensin is, compared to cohesin, less well understood. Condensin consists of a heterodimer of Smc2 and Smc4. In yeast only one condensin complex is present in which the kleisin subunit is Brn1 and three additional subunits are present, Ycs1, Ycs4 and Ycs5. Most other eukaryotes harbor two condensin complexes (condensin I and condensin II), both are comprised of the Smc2 and Smc4 heterodimer but each have a specific set of three additional subunits. The yeast condensin subunits resemble condensin I (Hirano, 2012). *Caenorhabditis elegans* harbors a third version of the condensin complex, in this case Smc4 of condensin I is substituted with DPY-27 making a complex that specifically acts in gene dosage compensation of X-chromosomes (Chuang et al., 1994; Csankovszki et al., 2009).

It was proposed that condensin acts in DNA damage response and repair, recombination, maintenance of rDNA repeats, chromosome organization and that it has several roles during meiosis (Hirano, 2012). The exact molecular mechanism by which condensin exerts these functions remains poorly understood (Cuylen & Haering, 2011).

Like cohesin, condensin was recently also suggested to topologically embrace DNA molecules in *ex-vivo* experiments (Cuylen et al, 2011). Condensin compacts and disentangles sister chromatids, it was shown that this contributes to faithful chromosome segregation (Strick et al., 2004; Sullivan et al., 2004; Gerlich et al., 2006; Cuylen et al., 2011). It is thought that condensin may hold different loci within the chromatids together; making the chromatid fiber more rigid. This increased rigidity would facilitate better transmission of the pulling forces of the spindle at the centromere to the chromatid arms and thereby it could contribute in chromosome segregation (Cuylen & Haering, 2011).

Several lines of evidence suggest that condensin works together with the type II topoisomerase (Top2) to decatenate chromosomes presumably by exposing it as a substrate to Top2 (D'Ambrosio et al., 2008a; Cuylen et al., 2011; Jeppsson et al., 2014a). In several organisms post-translational modifications on condensin stimulate chromosome condensation (St-Pierre et al., 2009; Abe et al., 2011; Hirano, 2012). Next to the gene dosage compensation complex in *C. elegans*, other condensin complexes are also thought

to function in transcriptional regulation. For example, mutations in budding yeast condensin inhibit the repression of normally silenced loci (Bhalla et al., 2002). Condensin I and condensin II display different modes of localization during the cell cycle but are eventually both localized at the axial region of chromosomes shortly before the chromatids are separated. The functional implications of the difference in localization of condensin I and II are thus far poorly understood, although it is known that the relative levels on, and subsequent association with chromatids of the two complexes are important for proper establishment of mitotic chromosomes (Shintomi and Hirano, 2011; Jeppsson et al., 2014a).

In *C. elegans* and budding yeast, condensin was found to localize to, amongst other loci, tRNA genes. In addition, *C. elegans* condensin also localizes to promoters (D'Ambrosio et al., 2008b; Haeusler et al., 2008; Kranz et al., 2013). Budding yeast condensin was found to associate with the RNA polymerase III (pol III) transcription factor TFIIIC and to bind to the genes, including tRNA genes, which TFIIIC regulates. Condensin is mainly found in the centromeric region when cells are in G2/Mitosis phase (D'Ambrosio et al., 2008b; Haeusler et al., 2008). In fission yeast, condensin also localizes along the chromosome arms in a TFIIIC and certain kinetochore proteins dependent manner. This localization is influenced by histone subunits and post-translational modifications (D'Ambrosio et al., 2008b; Tada et al., 2011; Jeppsson et al., 2014a). Recently, condensin was shown to localize at the boundaries of topological associated domains within the *D. melanogaster* genome (Van Bortle et al., 2014).

2.4.3.3 The Smc5/6 complex

The Smc5/6 complex is composed of a heterodimer of, as the name implies, Smc5 and Smc6 and a minimum of four additional subunits. The Smc5/6 complex is mostly known and studied for its non-essential role in DNA repair (De Piccoli et al., 2009; Potts, 2009), several lines of evidence showed that the complex has essential functions in chromosome stability and dynamics (Kegel & Sjögren, 2010; Jeppsson et al., 2014a).

It was suggested that non-functional Smc5/6 causes chromatid cohesion defects in chicken, yeast and human (Stephan et al., 2011; Almedawar et al., 2012; Gallego-Paez et al., 2014). Smc5/6 was also reported to have roles in DNA replication (Gallego-Paez et al., 2014; Wolters et al., 2014). In yeast the complex promotes replication of rDNA, it was suggested that it does this by promoting and ensuring stable replication fork progression through the rDNA region (Torres-Rosell et al., 2007). In addition, the Smc5/6 complex allows proper timing of replication of longer budding yeast chromosomes (Torres-Rosell et al., 2007; Kegel et al., 2011). Depletion of Smc5 or Smc6 in human alters the binding pattern of Top2 and condensin on the mitotic chromosome (Gallego-Paez & Tanaka, 2014). Moreover, the Smc5/6 complex was suggested to have an influence on transcription as well (Zhao & Blobel, 2005, Jeppsson et al., 2014a).

Smc5/6 localizes to the chromosome during S phase when chromosomes are being replicated in yeast and human (Kegel et al., 2011; Gallego-Paez et al., 2014). The localization of the complex shows overlap with the localization of cohesin and it was suggested that the chromosomal association of Smc5/6 requires cohesin bound to the chromosome (Ström et al., 2004; Ünal et al., 2004; Gallego-Paez et al., 2014;

Jeppsson et al., 2014b;). Temporal localization of Smc5/6 and cohesin also overlaps, with its presence during most of the cell cycle but release just before chromosomes segregate (Gallego-Paez & Tanaka, 2014). Although, in contrast, Smc5/6 remains present on rDNA and specific telomeres during the entire cell cycle (Torres-Rosell et al., 2005). In fission yeast the localization partially overlaps that of condensin by localizing to tRNAs and TFIIIC binding sites, Smc5/6 also localizes to centromeres in this organism (Pebernard et al., 2008; Jeppsson et al., 2014a).

2.4.4 Prokaryotic Smc complexes

In bacteria several Smc complexes are known such as Smc with the prokaryotic kleisin ScpA (Segregation and Condensation Protein A) and additional subunit ScpB. In *E. coli* and related bacteria a complex called MukBEF is present, the MukB subunit has low sequence homology to SMC proteins but shares structural features with the canonical SMC proteins (Nolivos and Sherratt, 2014). A third Smc-like complex was identified by sequence similarity to MukB recently, called MksBEF for MukBEF-like. These complexes contain significantly shorter coiled-coils than the aforementioned Smc complexes and often co-exist with Smc-ScpAB, MukBEF and sometimes other MksBEF complexes. The precise functions of this complex are not well studied (Petrushenko et al., 2011).
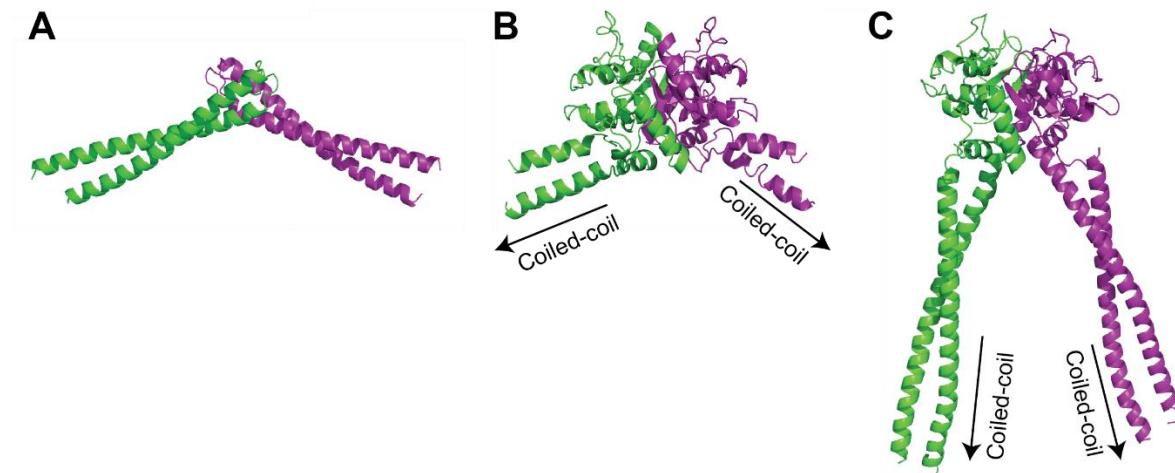
Figure 5. Different hinge domains of Smc and Smc-like complexes
  A. Zinc hook dimerization domain of *Pyrococcus furiosis* Rad50, PDB 1L8D (Hopfner et al., 2002)
  B. Hinge dimerization domain of Smc from *Thermotoga maritima*, PDB 1GXL (Haering et al., 2002)
  C. Hinge dimerization domain of Smc from *P. furiosis*, PDB 4RSJ (Soh et al., 2014)
      Images created with help of Dr. M-L. Durand-Diebold.

Other related Smc-like complexes include SbcC, a homolog of the archaeal and eukaryotic Rad50. In this complex a zinc-hook dimerization domain (Fig. 5A) is placed where typical Smc complexes have their hinge domain, it does have a ~50 nm coiled-coil and ABC-type ATPase head domain which is bridged by SbcD/Mre11. SbcC/Rad50 is known to play roles in DNA repair at double strand breaks (Hopfner et al., 2002; Lim et al., 2011; Lammens et al., 2011; Möckel et al., 2012). Another Smc-like complex is RecN, this

complex has shorter coiled-coils than the typical ~50 nm and no additional proteins are known. RecN was suggested to function in DNA repair and recombination (Pellegrino et al., 2012, Nolivos & Sherratt, 2014). Below I will introduce the most widely studied MukBEF and Smc-ScpAB complexes into more detail.

2.4.4.1 MukBEF

MukB was first identified in *E. coli* because MukB mutants generate anucleate cells (Hiraga et al., 1989). MukB forms an ATP-binding head domain with its N- and C-termini, has a ~50 nm coiled-coil and a hinge domain on the opposite end of this coiled-coil (Niki et al., 1991; Niki et al., 1992) displaying a similar structure as the aforementioned SMC proteins. MukB is encoded by the same operon as its additional proteins, MukE and MukF of which MukF binds to the head domains (Fig. 6). MukF does this by dimerizing at its N-terminus, the C-termini of the dimer bind to the two heads of the two MukB proteins in the complex, MukE associates with MukF (Woo et al., 2009; Upton & Sherratt, 2013; Nolivos & Sherratt, 2014). ATP binding to the MukB dimer disrupts one binding site of MukF with one MukB, this MukF can subsequently bind to another MukB-MukF complex and make dimers of dimer formations (Fig. 6) (Woo et al., 2009; Upton & Sherratt, 2013).
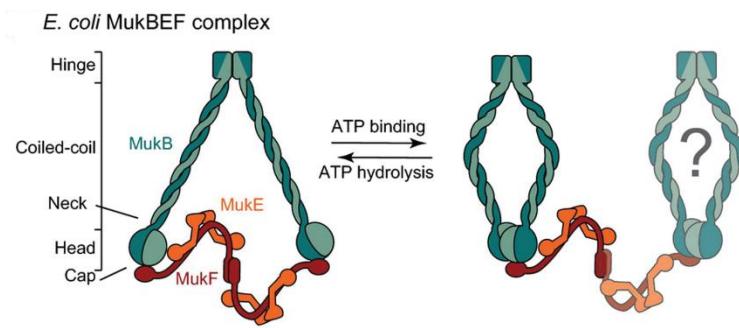
Figure 6. Architecture of *E. coli* MukBEF and the impact of ATP hydrolysis
MukF dimers interact with the cap region on the MukB head with their C-termini, four MukEs associate with the MukF dimer. ATP binding disrupts one binding site of MukF with one MukB which may subsequently interact with another MukB-MukF complex. Taken from (Nolivos & Sherratt, 2014).

Deletion of any of the MukBEF subunits leads to an increased fraction of anucleate cells and temperature sensitive growth, indicating that these mutants have a direct or indirect role in chromosome segregation (Niki et al., 1991; Sawitzke & Austin, 2000). In addition, these mutants are more sensitive to gyrase inhibitors which cause decreased negative supercoiling of chromosomal DNA (Adachi & Hiraga, 2003). An increase in negative supercoiling (by e.g. TopA, a DNA topoisomerase I, impairment) suppresses the temperature sensitive phenotype (Sawitzke & Austin, 2000). Overexpression of MukBEF leads to more condensed chromosomes suggesting a role in chromosome condensation as well (Wang et al., 2011). In addition, mutants show mispositioning of the *oriC* regions and chromosomal arms, a process independent of DNA replication, indicating a role for MukBEF in chromosome organization (Danilova et al., 2007; Badrinarayanan et al., 2012a).

Other evidence for a role of MukBEF in chromosome segregation comes from studies that show a direct physical interaction of MukBEF with topoisomerase IV in *E. coli*. MukB was shown to directly interact with

topoisomerase IV and to stimulate its activity, it could thereby have an influence on chromosome segregation and organization via the decatenation activity of topoisomerase IV (Hayama & Marians, 2010; Li et al., 2010).

Information about MukBEF localization is derived exclusively from microscopy experiments, as there is no ChIP data available. MukBEF was shown to form 2-4 foci that colocalize with the *oriC* (Danilova et al., 2007; Badrinarayanan et al., 2012a). New advanced microscopy techniques revealed that the measured turn-over rate for MukBEF foci *in vivo* is slower than the measured ATPase rate of MukBEF *in vitro*, therefore a model was proposed in which two dimers of dimers bind to DNA, upon ATP hydrolysis one dimer releases from the DNA and, similar to the action of a rock climber, looks for a new hand hold where it attaches to the DNA again (Badrinarayanan et al., 2012b). This model is supported by the observation that a mutant containing the E1407Q mutation in the walker B motif, capable of binding ATP but not hydrolyzing it, is able to form foci but does not turnover. Mutants incapable of binding ATP or engage heads, do not localize to the DNA. The mutant blocked in ATP hydrolysis also has an altered chromosomal localization as observed by microscopy. This suggests that although engaged heads are sufficient to localize to the chromosome, ATP hydrolysis is required to translocate to the wild-type chromosomal location (Badrinarayanan et al., 2012b; Nolivos & Sherratt, 2014), similar to the observation that was made by ChIP experiments for cohesin (Hu et al., 2011).

2.4.4.2 Smc-ScpAB

Smc complexes of the Smc-ScpAB type are studied in several organisms. The Smc-ScpAB complex consists of two Smc proteins that dimerize at the hinge domain. ScpA is the prokaryotic kleisin that bridges the two Smc proteins at their head domains by binding with its N-terminal domain to the neck, and with its C-terminal domain to the cap of the other Smc protein in *B. subtilis* (Fig. 2A). A dimer of ScpB associates with ScpA (Mascarenhas et al., 2002; Volkov et al., 2003; Bürmann et al., 2013; Kamada et al., 2013).

Smc-ScpAB has been studied in a diversity of prokaryotic organisms and mutations sometimes lead to an increased fraction of anucleate cells or aberrant nucleoid morphologies (Britton et al., 1998; Moriya et al., 1998; Jensen & Shapiro, 1999; Minnen et al., 2011). It is also suggested that Smc-ScpAB mutations increase sensitivity to gyrase inhibitors (Lindow et al., 2002a; Bouthier de la Tour et al., 2009). In *B. subtilis,* but not *S. pneumoniae,* Smc-ScpAB is essential under fast growth conditions (Moriya et al., 1998; Minnen et al., 2011; Nolivos & Sherratt, 2014). In *C. crescentus*, chromosome conformation capture followed by deep sequencing (Hi-C) experiments indicate that Smc-ScpAB may play a role in positioning the chromosome arms relative to each other (Le et al., 2013).

Localization of Smc-ScpAB is studied in detail in the Firmicutes *B. subtilis* and *S. pneumoniae.* Smc-ScpAB is mostly found on the *oriC* region of the chromosome and possibly at highly transcribed genes, the majority of its localization depends on ParB bound to *parS* sites. However, a *parB* deletion results in a milder phenotype than the *smc-scpAB* phenotype suggesting that decreased amounts of Smc-ScpAB on the chromosome can perform at least part of the function of Smc-ScpAB (Gruber & Errington, 2009; Sullivan

et al., 2009; Minnen et al., 2011; Nicolas et al., 2012). Very little is known about the interaction between ParB and Smc-ScpAB. More recently, evidence was provided that Smc-ScpAB of *B. subtilis* plays a crucial role in origin, but not terminus, segregation under fast growth conditions (Gruber et al., 2014; Wang et al., 2014).

The Graumann lab recently focused on the dynamics of Smc-ScpAB in live cells using fluorescence recovery after photo bleaching (FRAP) and single molecule fluorescence microscopy. They found that Smc-ScpAB has exchange rates of a few minutes in scale on the chromosome. In addition, they claim that Smc in the absence of ScpAB can freely diffuse through the chromosome whereas Smc in the presence of ScpAB is stationary bound to the chromosome and thereby forms condensation centers in the chromosome (Kleine Borgmann et al., 2013a; Kleine Borgmann et al., 2013b). Data other than their microscopy observations to support these conclusions is, however, currently lacking.

The most widely studied Smc-ScpAB complex *in vitro* is the *B. subtilis* Smc complex. The *B. subtilis* Smc protein is a dimer in solution and binds both single and double stranded DNA. The ATPase rate of Smc is stimulated by DNA binding, addition of ScpAB stimulates the ATPase rate in the absence of DNA (Hirano & Hirano, 2004; Kamada et al., 2013). ATP binding mutants, K37I – a Walker A motif mutant and D1117A – a Walker B motif mutant (Fig. 4), do not show ATP hydrolysis activity. Likewise, an ATP dependent dimerization mutant, S1090R – an ABC signature motif mutant (Fig. 4), which does bind ATP but cannot engage the heads does not show ATP hydrolysis activity. In the so called ATP hydrolysis mutant, E1118Q – a Walker B motif mutant (Fig. 4), ATP can bind and heads can engage. In this mutant ATP hydrolysis is drastically reduced and the heads remain in a (mostly) engaged state. In the presence of ATP, DNA binding of this mutant is greatly enhanced compared to wild type (Hirano & Hirano, 1998; Hirano et al., 2001; Kamada et al., 2013). Mutation of a conserved arginine (R59A) in *P. furiosis* resulted in an Smc dimer that had normal basal ATP hydrolysis activity but had reduced DNA stimulated ATP hydrolysis activity (Lammens et al., 2004). The corresponding mutation in *B. subtilis* (R57A) Smc showed reduced ATPase rates, both with and without the presence of DNA (Hirano & Hirano, 2006).

It was suggested that the Smc hinge plays a role in ATP hydrolysis. In a mutant that abolishes hinge-dimerization four conserved glycines are mutated to alanines in the hinge domain (Fig. 7). This protein showed to be a monomer *in vitro* that can still bind to DNA and is capable of hydrolyzing ATP although to much lower levels than wild-type Smc. From its capability of binding dsDNA and near wild-type levels of ATPase activity in the presence of ssDNA (Hirano & Hirano, 2002) conclude that the hinge domain of this mutant may still be partially active (Hirano et al., 2001; Hirano & Hirano, 2002). A combination of the monomeric hinge with the E1118Q mutation and the presence of ATP resulted in a protein that was pelletable more easily than the wild-type protein (Hirano & Hirano, 2004). It needs to be noted however that the majority of the *in vitro* work was carried out with proteins that contained his-tags and even his-tagged wild-type protein was not completely soluble (Hirano et al., 2001; Hirano & Hirano 2002; Hirano & Hirano 2004) suggesting that the studied proteins might be of compromised quality.
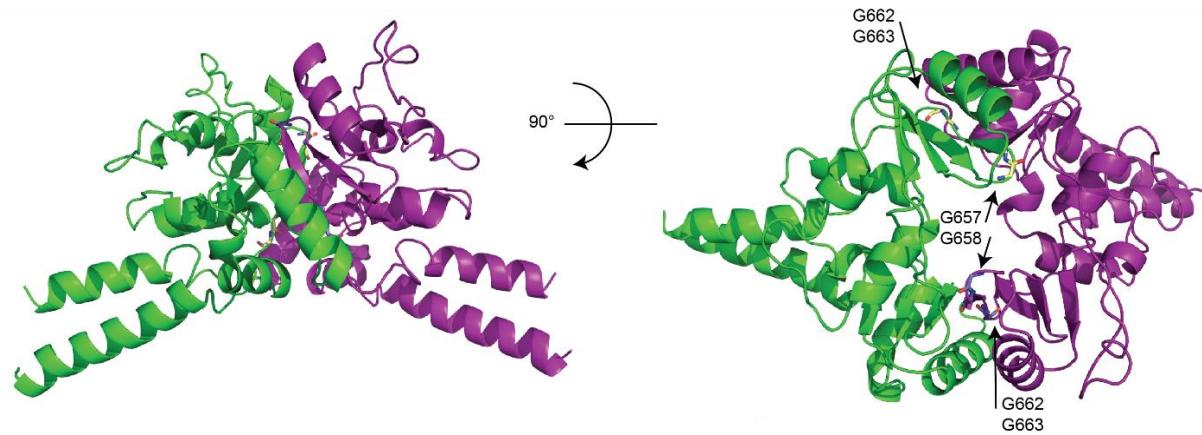
Figure 7. Superimposition of the _B. subtilis_ Smc hinge domain on the _T. maritima_ crystal structure (PDB 1GXL)
On the left a side view of the hinge dimer, on the right a top view of the hinge dimer. The four conserved glycines are indicated in yellow (on the green monomer) and blue (on the purple monomer) in sticks.
Image created with help of Dr. M-L. Durand-Diebold.

In _B. subtilis_, the K37I, D1117A, S1090R and E1118Q mutants render the Smc protein non-functional. Microscopy data shows that K37I, D1117A and S1090R Smc mutants do not localize to the chromosome, suggesting that at least ATP binding and head engagement are needed for proper localization (Mascarenhas et al., 2005). Measuring turnover by FRAP experiments of ScpA when Smc(E1118Q) was overexpressed led to the conclusion that Smc(E1118Q) has a slower turnover than wild-type Smc although this was not measured directly for the mutated Smc protein. In addition, overexpression of Smc(E1118Q) led to aberrant cell shapes, abnormal nucleoid morphologies and a strong growth defect (Kleine Borgmann _et al._, 2013a). In _C. crescentus_ over-expression of the corresponding EQ mutant protein led to unsegregated chromosomes resulting in multiple chromosomes per cell. _In vitro_ this protein bound DNA more readily than the corresponding wild-type protein and ATP hydrolysis was abolished. Pull down assays showed no evidence for an interaction between ParB and Smc in this organism (Schwartz & Shapiro, 2011). Thus far little is known about the interaction of the Smc-ScpAB loading factor (ParB for _B. subtilis_) and Smc-ScpAB. In addition, the role of ATP hydrolysis for Smcs is still poorly understood. A crystal structure of a dimer of ScpB with a peptide of ScpA showed that the ScpA peptide wraps around the ScpB dimer. In addition, it was demonstrated that the binding of ScpB to ScpA stimulates the ATPase activity in the Smc complex _in vitro_ (Bürmann et al., 2013; Kamada et al., 2013). Only very recently more insight was gained in the function of ATP-dependent head engagement, it was shown that ATP and DNA binding induce a conformational change in the coiled-coils close to the hinge region, the coiled-coils change from a rod shape to a more ring-like conformation (Soh et al., 2014). In addition, the authors show that the formation of the rod shape may be a conserved feature throughout Smc-ScpAB, condensin and cohesin. Proteins incapable of making rod-shapes were non-functional for Smc-ScpAB in _B. subtilis_, however it remains unclear what the function of these different conformational states of the Smc complex is inside the cell. Another study addressed chromosomal entrapment by Smc-ScpAB by covalently crosslinking Smc and ScpA into a ring.

After applying denaturing conditions, separating proteins from the chromosomes and subsequently isolating intact chromosomes it was shown that the covalently crosslinked Smc-ScpA ring remains entrapped on the chromosome. In addition, it was shown that ATP hydrolysis and ScpB are needed to achieve this (Wilhelm et al., submitted). It remains to be directly tested whether ATP hydrolysis and ScpB are required in a step preceding chromosomal entrapment, such as recruitment to the chromosome.

2.5 Aims of the thesis

Thus far the precise mechanism of action of SMC complexes is poorly understood. For functional SMC complexes ATP hydrolysis, the kleisin and all other subunits are required. What these components exactly do in the complex is however not fully understood. A model in the field is that ATP hydrolysis can introduce a conformational change in the SMC complex whereby the head domains facilitate a conformational change in the complex resulting in a conformationally changed hinge domain which would allow DNA loading into the ring. The kleisin and additional subunits could drive this ATP hydrolysis. In addition, as is the case in eukaryotic SMCs, the kleisin and additional subunits could make the difference in the various regulatory roles during different parts of the cell cycle. Post-translational modifications presumably have a similar role. This makes the regulation of SMC complexes in eukaryotes quite complex. To dissect the very basic mechanisms of SMC functioning it is therefore favorable to use a more simplistic system such as the prokaryotic SMC complexes. My previous work in *S. pneumoniae* showed that Smc is not essential under certain growth conditions in this organism (Minnen et al., 2011) suggesting that additional mechanisms play more pronounced roles in chromosome segregation in this organism. To understand the very basic mechanisms of functioning of SMC complexes it is therefore preferred to study an organism in which the SMC complex is essential under certain growth conditions. When the functionality of the complex and its growth phenotype are connected it facilitates an easier elucidation of the absolute essential basic mechanism to function. The Smc-ScpAB type of prokaryotic Smc complexes is most conserved between the eukaryotic and prokaryotic SMC complexes and widely studied in *B. subtilis*, therefore this was the organism of choice for this study.

It is clear that SMC complexes play roles in DNA segregation, organization and repair. To do so they must interact with chromosomes. Eukaryotic cohesin and condensin were suggested to topologically embrace DNA molecules and for a prokaryotic Smc complex it was shown to entrap chromosomes. The precise mechanism of SMC functioning in chromosome segregation is not well understood. In addition, it is not clear what the exact role of SMC in chromosome organization is and whether and how chromosome segregation and organization are interlinked. To investigate this it is pivotal to gain a deeper understanding of the specific chromosomal association of SMC. The first aim of this thesis was to study the initial recruitment of the Smc complex to the chromosome, and more specifically, the role of ATP hydrolysis in this process in more detail.

It is poorly understood how the distribution of SMC complexes is established and how this contributes to chromosome segregation. There is evidence that after initial loading of the SMC complex, the complex translocate to sites further away. The transcription machinery was suggested to aid SMC translocation along the chromosomes for yeast cohesin but it is unclear whether this is the only mode of translocation, whether this is a conserved feature and what the exact mechanism is. Therefore, to be able to investigate SMC translocation and its possible contribution to chromosome segregation in a simplistic system, the

second aim of this thesis was to gain insight into whether the Smc complex translocates on the chromosome in *B. subtilis*.

To gain a better comprehension of the specific chromosomal association of SMC it is important to understand precisely how it associates with the chromosome. Therefore the third aim of this thesis was to elucidate whether the Smc complex can hold chromosomal loci together in a prokaryote by using chromosome conformation capture derived methods.

ChIP-3C, ChIA-PET, genetics, colony formation assays, ChIP and fluorescence microscopy were used in this thesis work.

3. Material and methods

3.1 Strain generation

Genetic modifications were introduced via plasmid DNA through double cross over into the genome of *B. subtilis*. Plasmids were constructed using general cloning techniques or golden gate shuffling (Engler et al., 2009; Green & Sambrook, 2012) and checked by sequencing. *B. subtilis* cells were made competent by starvation as previously described (Bürmann et al., 2013), however slight modifications were made to transform 'sick' cells. From 5 ml overnight cultures in competence medium (SMM solution (15 mM ammonium sulfate, 80 mM dipotassium hydrogen phosphate, 44 mM potassium dihydrogen phosphate, 3.4 mM trisodium citrate, 0.8 mM magnesium sulfate, 6 g L^{-1} potassium hydrogen phosphate) supplemented with 5 g L^{-1} glucose, 20 mg L^{-1} tryptophan, 20 mg L^{-1} casamino acids, 6 mM magnesium sulfate and 110 mg L^{-1} feric ammonium citrate) 600, 900 or 1200 µl were diluted into 10 ml fresh competence medium for wild-type, Δ*smc* or *smc(E1118Q)* viable cells, respectively. Cells were grown for 3, 3.5 and 4 hours, respectively, at 37°C depending on their sickness and diluted 1:1 with prewarmed starvation medium (SMM supplemented with 5 g L^{-1} glucose and 6 mM magnesium sulfate) and grown for another 1, 1.5 or 2 hours depending on their sickness wild-type, Δ*smc* or *smc(E1118Q)*, respectively. DNA was added to 400 µl of cells, the cells were incubated at 37°C shaking for at least 2 hours. The longer the incubation with the DNA the greater the number of transformants obtained. *B. subtilis* strains were generated on SMG medium (SMM supplemented with 5 g L^{-1} glucose, 20 mg L^{-1} tryptophan, and 1 g L^{-1} glutamate) supplemented with 5 µg/ml chloramphenicol, 70 µg/ml spectinomycin, 10 µg/ml tetracycline or 0.4 µg/ml erythromycin with 10 µg/ml lincomycin when appropriate. Colonies were picked and streaked for single colonies and a single colony was patched to a fresh plate. Correct cell material was stored in 25% glycerol at -80°C. Strains were subsequently grown in the absence of antibiotics.

Table 1. *B. subtilis* **strains used**

Strain name	Genotype	Constructor
BSG1001	*1A700, trpC2*	Bacillus Genetic Stock Center
BSG1002	*1A700, smc ftsY::ermB, trpC2*	Stephan Gruber
BSG1007	*1A700, Δsmc ftsY::ermB, trpC2*	Stephan Gruber
BSG1008	*1A700, smc(E1118Q) ftsY::ermB, trpC2*	Stephan Gruber
BSG1016	*1A700, smc-TAP ftsY::ermB, trpC2*	Anita Minnen
BSG1017	*1A700, smc(Bacillus thuringiensis hinge) ftsY::ermB, trpC2*	Jens Stadler
BSG1018	*1A700, smc(Streptococcus pneumoniae hinge) ftsY::ermB, trpC2*	Jens Stadler
BSG1045	*1A700, smc(K37I) ftsY::ermB, trpC2*	Frank Bürmann
BSG1046	*1A700, smc(S1090R) ftsY::ermB, trpC2*	Frank Bürmann
BSG1047	*1A700, smc(D1117A) ftsY::ermB, trpC2*	Frank Bürmann
BSG1050	*1A700, ΔparB::kanR, trpC2*	Frank Bürmann

BSG1051	*1A700, smc ftsY::ermB, parAB::kanR, trpC2*	Frank Bürmann
BSG1052	*1A700, smc ftsY::ermB, ΔparB::kanR, trpC2*	Frank Bürmann
BSG1067	*1A700, smc-mGFPmut1 ftsY::ermB, trpC2*	Thomas Gerland
BSG1068	*1A700, smc(E1118Q)-mGFP1mut1 ftsY::ermB, trpC2*	Thomas Gerland
BSG1075	*1A700, smc(Pf Rad50 Zinc hook hinge M->D) ftsY::ermB, trpC2*	Stephan Gruber
BSG1083	*1A700, smc(R57A) ftsY::ermB, trpC2*	Frank Bürmann
BSG1095	*1A700, Δsmc ftsY::ermB, ΔamyE::smc(Pf Rad50 Zinc hook hinge M->D)::cat, trpC2*	Stephan Gruber
BSG1134	*1A700, smc-mGFP1mut1 ftsY::ermB, ΔamyE::smc(Pf Rad50 Zinc hook hinge M->D)::cat, trpC2*	Stephan Gruber
BSG1135	*1A700, smc(E1118Q)-mGFP1mut1 ftsY::ermB, ΔamyE::smc(Pf Rad50 Zinc hook hinge M->D)::cat, trpC2*	Stephan Gruber
BSG1378	*1A700, smc-mGFPmut1 ftsY::ermB, specR::ΔscpA scpB, trpC2*	Anita Minnen
BSG1387	*1A700, smc(E1118Q) ftsY::ermB, ΔparB::kanR, trpC2*	Anita Minnen
BSG1406	*1A700, smc(E1118Q) ftsY::ermB, parAB::kanR, trpC2*	Anita Minnen
BSG1413	*1A700, smc(E1118Q)-mGFP1mut1 ftsY::ermB, specR::ΔscpA scpB, trpC2*	Anita Minnen
BSG1469	*1A700, smc ftsY::ermB, ΔamyE::parS-359::cat, trpC2*	Anita Minnen
BSG1470	*1A700, smc ftsY::ermB, ΔamyE::mtparS-359::cat, trpC2*	Anita Minnen
BSG1471	*1A700, smc(E1118Q) ftsY::ermB, ΔamyE::parS-359::cat, trpC2*	Anita Minnen
BSG1475	*1A700, smc(E1118Q)-TAP ftsY::ermB, trpC2*	Anita Minnen
BSG1488	*1A700, smc(C119S, C437S, C826S, C1114S, K1151C, E1118Q)-TEV-His12-HaloTag(C61V, C262A) ftsY::ermB, trpC2*	Frank Bürmann
BSG1512	*1A700, smc(C119S, C437S, C826S, C1114S, K1151C, E1118Q)-TEV-His12-HaloTag(C61V, C262A) ftsY::ermB, specR::ΔscpA scpB, trpC2*	Frank Bürmann
BSG1518	*1A700, smc-TAP ftsY::ermB, specR::scpAB, trpC2*	Anita Minnen
BSG1520	*1A700, smc(E1118Q)-TAP ftsY::ermB, specR::ΔscpA, trpC2*	Anita Minnen
BSG1521	*1A700, smc(E1118Q)-TAP ftsY::ermB, specR::scpAB trpC2*	Anita Minnen
BSG1541	*1A700, smc(E1118Q) ftsY::ermB, ΔamyE::parS-355::cat, trpC2*	Anita Minnen
BSG1542	*1A700, smc(E1118Q) ftsY::ermB, ΔamyE::parS-354::cat, trpC2*	Anita Minnen
BSG1543	*1A700, smc(E1118Q) ftsY::ermB, ΔamyE::parS-90::cat, trpC2*	Anita Minnen
BSG1544	*1A700, smc(E1118Q) ftsY::ermB, ΔamyE::parS-optimal::cat, trpC2*	Anita Minnen
BSG1547	*1A700, smc(G657A, G658A, G662A, G663A, E1118Q)-ftsY::ermB, trpC2*	Anna Anchimiuk
BSG1592	*1A700, smc(T.m. Hinge, L-E version) ftsY::ermB, trpC2*	Anita Minnen
BSG1598	*1A700, smc(C119S, C437S, G657A, G658A, G662A, G663A, C826S, C1114S, E1118Q, K1151C)-TEV-His12-HaloTag(C61V, C262A) ftsY::ermB, trpC2*	Frank Bürmann
BSG1604	*1A700, smc(T.m. Hinge, L-E version (E1118Q) ftsY::ermB, trpC2*	Anita Minnen
BSG1619	*1A700, smc(1-499 GGGSGGGSGGG 674-1186, E1118Q) ftsY::ermB, trpC2*	Anita Minnen
BSG1620	*1A700, smc(G657A, G658A, G662A, G663A, E1118Q)-ftsY::ermB, specR::ΔscpA, trpC2*	Anita Minnen
BSG1621	*1A700, smc(G657A, G658A, G662A, G663A, E1118Q)-ftsY::ermB, specR::scpAB, trpC2*	Anita Minnen
BSG1623	*1A700, smc(G657A, G658A, G662A, G663A) ftsY::ermB, specR::ΔscpA, trpC2*	Anita Minnen
BSG1624	*1A700, smc(G657A, G658A, G662A, G663A) ftsY::ermB, specR::scpAB, trpC2*	Anita Minnen
BSG1626	*1A700, smc(1-499 GGGSGGGSGGG 674-1186) ftsY::ermB, trpC2*	Anita Minnen
BSG1662	*1A700, smc(G657A, G658A, G662A, G663A, E1118Q)-mGFP-ftsY::ermB, trpC2*	Verena Kuttenberger

BSG1671	*1A700, smc(G657A, G658A, G662A, G663A, E1118Q)-TAP-ftsY::ermB, specR::scpAB, trpC2*	Anita Minnen
BSG1672	*1A700, smc(G657A, G658A, G662A, G663A)-TAP ftsY::ermB, specR::ΔscpA, trpC2*	Anita Minnen
BSG1677	*1A700, smc(G657A, G658A, G662A, G663A)-mGFP-ftsY::ermB, trpC2*	Verena Kuttenberger
BSG1687	*1A700, smc(T.m. Hinge, IE-KH version E1118Q) ftsY::ermB, trpC2*	Anita Minnen
BSG1688	*1A700, smc(T.m. Hinge, L-E version, S535N) ftsY::ermB, trpC2*	Anita Minnen
BSG1689	*1A700, smc(G657A, G658A, G662A, G663A, E1118Q)-TAP ftsY::ermB, specR::ΔscpA, trpC2*	Anita Minnen
BSG1690	*1A700, smc(G657A, G658A, G662A, G663A, E1118Q)-TAP ftsY::ermB, specR::scpA ΔscpB, trpC2*	Anita Minnen
BSG1691	*1A700, smc(G657A, G658A, G662A, G663A)-TAP ftsY::ermB, specR::scpAB, trpC2*	Anita Minnen
BSG1692	*1A700, smc(C119S, C437S, R643C, C826S, C1114S)-TEV-His12-HaloTag(C61V, C262A) ftsY::ermB, trpC2*	Frank Bürmann
BSG1694	*1A700, smc(C119S, C437S, R643C, C826S, C1114S, E1118Q)-TEV-His12-HaloTag(C61V, C262A) ftsY::ermB, trpC2*	Frank Bürmann
BSG1779	*1A700, smc(1-499 GGGSGGGSGGG 674-1186, E1118Q)-TAP::ermB, specR::ΔscpA, trpC2*	Anita Minnen
BSG1780	*1A700, smc(1-499 GGGSGGGSGGG 674-1186, E1118Q)-TAP::ermB, specR::scpAB, trpC2*	Anita Minnen
BSG1791	*1A700, smc(C119S, C437S, G657A, G658A, G662A, G663A, C826S, C1114S, E1118Q, K1151C)-TEV-His12-HaloTag(C61V, C262A) ftsY::ermB, specR::ΔscpA, trpC2*	Frank Bürmann
BSG1798	*1A700, smc(G657A, G658A, G662A, G663A, E1118Q)-mGFP-ftsY::ermB, specR::ΔscpA, trpC2*	Anita Minnen
BSG1799	*1A700, smc(G657A, G658A, G662A, G663A)-mGFP-ftsY::ermB, specR::ΔscpA, trpC2*	Anita Minnen
BSG1824	*1A700, smc(1-199 GGGSGGGSGGG 999-1186, E1118Q)-TAP::ermB, specR::ΔscpA, trpC2*	Anita Minnen
BSG1825	*1A700, smc(1-219 GPG 983-1186, E1118Q)-TAP::ermB, specR::ΔscpA, trpC2*	Anita Minnen
BSG1826	*1A700, smc(1-243 GGGSGGGSGGG 957-1186, E1118Q)-TAP::ermB, specR::ΔscpA, trpC2*	Anita Minnen
BSG1827	*1A700, smc(1-243 GGGSGGGSGGG 943-1186, E1118Q)-TAP::ermB, specR::ΔscpA, trpC2*	Anita Minnen
BSG1828	*1A700, smc(1-261 GGGSGGGSGGG 943-1186, E1118Q)-TAP::ermB, specR::ΔscpA, trpC2*	Anita Minnen
BSG1829	*1A700, smc(1-261 GGGSGGGSGGG 912-1186, E1118Q)-TAP::ermB, specR::ΔscpA, trpC2*	Anita Minnen
BSG1830	*1A700, smc(1-277 GGGSGGGSGGG 922-1186, E1118Q)-TAP::ermB, specR::ΔscpA, trpC2*	Anita Minnen
BSG1836	*1A700, smc(C119S, C437S, 494-GGSGG, R643C, 678-GGSGG, C826S, C1114S, E1118Q)-TEV-His12-HaloTag(C61V, C262A) ftsY::ermB, trpC2*	Frank Bürmann
BSG1837	*1A700, smc(C119S, C437S, 494-GGSGGSGG, R643C, 678-GGSGGSGG, C826S, C1114S, E1118Q)-TEV-His12-HaloTag(C61V, C262A) ftsY::ermB, trpC2*	Frank Bürmann
BSG1838	*1A700, smc(C119S, C437S, 494-GGSGGSGGSGG, R643C, 678-GGSGGSGGSGG, C826S, C1114S, E1118Q)-TEV-His12-HaloTag(C61V, C262A) ftsY::ermB, trpC2*	Frank Bürmann
BSG1839	*1A700, smc(C119S, C437S, R643C, G657A, G658A, G662A, G663A, C826S, C1114S, E1118Q)-TEV-His12-HaloTag(C61V, C262A) ftsY::ermB, trpC2*	Frank Bürmann
BSG1852	*1A700, smc(C119S, C437S, 494-GGSGG, R643C, 678-GGSGG, C826S, C1114S)-TEV-His12-HaloTag(C61V, C262A) ftsY::ermB, trpC2*	Frank Bürmann
BSG1853	*1A700, smc(C119S, C437S, 494-GGSGGSGG, R643C, 678-GGSGGSGG, C826S, C1114S)-TEV-His12-HaloTag(C61V, C262A) ftsY::ermB, trpC2*	Frank Bürmann
BSG1854	*1A700, smc(C119S, C437S, 494-GGSGGSGGSGG, R643C, 678-GGSGGSGGSGG, C826S, C1114S)-TEV-His12-HaloTag(C61V, C262A) ftsY::ermB, trpC2*	Frank Bürmann
BSG1855	*1A700, smc(K37I)-mGFP1mut1 ftsY::ermB, trpC2*	Anita Minnen
BSG1856	*1A700, smc(S1090R)-mGFP1mut1 ftsY::ermB, trpC2*	Anita Minnen
BSG1857	*1A700, smc(D1117A)-mGFP1mut1 ftsY::ermB, trpC2*	Anita Minnen

BSG1871	*1A700, smc(1-468 GGGSGGGSGGG 705-1186, E1118Q)-TAP::ermB, specR::ΔscpA, trpC2*	Anita Minnen
BSG1872	*1A700, smc(1-437 GGGSGGGSGGG 736-1186, E1118Q)-TAP::ermB, specR::ΔscpA, trpC2*	Anita Minnen
BSG1873	*1A700, smc(1-315 GGGSGGGSGGG 858-1186, E1118Q)-TAP::ermB, specR::ΔscpA, trpC2*	Anita Minnen
BSG1874	*1A700, smc(1-370 GGGSGGGSGGG 803-1186, E1118Q)-TAP::ermB, specR::ΔscpA, trpC2*	Anita Minnen
BSG1875	*1A700, smc(1-414 GGGSGGGSGGG 785-1186, E1118Q)-TAP::ermB, specR::ΔscpA, trpC2*	Anita Minnen
BSG1876	*1A700, smc(1-261 GGGSGGGSGGG 912-1186, V929S R933E V936S E1118Q)-TAP::ermB, specR::ΔscpA, trpC2*	Anita Minnen
BSG1877	*1A700, smc(1-261 GGGSGGGSGGG 912-1186, V929D R933E V936D E1118Q)-TAP::ermB, specR::ΔscpA, trpC2*	Anita Minnen
BSG1881	*1A700, smc(R57A)-mGFP1mut1 ftsY::ermB, trpC2*	Anita Minnen
BSG1888	*1A700, smc(Pf Smc hinge insert) ftsY::specR, trpC2*	Stephan Gruber
BSG1889	*1A700, smc ftsY::ermB, specR::ΔscpA scpB, trpC2*	Anita Minnen
BSG1890	*1A700, smc ftsY::ermB, specR::scpAB scpB, trpC2*	Anita Minnen
BSG1891	*1A700, smc ftsY::ermB, specR::scpA ΔscpB, trpC2*	Anita Minnen
BSG1892	*1A700, smc(E1118Q) ftsY::ermB, specR::ΔscpA scpB, trpC2*	Anita Minnen
BSG1893	*1A700, smc(E1118Q) ftsY::ermB, specR::scpAB, trpC2*	Anita Minnen
BSG1894	*1A700, smc(E1118Q) ftsY::ermB, specR::scpA ΔscpB, trpC2*	Anita Minnen
BSG1895	*1A700, smc(1-499 GGGSGGGSGGG 674-1186)-TAP ftsY::ermB, specR::ΔscpA scpB, trpC2*	Anita Minnen
BSG1896	*1A700, smc(1-499 GGGSGGGSGGG 674-1186)-TAP ftsY::ermB, specR::scpA scpB, trpC2*	Anita Minnen
BSG1900	*1A700,smc(Pf Smc hinge insert)(E1118Q) ftsY::ermB, trpC2*	Anita Minnen
BSG1922	*1A700, smc(C119S, C437S, A715C, C826S, C1114S, E1118Q)-TEV-His12-HaloTag(C61V, C262A) ftsY::ermB, trpC2*	Frank Bürmann
BSG1924	*1A700, smc(C119S, C437S, G657A, G658A, G662A, G663A, A715C, C826S, C1114S, E1118Q)-TEV-His12-HaloTag(C61V, C262A) ftsY::ermB, trpC2*	Frank Bürmann
BSG1943	*1A700, smc ftsY::ermB, parB(G77S)::kanR, trpC2*	Anita Minnen
BSG1944	*1A700, smc ftsY::ermB, parB(R80A)::kanR, trpC2*	Anita Minnen
BSG1950	*1A700, smc(C119S, C437S, A715C, C826S, C1114S, E1118Q)-TEV-His12-HaloTag(C61V, C262A) ftsY::ermB, specR::ΔscpA, scpB, trpC2*	Frank Bürmann
BSG1955	*1A700, smc(1-588)-SGSG-Pfhinge-SGSG-smc(589-1186) ftsY::ermB, trpC2*	Anita Minnen
BSG1956	*1A700, smc(1-588)-GGGSGGGSGGG-Pfhinge-GGGSGGGSGGG-Smc(589-1186) ftsY::ermB, trpC2*	Anita Minnen
BSG1958	*1A700, smc(1-588)-GGGSGGGS-Pfhinge-SGGGSGGG-smc(589-1186) ftsY::ermB, trpC2*	Anita Minnen
BSG1959	*1A700, smc(1-588)-SSGGSGSGSGSGSGGSS-Pfhinge-SSGSGSGSTSGGSGSGS-smc(589-1186) ftsY::ermB, trpC2*	Anita Minnen
BSG1972	*1A700, smc(G657A, G658A, G662A, G663A, E1118Q)-ftsY::ermB, parB(G77S)::kanR, trpC2*	Anita Minnen
BSG1973	*1A700, smc(G657A, G658A, G662A, G663A, E1118Q)-ftsY::ermB, parB(R80A)::kanR, trpC2*	Anita Minnen
BSG1974	*1A700, smc(G657A, G658A, G662A, G663A, E1118Q)-ftsY::ermB, parAB::kanR, trpC2*	Anita Minnen
BSG1975	*1A700, smc(1-588)-SGSG-Pfhinge(S646A, G647A, G651A, G652A)-SGSG-smc(589-1186) ftsY::ermB, trpC2*	Anita Minnen
BSG1976	*1A700, smc(1-588)-GGGSGGGS-Pfhinge(S646A, G647A, G651A, G652A)-SGGGSGGG-smc(589-1186) ftsY::ermB, trpC2*	Anita Minnen
BSG1977	*1A700, smc(1-588)-GGGSGGGSGGG-Pfhinge(S646A, G647A, G651A, G652A)-GGGSGGGSGGG-Smc(589-1186) ftsY::ermB, trpC2*	Anita Minnen

BSG1978	*1A700, smc(1-588)-SSGGSGSGSGSGSGGGSS-Pfhinge(S646A, G647A, G651A, G652A)-SSGSGSGSTSGGSGSGS-smc(589-1186) ftsY::ermB, trpC2*	Anita Minnen
BSG1981	*1A700, smc(1-588)-SGSG-Pfhinge-SGSG-smc(589-1186 E1118Q) ftsY::specR, trpC2*	Anita Minnen
BSG1982	*1A700, smc(1-588)-GGGSGGGS-Pfhinge-SGGGSGGG-smc(589-1186) ftsY::specR, trpC2*	Anita Minnen
BSG1983	*1A700, smc(1-588)-GGGSGGGS-Pfhinge-SGGGSGGG-smc(589-1186 E1118Q) ftsY::specR, trpC2*	Anita Minnen
BSG1984	*1A700, smc(1-588)-GGGSGGGSGGG-Pfhinge-GGGSGGGSGGG-Smc(589-1186) ftsY::specR, trpC2*	Anita Minnen
BSG1985	*1A700, smc(1-588)-GGGSGGGSGGG-Pfhinge-GGGSGGGSGGG-Smc(589-1186 E1118Q) ftsY::specR, trpC2*	Anita Minnen
BSG1986	*1A700, smc(1-588)-SSGGSGSGSGSGSGGGSS-Pfhinge-SSGSGSGSTSGGSGSGS-smc(589-1186) ftsY::specR, trpC2*	Anita Minnen
BSG1987	*1A700, smc(1-588)-SSGGSGSGSGSGSGGGSS-Pfhinge-SSGSGSGSTSGGSGSGS-smc(589-1186 E1118Q) ftsY::specR, trpC2*	Anita Minnen
BSG1996	*1A700, smc(Pf Rad50 Zinc hook hinge M->D) ftsY::ermB, ΔamyE::parS-359::cat, trpC2*	Anita Minnen
BSG1997	*1A700, smc(Pf Rad50 Zinc hook hinge M->D) ftsY::ermB, ΔamyE::mtparS-359::cat, trpC2*	Anita Minnen
BSG1998	*1A700, smc(T.m. Hinge, L-E version) ftsY::ermB, ΔamyE::parS-359::cat, trpC2*	Anita Minnen
BSG1999	*1A700, smc(T.m. Hinge, L-E version) ftsY::ermB, ΔamyE::mtparS-359::cat, trpC2*	Anita Minnen
BSG2000	*1A700, smc(T.m. Hinge, L-E version, S535N) ftsY::ermB, ΔamyE::parS-359::cat, trpC2*	Anita Minnen
BSG2001	*1A700, smc(T.m. Hinge, L-E version, S535N) ftsY::ermB, ΔamyE::mtparS-359 ::cat, trpC2*	Anita Minnen
BSG2036	*1A700, smc(C119S, C437S, G657A, G658A, G662A, G663A, A715C, C826S, C1114S, E1118Q)-TEV-His12-HaloTag(C61V, C262A) ftsY::ermB, specR::ΔscpA scpB, trpC2*	Frank Bürmann
BSG2050	*1A700, smc(K37I, E1118Q) ftsY::ermB, trpC2*	Anita Minnen
BSG2051	*1A700, smc(S1090R, E1118Q) ftsY::ermB, trpC2*	Anita Minnen

3.2 Antibodies used

α-ScpB antiserum was generated in rabbit and available in the lab at the start of this work. α-Smc antiserum and α-ParB antiserum were generated in rabbit during this thesis work (but were not part of the work) and tested for this thesis work by ChIP experiments. α-GFP was purchased from Life Technologies, A6455. Rabbit IgG was purchased from Sigma, I5006. Peroxidase Anti-Peroxidase was available in aliquots in the lab.

3.3 Western blots

Overnight cultures in SMG medium were diluted to an OD of 0.005 and grown to an OD of 0.02-0.03, resuspended in 2 ml PBSG (PBS + 0.1% glycerol) and washed once. The OD was measured and the amount of cells for an OD of 0.02 for all samples was taken. Cells were resuspended in PBSG, ß-mercaptoethanol was added to a final concentration of 28.6 mM and kept on ice for 3 min. Ready lyse lysozyme (Epicentre) (12.8U/µl final), *Roche Complete* protease inhibitor cocktail and Benzonase (1:625 final from Sigma) were added and the samples were incubated at 37°C for 20 min. After addition of NuPage LDS loading dye (final 1x) and DTT (final 100 mM) the samples were incubated at 70°C for 10 min. The extracts were loaded on a 4-12% NuPAGE Bis-Tris gel (Invitrogen) and run in MOPS buffer for 50 min at

200 V. Proteins were transferred to a PVDF membrane via a semi-dry method, the membrane was treated with α-Smc, α-GFP or Peroxidase Anti-Peroxidase (PAP). α-Smc and α-GFP blots were treated with ECL Anti-rabbit IgG, HRP-linked whole antibody (from donkey) (GE Healthcare). The blots were incubated with Supersignal west Femto (Thermo Scientific) and were imaged in a LAS 4000 scanner.

3.4 Colony formation assay

Cells were grown in 250 µl SMG medium overnight into stationary phase, diluted 81-fold and 59049-fold and 5 µl was spotted on nutrient agar plates (Oxoid) and 7.5 µl on SMG agar plates. Plates were incubated at 37°C for ~14 hr on NA or ~38 hr on SMG agar or as specified in the figures.

3.5 Microscopy

Overnight cultures in SMG medium were diluted to an OD of 0.005 and grown to OD 0.02-0.03 in SMG medium. Cells were mounted on agarose pads and visualized on an APPLIED PRECISION (Issaquah, WA, USA) DeltaVision Elite system equipped with an OLYMPUS (Tokyo, Japan) IX-71 inverted base microscope, an OLYMPUS UPlanSApo 100x/NA1.40 oil immersion objective and a PCO (Romulus, Michigan, USA) pco.edge gold 5.5 deep cooled CMOS camera at the Imaging Facility of the Max Planck Institute of Biochemistry, Martinsried.
Images were all modified equally using Fiji (Schindelin et al., 2012).

3.6 Chromatin immuno-precipitation (ChIP) and qPCR

ChIP was performed by modification of a previously described protocol (Gruber & Errington, 2009).
Cells were grown in SMG medium at 37ºC overnight and diluted to OD 0.005 in 400 ml SMG. At OD 0.02-0.03, 40 ml of fixing solution (50mM Tris/HCl pH 8.0, 100mM NaCl, 1mM EDTA, 0.5mM EGTA, 11% formaldehyde) was added and incubated at room temperature for 30 minutes. Cells were harvested using filtering and washed in 2 ml ice-cold PBS and the OD was measured. Cells were resuspended in 1 ml TESS (50mM Tris/HCl 7.4, 10mM EDTA, 50mM NaCl, 500mM sucrose) and protoplasted by incubating in 1 ml TESS supplemented with 20mg/ml lysozyme (Sigma) and Roche Complete protease inhibitor cocktail for 30 min at 37°C with shaking. Cells were washed once more in 1 ml TESS, aliquoted according to the previously measured OD and stored at -80°C.
One aliquot of fixed cells was resuspended in 2 ml lysis buffer (50mM Hepes/KOH pH 7.5, 140mM NaCl, 1mM EDTA, 1% (v/v) Triton X-100, 0.1% (w/v) sodium deoxycholate, 100mg/ml RNase, *Roche Complete* protease inhibitor cocktail) and transferred to a 5 ml round-bottom tube. The samples were sonicated 3 x 20 sec on a Bandelin Sonoplus with a MS-72 tip at 90% pulse and 35% power outlet. Lysates were transferred into 2 ml tubes and centrifuged 5 min, 21000g at 4°C. The supernatant was subsequently centrifuged at 21000g for 10 min at 4°C.
200 µl of the cleared lysates was kept separate as the input sample. 50 µl Protein G coupled DynaBead (Invitrogen) were incubated with 50 µl antibody serum (α-Smc, α-ScpB or α-ParB) or 2.5 µl α-GFP

antibodies for at least 1 hr rotating at 4°C. Beads were washed in lysis buffer and added to 800 µl of the cleared lysates. For experiments involving TAP-tagged strains, rabbit IgG coupled to 50 µl magnetic Dynabeads (prepared according to the manufacturer's protocol) was added to 800 µl cleared lysate. The beads with cleared lysate were incubated at 4°C rotating for 2-4 hours. Beads were washed once with each of the following buffers: lysis buffer, lysis buffer with high salt (500mM NaCl) and wash buffer (10mM Tris/HCl pH 8.0, 250mM LiCl, 1mM EDTA, 0.5% (w/v) NP-40, 0.5% (w/v) sodium deoxycholate). Beads were resuspended in 520 µl TES (50mM Tris/HCl pH 8.0, 10mM EDTA, 1% SDS) and the input samples were combined with 300 µl TES and 20 µl 10% SDS solution and incubated overnight at 65°C shaking. DNA was purified by phenol chloroform extraction and ethanol precipitation. The DNA was dissolved in 100µl TE at 65°C for 20 min and purified on a Qiagen PCR purification column and eluted in 30 µl EB.

For qPCR 4 µl of the input DNA (diluted 1:200) and IP samples (diluted 1:20) was used in a 10 µl reaction using 5 µl Takyon no ROX SYBR Mastermix blue dTTP (Eurogentec) and 1 µl primer pair stock solution (3 µM each primer) (Table 2) on a Qiagen Roto-Gene Q in a 72 well rotor according to manufacturer's instructions. CT values were calculated using the Real-time PCR miner software (http://ewindup.info) (Zhao & Fernald, 2005) and averaged between duplicates. IP efficiencies were calculated as follows: ((IP/input)*100) for each primer pair.

3.7 ChIP-seq

Samples were prepared as described above with the exception that several IP samples were loaded onto the same PCR purification column to obtain sufficient DNA. 1-5 ng of IP DNA and 250-400 ng of input DNA were sequenced on a HiSeq2500 (Illumina) with 100 bps single reads at the Max Planck Genome Centre in Cologne (http://mpgc.mpipz.mpg.de/home/). The obtained reads (1 – 5 million) were mapped to the corresponding genomes with Bowtie on the Galaxy platform (http://galaxyproject.org/) using default settings. Subsequent analysis was performed using SeqMonk version 0.27.0 (http://www.bioinformatics.babraham.ac.uk/projects/seqmonk/). For comparisons between different strains, the number of reads were normalized to the largest dataset. For genome-wide overviews, the reads were counted in 5000 bp windows every 5000 bps, for detailed regions the reads were counted in 1000 bp windows every 100 bps. The number of reads in a windows for the IP sample was always divided by the number of reads of the corresponding window of the input sample. Graphs were plotted in Microsoft Excel and modified in Adobe Illustrator.

3.8 ChIP-3C

The ChIP procedure described above was used up to and including the final wash step of the beads with the wash buffer with the exception that sonication took place 2x 20sec instead of 3x 20 sec. Beads were subsequently washed once in 500 µl digestion buffer (1x NEB digestion buffer 2 and 0.5% Triton X-100) and subsequently resuspended in 530 µl digestion buffer with 2000 Units *Hind*III and kept at 37°C for 2 hours shaking 900 rpm. Beads were washed once in 500 µl digestion buffer and subsequently washed in

200 µl ligation buffer (1x T4 DNA ligation buffer, 0.5% Triton X-100, 2 µg Bovine Serum Albumin (BSA)). Finally the beads were resuspended in 693 µl ligation buffer with 10 Units T4 DNA ligase and kept at 16°C shaking 1000 rpm O/N. Next, 250 µg of proteinase K, 42.5 µl of 1M Tris pH 8.0, 17.0 µl 0.5M EDTA and 85.0 µl 10% SDS was added and incubated at 65°C at 1400 rpm O/N. The supernatant was collected and purified as described in Chapter 3.6. qPCR was performed using FAST qPCR mastermix Plus-dTTP-NoROX (Eurogentec) with 100nM of Taqman probe, 50nM of each primer (Table 2), 10-fold diluted IP DNA and 100-fold diluted input DNA in a 15 µl reaction.

Table 2. Overview of qPCR primers

locus	Primer name	Sequence 5' – 3'
For Sybr green qPCR		
parS-359	STG097	aaaaagtgattgcggagcag
	STG098	agaaccgcatctttcacagg
yocGH	STG099	tccatatcctcgctcctacg
	STG100	attctgctgatgtgcaatgg
dnaA	STG199	gatcaatcggggaaagtgtg
	STG200	gtagggcctgtggatttgtg
parS-356	STG236	tgaaaagaatgcccatcaca
	STG237	tgcaagcaacaacccttttac
soj	STG238	tttccctgcggatcaatatc
	STG239	tgacatcgtgggaaaaatca
parS-4	STG250	ttcgtcgaacacctttgtg
	STG251	tttgcccgttcaataacctc
dnaN	STG252	gaattccttcaggccattga
	STG253	gatttctggcgaattggaag
cheC	STG396	tttgcatgaactgggcaata
	STG397	tccgaacatgtccaatgaga
parS-355	STG493	taattcatcatcgcgctcaa
	STG494	aatgccgattacgagtttgc
parS-354	STG495	ttgcagctaactgccatttg
	STG496	aaaactgaacaggggtcacg
trnS	STG598	atttgtcttttgcgggtgt
	STG599	acagatttgcgtgcactttg
noc	STH597	gcatgcgcttcctcaatag
	STH598	aggtgaaagacgctggagag
gidB	STH599	tccacgattgtgacatggag
	STH600	tgtcgacttcaatcaggtgaac
gidA	STH601	agaaggctgctggttattcg
	STH602	ttatcgtgcgaaagcagttg
spoIIIJ	STH605	gcatcgctttcgaacttctc

	STH606	gggagataactacgggctttc
non-endogenous sequences integrated at amyE	STH672	agagacaggtggtccctatcag
	STH673	gggacaggaccatattgagg
For Taqman qPCR		
parS-359 fw	STH540	gttggcgaacattgagctg
noc rv	STH541	aagcgcatgcttatgctagg
gidB rv	STH542	tcgtggattcactaaacaaacg
gidA rv	STH543	cgtatcattcttggcgatctg
trnE rv	STH544	atgtcccgatcgacatgg
dnaA rv	STH545	ccgatcgcatgcattaag
dnaN rv	STH546	ttctgacaggaaggataagctg
probe at parS-359 5'FAM 3'TAMRA	STH582	tccgcaatcactttttgtaccagcg
parS-4 rv	STH593	tctgcctctaaacgagggaac
parS-354 rv	STH594	aaggcgtctacacccatcac
parS-355 rv	STH595	gatgaagggatcggcattc
parS-356 rv	STH596	aggaataaggtgaagtgaacatgag
jag rv	STH603	ggtggatgcagaaaactatcg
spoIIIJ rv	STH604	tcgtttattaattttaccgctgatg

3.9 Chromatin Interaction Analysis using Paired End Tag sequencing (ChIA-PET)

The following protocol is based to a large extent on (Fullwood et al., 2010) and modified for *B. subtilis.* Sequences of the linkers and adapters were identical to the ones described, and preparation of linkers, adapters and primers was performed exactly as described (Fullwood et al., 2010). In addition, a linker D was designed which consists of two half linkers: GGCCGCGAT*AT**TCAT**TCCAAC and GTTGGA**ATGA**ATATCGC, a biotin label was present on T*, the bold four bases indicate the index. *B. subtilis* cells were fixed and sonicated as described in chapter 3.6. The beads were washed according to the protocol described in chapter 3.6. The beads of five IP samples were combined and washed in 1 ml ice-cold TE pH 8.0 and subsequently resuspended in 1 ml ice-cold TE pH 8.0. To check whether the initial ChIP was successful, 100 µl of the beads was kept to purify and analyzed as described in chapter 3.6. The remaining 900 µl of beads was split into two equal aliquots. Blunt ending of the DNA: The beads in each tube were resuspended in 70 µl 10× T4 DNA polymerase buffer, 7 µl 10 mM dNTP mix, 615.8 µl nuclease-free water and 7.2 µl 9.7 U/µl T4 DNA polymerase (Promega, M4215) and incubated at 37°C for 20 min shaking at 1100 rpm. Ligation of biotinylated half-linkers to ChIP-DNA: The beads were washed three times in 1 ml ice-cold wash buffer (10 mM Tris pH 7.5, 1 mM EDTA, 500 mM sodium chloride), the beads were pelleted and the following reagents were added one by one: 786 µl $_{dd}H_2O$, 10 µl 200 ng/µl biotinylated half-linker (A or B), 200 µl 5x T4 DNA ligase buffer with PEG (Invitrogen 46300018) and 4 µl 30 U/µl T4 DNA ligase (Fermentas EL0013). The beads were incubated at 16°C on a turning wheel overnight. Addition of

phosphate groups to 5'ends: The contents of the two tubes were combined and the beads were washed three times in ice cold wash buffer and resuspended in 900 µl 1x T4 DNA ligase buffer (no PEG) with 200 Units T4 DNA polynucleotide kinase (NEB M0201s). This reaction was incubated at 37°C for 30 min shaking at 1100 rpm. Proximity ligation of the DNA fragments on the beads: The beads were pelleted and resuspended in 2 ml 1x T4 DNA ligase buffer (no PEG) with 200 Units T4 DNA ligase and kept at 22°C on a turning wheel for 20 hours. Reversion of cross-links and purification of the DNA: Beads were collected and 1510.8 µl of supernatant was removed. The remaining 489.2 µl was combined with 176 µg Proteinase K, 50mM Tris/HCl pH 8.0, 10mM EDTA and 1% SDS in a final volume of 600 µl and incubated overnight with shaking at 1400 rpm at 65°C. The beads were pelleted and the supernatant transferred to a 2 ml phase lock gel tube (Eppendorf) and the DNA was purified using phenol chloroform extraction followed by ethanol precipitation. The pellet was resuspended in 100 µl TE pH 8.0 and DNA was further purified on a Qiagen PCR purification column and eluted in 34 µl Elution Buffer (EB). *Mme*I digestion: The DNA in 34 µl EB was combined with 5 µl 10x NEBuffer 4, 5 µl 500 µM SAM, 5 µl 200 ng/µl nonbiotinylated linker and 1 µl 2U/µl MmeI (NEB) and incubated at 37°C for 2 hours without rotation. Immobilization of ChIA-PETs on Dynabeads: 50 µl of resuspended Dynabeads (M-280 Streptavidin, Invitrogen) were transferred to a 1.5 ml Eppendorf LoBind tube, washed twice in 150 µl 2x B&W buffer (10 mM Tris pH 7.5, 1 mM EDTA pH 8.0, 2 M sodium chloride) and resuspended in 50 µl 2x B&W buffer. The 50 µl digested DNA from the previous step was added and mixed well. The beads were kept at 22°C for 30 min at 1100 rpm. The supernatant was removed and the beads were washed twice in 1x B&W buffer (5 mM Tris pH 7.5, 0.5 mM EDTA pH 8.0, 1 M sodium chloride). Ligation of the sequencing adapters: To the pelleted beads a premix of 5 µl 10x T4 DNA ligase buffer, 8 µl 200 ng/µl Adapter A, 8 µl 200 ng/µl Adapter B and 28 µl $_{dd}$H$_2$O was added followed by 1 µl 30 U/µl T4 DNA ligase. The beads were incubated at 22°C on a turning wheel overnight. Nick translation: The beads were washed twice with 150 µl 1x B&W buffer and a premix of 5 µl 10x NEBuffer 2, 2.5 µl 10 mM dNTPs, 38.5 µl $_{dd}$H$_2$O and 4 µl 10 U/µl *E. coli* DNA polymerase I (NEB) was added and incubated at 22°C for 2 hours at 1100 rpm. PCR amplification of the ChIA-PETs: The beads were washed twice in 150 µl 1x B&W buffer, resuspended in 50 µl EB and transferred to a fresh 1.5 ml LoBind tube and stored at -20°C. For PCR, 2 µl of the beads were used in a 25 µl reaction using Phire Hot Start II DNA Polymerase (Thermo Scientific) for 25 cycles. The short primers with five random nucleotides at the 5'end used for amplifying the library had the following name and sequence: STH721 NNNNNCCCTCCCTGTCTCAG and STH722 NNNNNTGTTGCGTGTCTCAG. The primers with five random nucleotides and the Illumina adapters to be used on the 454 adapters libraries had the following name and sequence: STH944 CAAGCAGAAGACGGCATACGAGATCGTGATGTGACTGGA GTTCAGACGTGTGCTCTTCCGATCTNNNNNCCCTCCCTGTCTCAG and STH945 AATGATACGGCG ACCACCGAGATCTACACTCTTTCCCTACACGACGCTCTTCCGATCTNNNNNTGTTGCGTGTCTCAG.

The PCR reactions were loaded onto a 6% TBE PAGE gel and visualized with ethidium bromide. The fragments of the correct size were excised from the gel and transferred to a 0.6 ml centrifuge tube that was pierced with a needle in the bottom prior to use. The tube was placed inside a 1.5 ml tube and centrifuged

for 5 min at 4°C at maximum speed. To the gel pieces collected in the 1.5 ml tube 200 µl TE pH 8.0 was added, frozen at -80°C for at least 1 hour and incubated at 37°C O/N. The gel pieces and the buffer were transferred to a Corning Costar Spin-X 0.45 µm column and centrifuged for 10 min at 4°C at maximum speed. The tube was rinsed with another 200 µl TE pH 8.0 and added to the Spin-X column which was subsequently centrifuged for another 10 min at 4°C at maximum speed. The flow through was collected and isopropanol precipitation was performed. The pellet was resuspended in 100 µl TE pH 8.0, Qiagen PCR purification column purified and eluted in 30 µl EB. This solution was subsequently used for cloning into the blunt end cloning vector pJET1.2 (Life technologies), for PCR amplification or pooled for high throughput sequence 100 bps Single End (SE) on an Illumina HiSeq 2000 at GATC Biotech, Constance, Germany.

3.9.1 Modifications for proximity ligation in solution in a larger volume

For ligation in solution the total volume for blunt ending of the DNA and ligation of biotinylated half-linkers to ChIP-DNA was 700 µl. The proximity ligation step was replaced by the following steps: The beads were pelleted, resuspended in 200 µl TE with 1% SDS and incubated at 37°C for 30 min with rotation. The eluate was transferred to a fresh tube and the beads were washed once with 900 µl EB which was subsequently added to the initial eluate. The solution was transferred to a Spin-X column and spun for 1 min at 16, 1100 g at room temperature. The SDS was sequestered by adding 90 µl of 20% Triton X-100 which was incubated at 37°C for 1 hour. The DNA fragments were proximity ligated by adding 7776 µl $_{dd}$H$_2$O, 1000 µl $_{dd}$H$_2$O 10x T4 DNA ligase buffer and 33.33 µl 30 U/ µl T4 DNA ligase which was incubated O/N at 16°C. Cross-links were reversed by adding 184 µl 20 mg/ml Proteinase K, 625 µl 1 M Tris pH 8.0, 250 µl 0.5 M EDTA, 1250 µl 10% SDS and 191 µl $_{dd}$H$_2$O. The solution was incubated overnight at 65°C with rotation. The mixture was transferred to a 50 ml MaXtract High Density tube and 6.5 ml of $_{dd}$H$_2$O was added to obtain exactly 19 ml. The DNA was purified by adding 25:24:1 Phenol—Chloroform-Isoamyl alcohol pH 7.9 and recovering the aqueous phase after centrifugation, the DNA was precipitated via isopropanol precipitation. The pellet was dissolved in 100 µl EB after which the steps described from the Immobilization of ChIA-PETs on Dynabeads step onwards were executed.

3.9.2 Procedure of manual data treatment for ChIA-PET analysis

The linkers and adapters were cut off the obtained sequence and the genomic sequences were uniquely mapped using Tophat version 2.0.11. Duplicates were removed and the mapped files were then analyzed for chromosomal interactions between 1000 bps windows using SeqMonk version 0.27.0. To counteract for the bias in ligations occurring more often between DNA fragments that are enriched, the observed interactions were normalized. All reads in a certain window were counted, the amount of interactions between two windows was divided by the total amount of reads in the first window and subsequently by the total amount of reads in the second window, see Table 3 for an example. The very small obtained values were multiplied with 10,000. To counteract for non-specific ligations, the normalized value for the non-

chimeric linkers was substracted by the normalized value of the chimeric linkers. To reduce the background signal in the plots all square windows with initial interaction values of less than 100 were omitted, the remaining values were plotted (Fig. 35).

	1A	2A	3A	4A	5A	number of reads
1B	50	100	15	100	25	290
2B		35	40	100	20	195
3B			5	100	15	120
4B				500	100	600
5B					5	5
Number of reads	50	135	60	800	165	

Table 3. Example of normalization for ChIA-PET data

In blue are the number of interactions between two windows. For example, 3A and 2B have 40 interactions. In red are the total number of interactions (and thus reads) counted for every window, 3A has a total of 60 reads, 2B a total 195. For the normalization the total number of interactions (and thus reads) derived from window 3 (3A + 3B = 60 + 120 = 180) and window 2 (2A + 2B = 135 + 195 = 330) are counted. The number of interaction between two windows (3A and 2B had 40) was divided by the total number of reads in window 3 and subsequently divided by the total number of reads in window 2 to counteract for the frequency of ligation compared to amount of DNA bias.

4. Results

4.1 Requirements for the recruitment of the Smc complex to the *B. subtilis* chromosome

SMC complexes play a pivotal role in chromosome segregation, however the precise mechanism of action by which they function is not well understood. To gain more insight in this mechanism it is important to get a deeper understanding of the specific chromosomal association of SMC complexes. It was previously shown that yeast cohesin does not require ATP hydrolysis for initial recruitment to the chromosome (Hu et al., 2011), however our understanding of what structural and functional effects the ATP hydrolysis cycle has on the SMC complex is poor. In addition, it was shown that efficient recruitment of SMC to the chromosome requires a loading factor which is ParB in *B. subtilis* (Gruber & Errington, 2009; Sullivan et al., 2009). It is however poorly understood how ParB and the Smc complex interact. Furthermore, it has been suggested that DNA is loaded into the cohesin ring via opening of the hinge domain (Gruber et al., 2006) implying that opening of the hinge domain may be important for the chromosomal association of SMC. To obtain a better understanding of the chromosomal association of SMC, the initial recruitment of SMC to the chromosome was studied by investigating several aspects of SMC including the role of ATP hydrolysis, the interaction with ParB and the hinge domain in more detail in *B. subtilis*.

4.1.1 The Smc complex in a pre-hydrolysis state targets to *parS* sites/ParB and ATP hydrolysis is needed for wild-type distribution on the chromosome

To investigate the role of the ATP hydrolysis cycle in the cellular and chromosomal localization of the Smc complex, well characterized single-amino acid substitutions were introduced in *smc* generating mutant proteins, which fail to bind ATP (K37I and D11117A), block ATP dependent head dimerization (S1090R), drastically reduce ATP hydrolysis (E1118Q) (Fig. 4) or are reduced in ATPase activity *in vitro* (R57A). The mutations were introduced at the endogenous *smc* locus, under the control of the endogenous promoter and as the only copy of *smc*. A western blot confirmed similar expression levels for all variants of the Smc proteins (Fig. 8A). A colony formation assay showed that *B. subtilis* harboring wild-type Smc is capable of forming colonies on rich media agar (nutrient agar (NA)) supporting fast growth rates and on minimal media agar (SMG) on which cells grow slower (Fig. 8B), as previously reported (Bürmann et al., 2013). All ATPase mutants, with the exception of *smc(R57A)*, do not form colonies on NA indicating that those mutants harbor non-functional *smc* alleles. Colonies of *smc(R57A)* cells are of the same size as wild-type colonies on NA and SMG-agar indicating normal growth rates. Colonies of *smc(K37I), smc(D1117A)* and *smc(S1090R)* formed slightly smaller colonies on SMG-agar comparable to growth of colonies of an *smc* deletion strain (Fig. 8B). *smc(E1118Q)* displays even smaller colonies suggesting that the non-functional Smc(E1118Q) protein is somewhat toxic for cells (Fig. 8B).
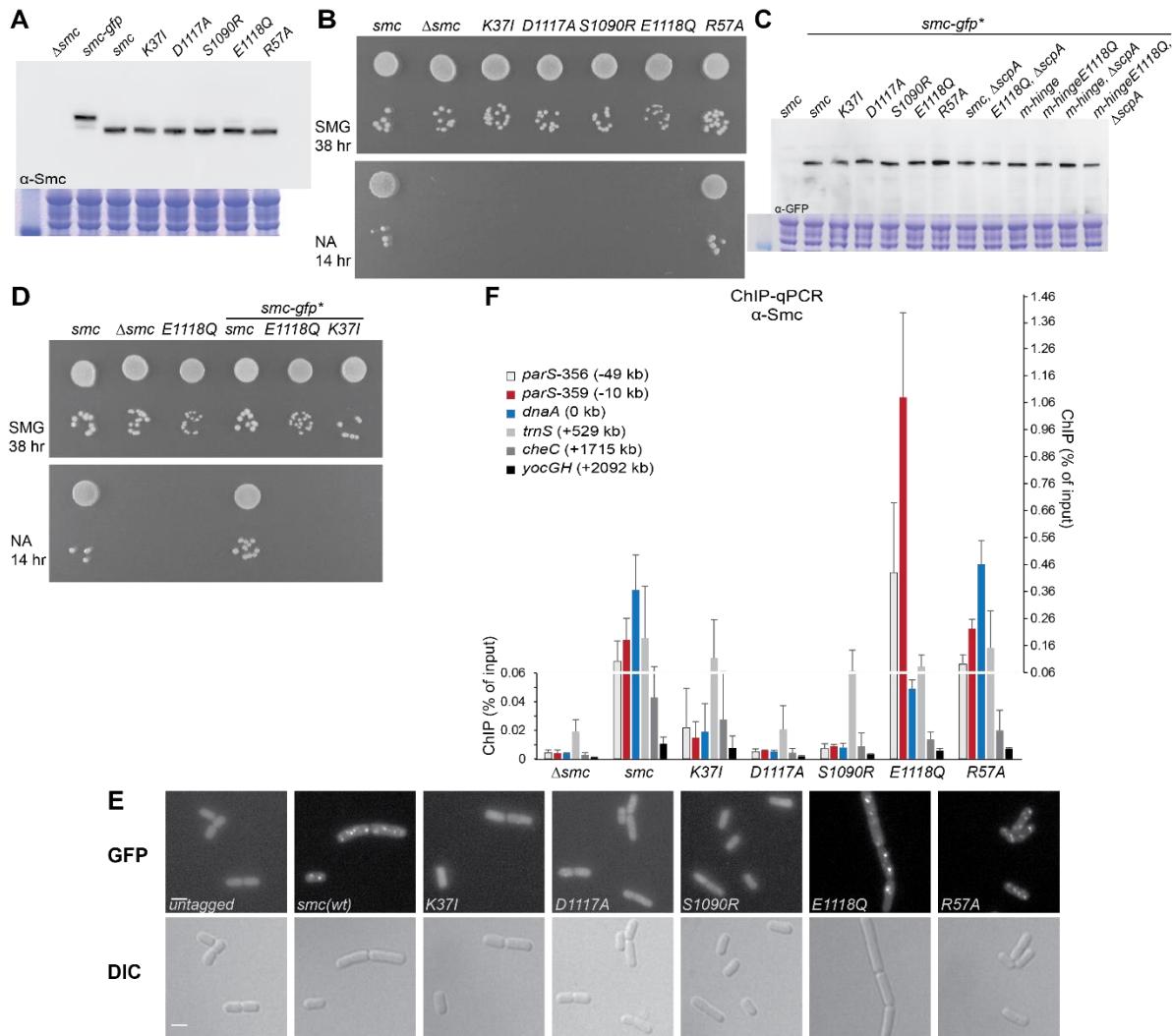
Figure 8. Smc in a pre-hydrolysis state is slightly toxic and accumulates at *parS* sites

- A. Western blot using α-Smc antiserum with different ATPase mutants, used strains are BSG 1007, 1067, 1002, 1045, 1047, 1046, 1008 and 1083. For a loading control a coomassie stained SDS gel is shown.
- B. Colony formation assay of the ATPase mutants. Used strains BSG 1002, 1007, 1045, 1047, 1046, 1008 and 1083.
- C. Western blot using α-GFP antibodies on GFP-tagged strains. Used strains BSG 1002, 1067, 1855, 1857, 1856, 1068, 1881, 1378, 1413, 1677, 1662, 1799 and 1798. A coomassie stained SDS gel is shown as loading control.
- D. Viability assay of untagged and GFP-tagged Smc strains, used strains BSG 1002, 1007, 1008, 1067, 1068 and 1855.
- E. Fluorescence microscopy of strains BSG1002, 1067, 1855, 1857, 1856, 1068 and 1881. Scale bar represents 2 μm.
- F. ChIP-qPCR of strains BSG1007, 1002, 1045, 1047, 1046, 1008 and 1083 using α-Smc antiserum. The data is plotted onto two different axes with different scales to be able to show the background (left axes) and real ChIP signals (right axes). Plotted are mean values from two independent experiments, error bars indicate the standard deviation.

Next, the cellular localization of the ATPase mutants was studied by fluorescence microscopy. The mutant and wild-type genes were tagged at the C-terminus with a monomeric version of GFP. Western blot revealed similar expression levels for all GFP-tagged Smc mutants (Fig. 8C) and a colony formation assay showed that the phenotypes are similar to the untagged counterparts (Fig. 8D). Fluorescence microscopy showed 2-4 foci for wild-type Smc, as previously reported (Fig. 8E) (Gruber & Errington, 2009; Sullivan et al., 2009). Smc(R57A) showed similar cellular localization as wild type. For Smc(K37I), Smc(D1117A) and

Smc(S1090R) no foci formation was observed indicating that these proteins are dispersed throughout the cell. This is consistent with previously published observations (Fig. 8E) (Mascarenhas et al., 2005). Interestingly, Smc(E1118Q) displayed brighter foci and usually had fewer foci per cell, although wild-type-like localization was also observed (Fig. 8E). This data suggests that the Smc complex does not need ATP hydrolysis to form foci.

The differences in foci formation observed for the different mutants could be due to defects in chromosome segregation or chromosomal arrangement caused by the lack of a functional Smc complex. Alternatively, the differences could be a direct effect of the chromosomal localization of these mutant proteins. To test whether the mutant proteins have a different chromosomal localization than wild type, chromatin immuno-precipitation (ChIP) was applied with the untagged mutants using an α-Smc antiserum (Fig. 8F). Primer pairs specific for two *parS* sites (*parS*-356 and *parS*-359), the *oriC* (*dnaA*), a highly transcribed gene (*trnS*) and two terminus proximal loci (*cheC* and *yocGH*) were used in quantitative PCR (qPCR) to determine the ChIP enrichment. As expected, an *smc* deletion strain showed very little DNA precipitation. Wild-type Smc in contrast is enriched at origin proximal loci such as *parS*-356, *parS*-359 and *dnaA* and in addition at the highly transcribed gene *trnS* (Fig. 8F). This is consistent with previous results (Gruber & Errington, 2009). In contrast, the ATPase mutants Smc(K37I), Smc(D1117A) and Smc(S1090R) had poor ChIP enrichments similar to the *smc* deletion strain. This, together with the microscopy data above and previous data (Mascarenhas et al., 2005), indicates that the ATPase mutants do not localize to the chromosome. Smc(E1118Q) showed higher enrichment at the two tested *parS* sites than wild-type Smc. The enrichment at *dnaA* is, however, lower compared to wild type. Thus, this ChIP and microscopy data clearly demonstrate that Smc(E1118Q) is capable of localizing to the chromosome although the distribution is different from wild type. Smc(R57A) showed ChIP enrichment levels and distribution comparable to wild type, which is also consistent with the microscopy data above. This suggests that the ATPase activity of this mutant might be only mildly (if at all) affected *in vivo*.

To get a chromosome wide overview of the differences in distribution between wild-type Smc and Smc(E1118Q), high throughput sequencing was performed on ChIP input samples and IP samples (ChIP-seq).The bioinformatic ChIP-seq analysis approach was set up in the lab as part of this thesis. ParB, a protein binding to *parS* sites, was previously shown to recruit the Smc complex to the chromosome. Smc(E1118Q) had high ChIP enrichment at *parS* sites. To establish the differences and similarities in chromosomal distribution between Smc(E1118Q) and ParB, ChIP-seq with an α-ParB antiserum was also performed using the same protocol (Fig. 9A and 9B). The mapped reads were counted in 5000 bp sliding windows. To normalize for the input in the ChIP experiment, the number of reads in a 5000 bp window of the IP sample was divided by the number of reads in the corresponding 5000 bp window of the input sample. In general the ChIP-qPCR and ChIP-seq results were very similar. Smc(E1118Q), and also ParB, showed peaks of enrichment at *parS* sites (Fig. 9A and 9B). Wild-type Smc in contrast localized most strongly to the *oriC* region. In addition, enrichments for Smc, Smc(E1118Q) and ParB were found at highly transcribed genes such as rRNA and tRNA clusters, a feature that was previously reported for a tagged Smc but not
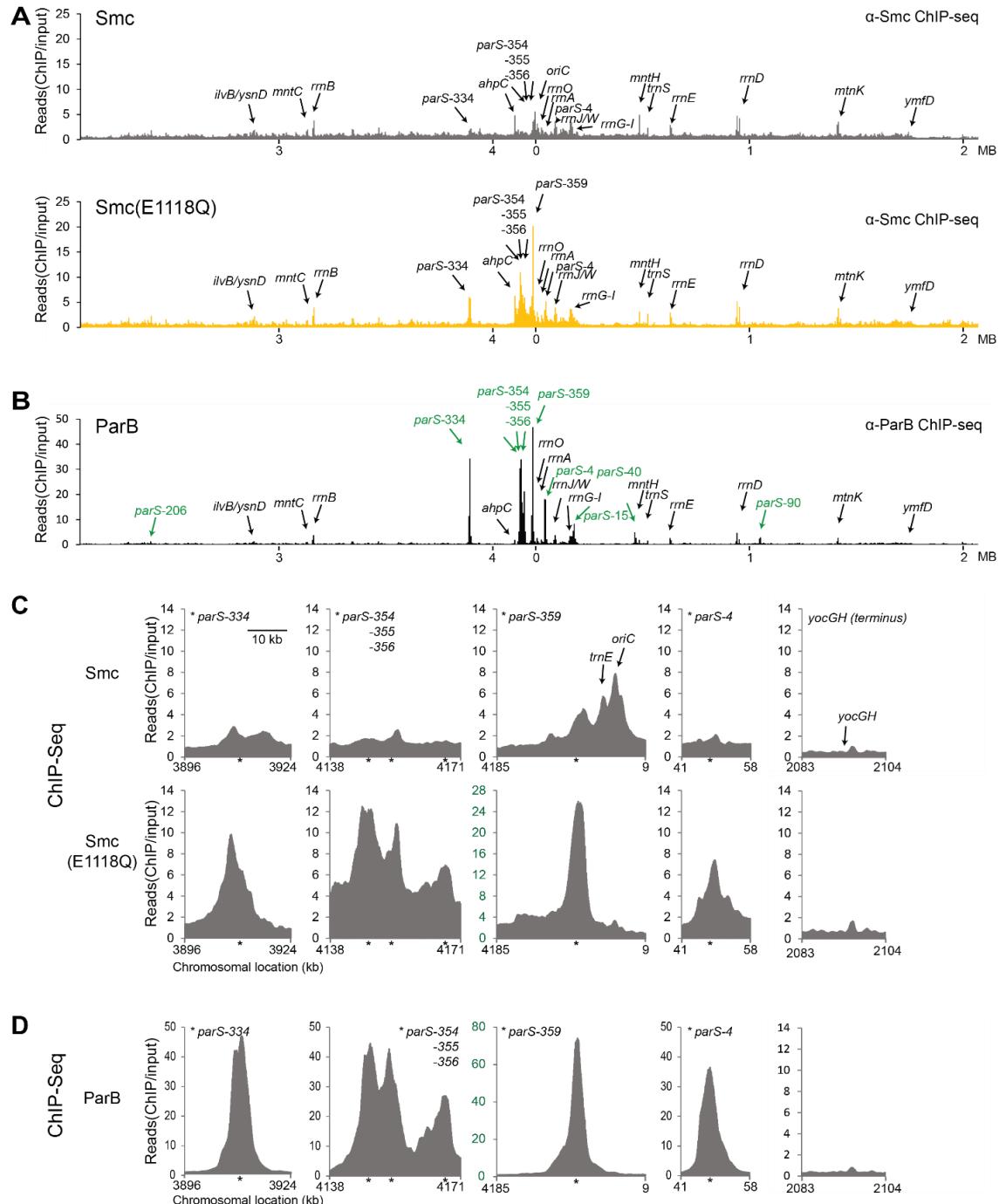
Figure 9. Smc in a pre-hydrolysis state accumulates at *parS* sites/ParB and ATP hydrolysis is needed for wild-type distribution on the chromosome

A. ChIP-seq using α-Smc antiserum on BSG 1002 and 1008. Mapped reads were counted in 5000 bps windows and normalized as described in Chapter 3.7

B. ChIP-seq using α-ParB antiserum on BSG 1470. Mapped reads were counted in 5000 bps windows and normalized as described in Chapter 3.7. The ten *parS* sites in the *B. subtilis* genome are marked in green.

C. ChIP-seq on strains BSG 1002 and 1008 using α-Smc antiserum. Mapped reads were counted in 1000 bps windows every 100 bps and normalized as described in Chapter 3.7. Axes in green indicate different scaling as for the other graphs of the same sample. Stars represent *parS* sites.

D. ChIP-seq on strain BSG 1470 using α-ParB antiserum. Mapped reads were counted in 1000 bps windows every 100 bps and normalized as described in Chapter 3.7. For legends see C.

ParB (Breier & Grossman, 2007; Gruber & Errington, 2009; Nicolas et al., 2012). ChIP-qPCR on an *smc* deletion strain with α-Smc antiserum also showed enrichment at the highly transcribed gene *trnS* (Fig. 8F), and enrichment of Smc is also found in the absence of ParB on highly transcribed genes (Gruber & Errington, 2009), which may suggest that localization to highly transcribed genes is an artifact of the ChIP protocol. Examining the *parS* sites, *oriC* region and terminus region in more detail revealed that Smc(E1118Q) and ParB have almost perfectly overlapping localization at *parS* sites. Wild type also showed localization to the *parS* sites but the signal was broader with higher enrichment towards the *oriC* region (Fig. 9C and 9D). These experiments demonstrate that Smc blocked in ATP hydrolysis (Smc(E1118Q)) accumulates more pronouncedly at ParB binding sites (*parS* sites). The poor localization of Smc(S1090R), which cannot engage the head domains, to the chromosome in combination with the localization of Smc(E1118Q) to the chromosome indicates that engaged heads are needed for the Smc complex to be targeted to the chromosome on the *parS* sites. However, ATP hydrolysis is not required for the Smc complex to localize to the chromosome. Wild-type distribution is obtained after at least one full cycle of ATP hydrolysis.
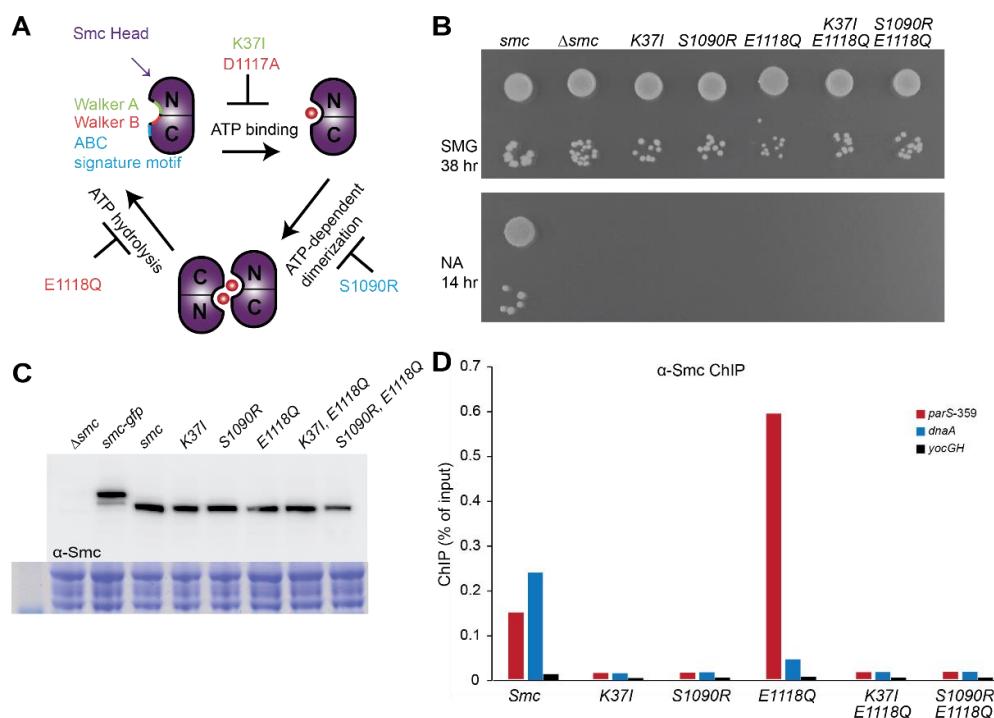
Figure 10. Smc(E1118Q) affects growth and chromosomal localization by increased head engagement efficiency
   A. Overview of the ATPase hydrolysis cycle of the Smc heads, mutations inhibiting steps in this cycle are shown for *B. subtilis*. Same image as figure 4.
   B. Colony formation assay using strains BSG 1002, 1007, 1045, 1046, 1008, 2050 and 2051.
   C. Western blot against Smc using strains BSG 1007, 1067, 1002, 1045, 1046, 1008, 2050 and 2051.
   D. ChIP-qPCR using α-Smc antiserum on strains BSG 1002, 1008, 1045, 1046, 2050 and 2051.

Smc(E1118Q) *in vitro* shows strongly enhanced DNA binding compared to wild type (Hirano & Hirano, 1998; Hirano et al., 2001; Kamada et al., 2013). Cells harboring *smc(E1118Q)* also show a strong

phenotype *in vivo* (see above). To test whether the observed growth phenotype and increased localization to *parS* sites are dependent on ATP binding and head engagement in Smc(E1118Q) and not due to a non-physiological change in the protein, an ATP binding mutation (K37I) and ATP dependent dimerization mutation (S1090R) (Fig. 10A) were independently combined with the E1118Q mutation. In these double mutants the step in the ATP hydrolysis cycle prior to head engagement should be blocked by either the presence of the K37I or S1090R mutation. When tested in the colony formation assay, the double mutants displayed growth phenotypes similar to *Δsmc* (Fig. 10B). A western blot showed similar expression levels for Smc(K37I, E1118Q) compared to wild type, and only slightly reduced levels for Smc(S1090R, E1118Q) (Fig. 10C). ChIP-qPCR revealed that both double mutants had low enrichments levels similar to Smc(K37I) and Smc(S1090R) (Fig. 10D) indicating that the double mutants do not localize to the chromosome. These results show that the slight toxicity of Smc(E1118Q) is lost when ATP cannot bind to this protein or ATP dependent head engagement cannot occur. This is consistent with the notion that Smc(E1118Q) affects growth and chromosomal localization by increased head engagement efficiency.

4.1.2 Smc in a pre-hydrolysis state is recruited to the chromosome independent of the reduced growth rates caused by this mutant

Cells harboring Smc(E1118Q) are very sick compared to wild type, presumably due to a chromosome segregation defect. It cannot be excluded that this defect influences the localization of Smc proteins. To investigate this, strains were generated by colleagues which express Smc(E1118Q) but had wild-type like growth rates by simultaneously expressing wild-type functioning Smc proteins. In these strains the hinge domain of *B. subtilis* Smc is replaced by the zinc hook dimerization domain of Rad50 from *P. furiosis* (Fig. 5A and 11A) (Hopfner et al., 2002). This dimerization domain does not structurally resemble the Smc hinge domain.
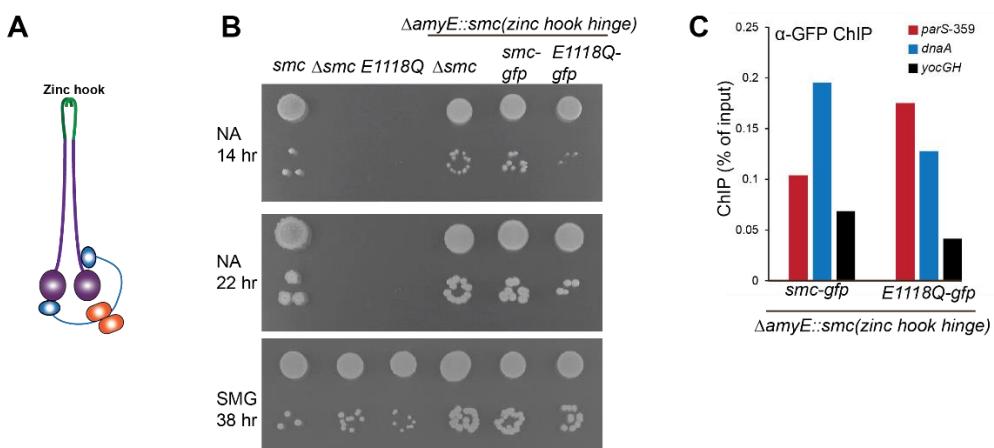
Figure 11. Smc in a pre-hydrolysis state is recruited to the chromosome independent of slightly toxic growth rates
    A.   Schematic drawing of a chimeric Smc with the Rad50 zinc hook as the dimerization domain instead of the hinge domain, the conformation of the coiled-coils in this protein is unknown.
    B.   Colony formation assay using strains BSG 1002, 1007, 1008, 1095, 1134 and 1135.
    C.   ChIP-qPCR using α-GFP antibodies on strains BSG 1134 and 1135. Cells were grown in competence medium.

When this chimeric Smc was expressed from the *amyE* locus as the only copy of Smc cells were viable on NA indicating that the chimeric protein is functional (Fig. 11B). For subsequent experiments, GFP-tagged Smc with and without the E1118Q mutation was expressed from the endogenous *smc* locus, in addition to the chimeric untagged Smc expressed from *amyE*. Because the hinge domains of these two proteins are structurally very different, no dimerization between the wild-type Smc hinge and the chimeric zinc hook Smc is expected. The strains expressing both proteins were viable on NA (Fig. 11B). The toxicity caused by Smc(E1118Q) is thus alleviated by the presence of the chimeric Smc expressed from *amyE* in these strains. ChIP-qPCR was performed using α-GFP antibodies where the GFP-tagged Smc or Smc(E1118Q) expressed from the endogenous *smc* locus was immunoprecipitated (Fig. 11C). As observed above, wild-type Smc localizes mostly to *dnaA*, whereas Smc(E1118Q) localizes mostly to the tested *parS* site. The different localization of Smc and Smc(E1118Q) is thus not a result of a chromosome segregation phenotype in cells harboring Smc(E1118Q). The increased levels of localization to the terminus region (*yocGH*) are possibly due to the higher levels of Smc proteins in these strains or the GFP tag on Smc.

4.1.3 Recruitment of wild-type Smc and Smc in a pre-hydrolysis state to the chromosome depends on ParB, ScpA and ScpB

Normal localization of wild-type Smc depends largely on ParB, which binds to *parS* sites (Gruber & Errington, 2009; Sullivan et al., 2009). The strong localization of Smc(E1118Q) to *parS* sites suggests that it might also depend on ParB. To directly test this, *parB* was deleted in the *smc* and *smc(E1118Q)* strain. *B. subtilis* is viable without the ParB protein on NA (Ireton et al., 1994; Autret et al., 2001) (Fig. 12A). The *smc(E1118Q)* strain in which *parB* was deleted was not viable on NA and only very small colonies were observed on SMG (Fig. 12A) indicating that the double mutant has very severe defects. Expression levels of Smc and Smc(E1118Q) were not changed in the Δ*parB* background (Fig. 12B). ChIP-qPCR clearly demonstrated that chromosomal localization of Smc and Smc(E1118Q) depends on ParB (Fig. 12C).

It has been shown that ScpA and ScpB are required for Smc complex functionality (Lindow, et al., 2002), however little is known about their precise role. To directly test whether ScpA and ScpB have a role in the chromosomal localization of Smc *scpA* or *scpB* was deleted in strains that harbored wild-type *smc* or *smc(E1118Q)*. Strains harboring wild-type *smc* in the absence of *scpA* or *scpB* did not grow on NA and formed small colonies on SMG-agar comparable to an *smc* deletion strain (Fig. 12D). This observation is consistent with the notion that the Smc complex in the absence of ScpA or ScpB is non-functional (Lindow et al., 2002). *smc(E1118Q)* in the absence of *scpA* or *scpB* also formed colonies with sizes similar to the *smc* deletion strain, indicating that the slight toxicity of *smc(E1118Q)* is dependent on *scpA* and *scpB* (Fig. 12D). Expression levels of the Smc proteins in all these strains were similar (Fig. 12B). ChIP-qPCR showed that chromosomal localization of Smc is indeed lost when ScpA or ScpB is absent for wild-type Smc. For Smc(E1118Q) the localization to *parS*-359 is drastically reduced but some residual localization might be observed (Fig. 12E). This data demonstrates that, in addition to engaged heads, ScpA, ScpB and ParB are needed for wild-type Smc and Smc(E1118Q) to localize efficiently to (*parS* sites on) the chromosome.
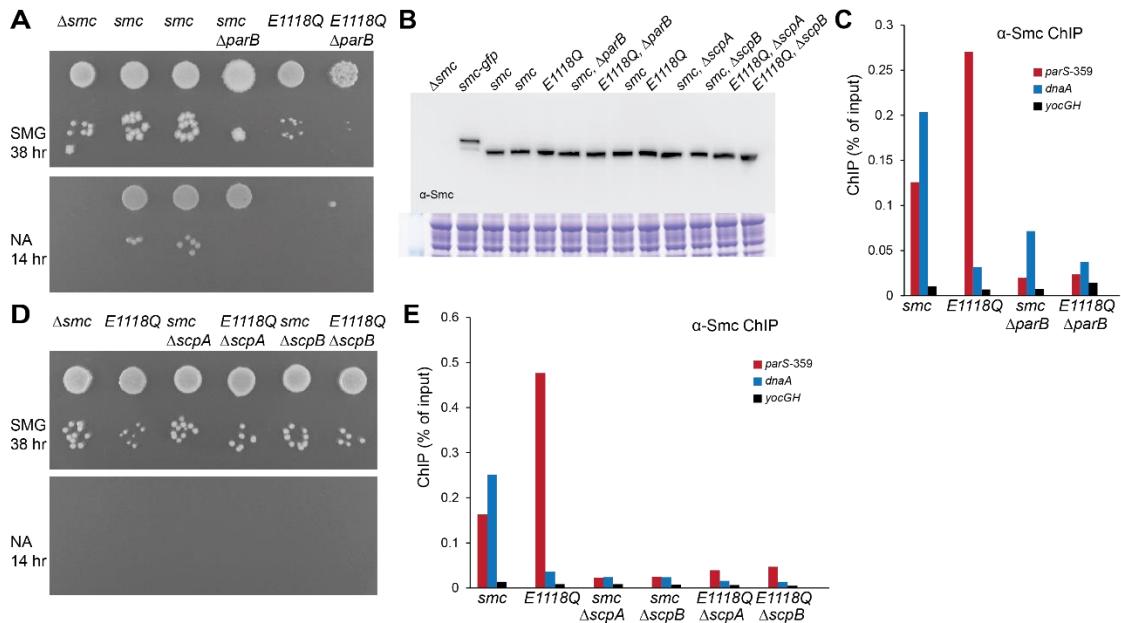
Figure 12. Recruitment of wild-type Smc and Smc in a pre-hydrolysis state to the chromosome depends on ParB, ScpA and ScpB

    A.   Colony formation assay using strains BSG 1007, 1002, 1051, 1052, 1406 and 1387.

    B.   Western blot using α-Smc antiserum with strains BSG 1007, 1067, 1002, 1051, 1406, 1052, 1387, 1890, 1893, 1889, 1891, 1892 and 1894.

    C.   ChIP-qPCR using α-Smc antiserum with strains BSG 1051, 1406, 1052 and 1387

    D.   Colony formation assay using strains BSG 1007, 1008, 1889, 1892, 1891 and 1894.

    E.   ChIP-qPCR using α-Smc antiserum of strains BSG1890, 1893, 1889, 1891, 1892 and 1894

4.1.4 Hinge dimerization hinders localization to the chromosome

From the above it is clear that the Smc complex localizes to ParB/*parS* loading sites on the chromosome in a pre-hydrolysis state. For localization to the chromosome of wild-type Smc and Smc(E1118Q) ScpA and ScpB are required. It is however unknown if there are other regions within the Smc protein that are involved in the initial recruitment to the chromosome. It was previously shown that mutations in four glycines in the hinge domain of *B. subtilis* Smc abolish hinge-dimerization *in vitro* (Chapter 2.4.4.2 and Fig. 7) and that this mutant has higher dsDNA binding affinities *in vitro* than wild type, presumably by exposing a DNA binding site at the bottom surface of the hinge (Hirano & Hirano, 2002, 2006). In addition, it was suggested that the combination of this abolished hinge-dimerization (monomeric hinges) with ATP dependent head engagement creates V-shaped Smc dimers, a state of the complex that may also exist in wild-type Smc (Hirano & Hirano, 2006) To test whether and to what levels a monomeric hinge allows chromosomal association, the mutations to generate the mutant Smc protein that abolishes hinge-dimerization were introduced into full length wild-type *smc* and *smc(E1118Q)*, in strains lacking and harboring the *scpA* gene.
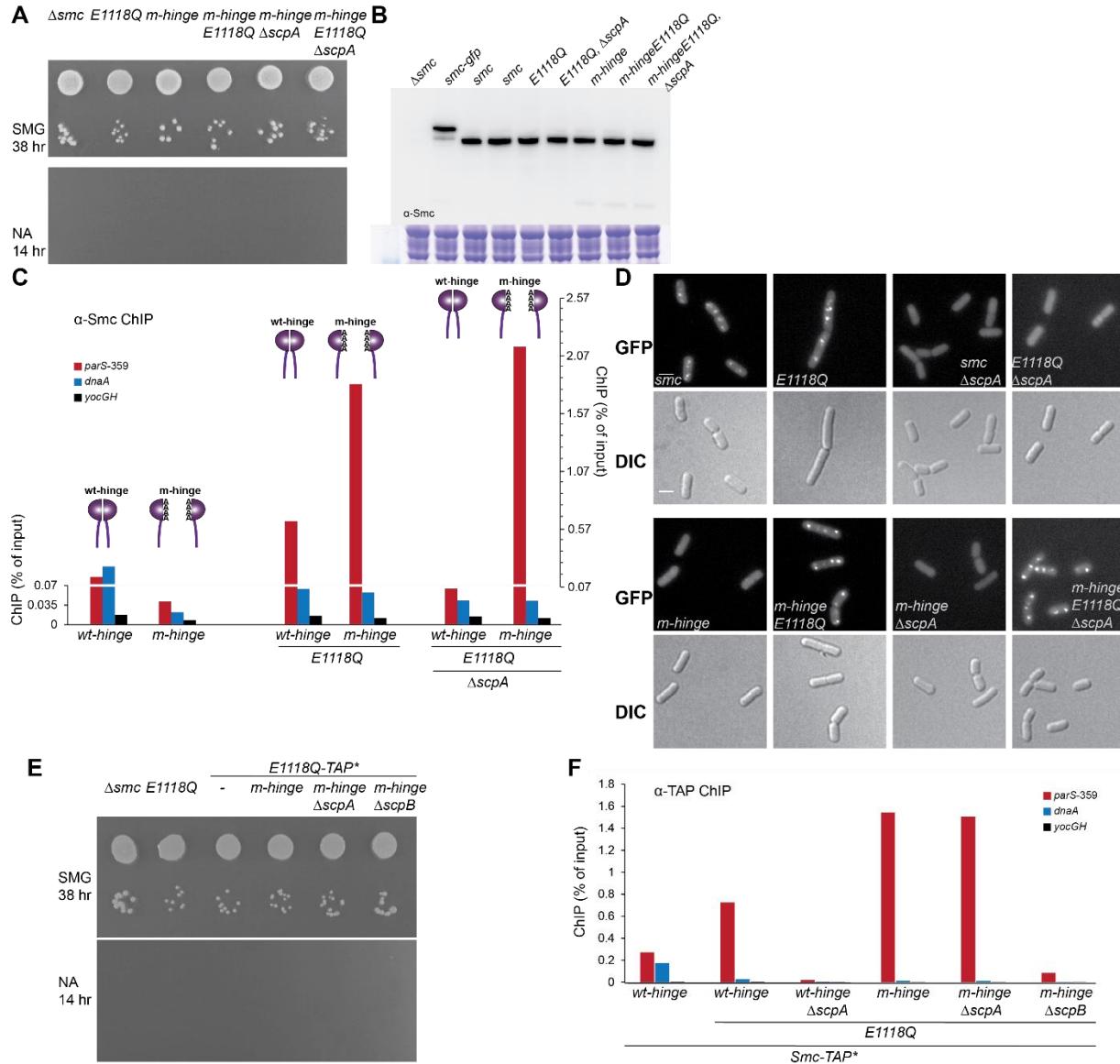
Figure 13. Hinge dimerization hinders localization to the chromosome

A. Colony formation assay using strains BSG 1007, 1893, 1624, 1621, 1623 and 1620
B. Western blot using α-Smc antiserum with strains BSG 1007, 1067, 1002, 1890, 1893, 1892, 1624, 1621 and 1620. Below the band of the Smc(m-hinge) proteins a faint additional band can be observed.
C. ChIP-qPCR using α-Smc antiserum of strains BSG1890, 1624, 1893, 1621, 1892 and 1620. The data is plotted onto two different axes with different scales to be able to show the background (left axes) and real ChIP signals (right axes).
D. Fluorescence microscopy of strains BSG 1067, 1068, 1378, 1413, 1677, 1662, 1799 and 1798. Scale bar represents 2 µm.
E. Colony formation assay using strains BSG 1007, 1008, 1521, 1671, 1689 and 1690.
F. ChIP-qPCR using IgG-coupled beads of strains BSG 1518, 1521, 1520, 1671, 1689, 1690.

The colony formation assay showed that cells of *smc(m-hinge)* (for monomeric hinge) make colonies similar in size to a *Δsmc* strain on SMG agar indicating that the Smc complex with monomeric hinges is non-functional (Fig. 13A). Sizes of colonies from *smc(m-hinge, E1118Q)* are slightly larger than colonies of *smc(E1118Q)* but smaller than colonies of *Δsmc.* This suggests that the Smc(m-hinge) proteins in

combination with E1118Q are not as toxic as Smc(E1118Q). *smc(m-hinge), ΔscpA* displayed colonies similar in size to *Δsmc*. *smc(m-hinge, E1118Q), ΔscpA* had colony sizes comparable to *smc(E1118Q)*, but also a few larger colonies (comparable to *Δsmc*) can be observed (Fig. 13A). Expression levels of the Smc proteins are similar in all these mutant strains (Fig. 13B). ChIP-qPCR analysis showed that Smc(m-hinge) does not localize to the chromosome (Fig. 13C). However, Smc(m-hinge, E1118Q) localizes to the chromosome. Surprisingly, this mutant protein shows even higher levels of localization to *parS*-359 than Smc(E1118Q) (Fig. 13C), indicating that a monomeric hinge promotes localization to the chromosome. Even more surprising was the finding that this localization does not depend on ScpA. Actually, even slightly more localization to *parS*-359 can be observed in the absence of ScpA (Fig. 13C). To verify that the surprising results above were not due to artifacts in the ChIP experiments the mutant proteins were GFP tagged and after confirmation of similar expression levels for all mutant proteins (Fig. 8C), applied to fluorescence microscopy. Wild-type Smc and Smc(E1118Q) did not show any foci formation in the absence of ScpA (Fig. 13D), which fits well with the ChIP data (Fig. 13C). Smc(m-hinge) in the presence and absence of ScpA also did not form foci (Fig. 13D). In contrast, Smc(m-hinge, E1118Q) in the presence and absence of ScpA displayed bright foci (Fig. 13D), these foci appear to be brighter than for Smc(E1118Q) suggesting a more pronounced localization. This is consistent with the notion that Smc(m-hinge, E1118Q) in the presence and absence of ScpA has increased localization to *parS*-359 as compared to Smc(E1118Q).

In addition, the role of ScpB in chromosomal localization of Smc(m-hinge, E1118Q) was investigated. Intriguingly, in the absence of ScpB Smc(m-hinge, E1118Q) displayed larger colonies (comparable to *Δsmc*) than in the absence of ScpA (Fig. 13E) suggesting that the toxicity of Smc(m-hinge, E1118Q) depends on ScpB. Furthermore, Smc(m-hinge, E1118Q) in the absence of ScpB showed lower localization to *parS*-359 than Smc(m-hinge, E1118Q) in the absence of ScpA (Fig. 13F), implying that ScpB in the presence of ScpA is necessary for efficient localization of Smc(m-hinge, E1118Q). ScpA might thus inhibit loading to *parS* sites when *Scpb* is deleted. This negative result should be investigated deeper by for example assessing the localization of the Smc(m-hinge, E1118Q) protein in the presence of ScpB containing mutations that were shown to inhibit Smc complex functioning *in vivo*, presumably by reduced binding to ScpA (Kamada et al., 2013). This should clarify whether functional ScpB is needed in the presence of ScpA for Smc(m-hinge, E1118Q) to localize strongly to ParB/*parS* sites. Nevertheless, this data demonstrates that Smc with engaged heads (E1118Q) and a monomeric hinge localizes to the loading sites on the chromosome very strongly, even in the absence of ScpA. This could resemble a state of the complex during the loading process.

4.1.5 Recruitment of the Smc complex to the chromosome is promoted by engaged heads in combination with reduced rod formation in the coiled-coils

The results above show that engaged heads are required for recruitment to *parS* sites. The engaged heads in combination with a monomeric hinge promote localization to the *parS* sites, which may indicate that a monomeric hinge increases the fraction of Smc complexes with engaged heads. This suggests that in the

wild-type situation a conformational change might be needed for recruitment to *parS* sites. This conformational change requires at least engaged heads and presumably an additional change in the hinge or hinge-proximal part of the complex. The different conformations of the Smc complex are being tested by other members in the lab using *in vivo* crosslinking of cysteine residues within the Smc complex. For these experiments strains are used in which the four endogenous cysteines in the Smc protein are replaced by serines. Cysteine residues are then introduced at the locations that are tested for their conformation by crosslinking. These Smc proteins are tagged with a TEV-His12-HaloTag. Thus far it was assumed that Smc(E1118Q) indeed has engaged heads as this was observed in crystal structures and other related proteins. Colleagues measured the levels of head engagement and found that these levels were poor for wild type, however the levels were significantly increased for Smc(E1118Q). Smc(m-hinge, E1118Q) displayed increased head engagement over Smc(E1118Q). These findings match with the localization as observed by ChIP in which proteins with engaged heads localize to the chromosome. However, in the absence of ScpA, head engagement was reduced for both Smc(E1118Q) and Smc(m-hinge, E1118Q), the latter protein localizes to *parS*-359 efficiently in the absence of ScpA. This suggests that there is no strict correlation between engaged heads and localization. However, another aspect of the conformation of the Smc complex that was tested by *in vivo* crosslinking was the formation of rods between the coiled-coils by measuring the crosslinking ability of two cysteines in the coiled-coil close to the hinge domain as was described in (Soh et al., 2014) (Fig. 14A).
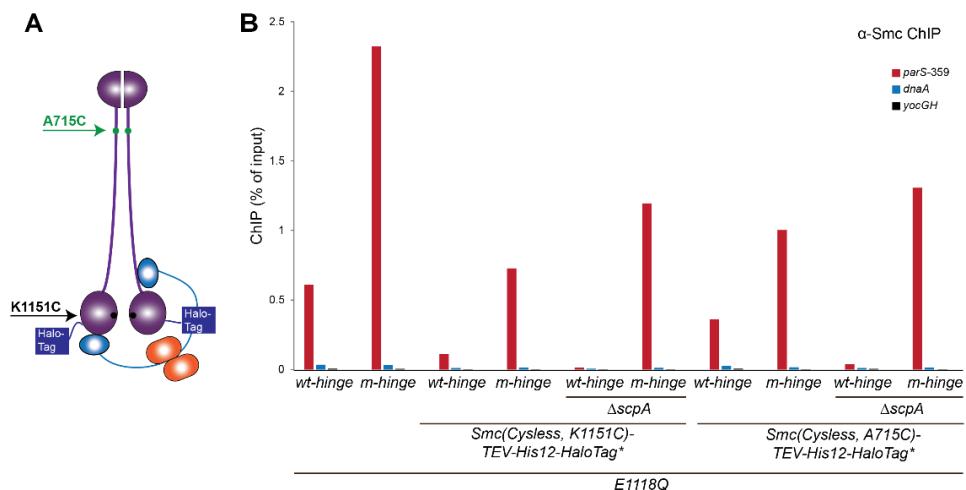
Figure 14. Smc(cysless, TEV-His12-HaloTag) displays a similar pattern of localization as wild-type Smc proteins
  A. Schematic representation of Smc(cysless, TEV-His12-HaloTag), indicated are the two mutated residues used for disulfide crosslinking.
  B. ChIP-qPCR with α-Smc antiserum using strains BSG 1008, 1547, 1488, 1598, 1512, 1791, 1922, 1924, 1950 and 2036.

Colleagues found that Smc(E1118Q) has reduced rod formation compared to wild type. Smc(m-hinge) had even more decreased rod formation, also in the presence of E1118Q and absence of ScpA or a combination of both. In summary, Smc(E1118Q) and Smc(m-hinge, E1118Q) have increased head engagement and largely decreased rod formation (both localize to the chromosome efficiently), Smc(E1118Q) in the absence

of ScpA has slightly increased head engagement and very slightly decreased rod formation (localizes to the chromosome poorly), Smc(m-hinge, E1118Q) in the absence of ScpA has slightly increased head engagement and largely decreased rod formation (localizes to the chromosome efficiently). This implies that a combination of head engagement and reduction in rod formation promotes localization to the chromosome.

The proteins used for crosslinking harbor several cysteine mutations and a large tag (Fig. 14A), which could influence their chromosomal localization. Therefore it was important to test the localization of these modified Smc proteins directly by ChIP-qPCR (Fig. 14B). The pattern of localization of these strains resembles that of wild type, however in general the levels of localization are reduced. Nevertheless, the consistency of the pattern of localization (high at *parS*-359 for Smc(E1118Q), increased levels at *parS*-359 for Smc(m-hinge, E1118Q) and Smc(m-hinge, E1118Q) in the absence of ScpA and poor localization for Smc(E1118Q) in the absence of ScpA) of the Smc(cysless, TEV-His12-HaloTag) proteins confirms that the measured levels of head engagement and rod formation correlate with chromosomal localization. Accordingly, a combination of increased head engagement and reduced rod formation promotes localization to the *parS* sites.

4.1.6 A flexible peptide insertion below the Smc hinge influences localization

Above it is shown that the Smc complex with a monomeric hinge domain localizes more efficiently to *parS* sites than Smc complexes with a wild-type hinge domain. This possibly suggests that an open hinge promotes localization to *parS* sites. Colleagues in the lab constructed three mutant strains in which three different lengths of flexible peptides (5, 8 and 11 residues) were inserted between residue 494 and 495 at the end of the N-terminal coiled-coil and residue 678 and 679 at the beginning of the C-terminal coiled-coil in strains lacking and containing the E1118Q mutation in Smc. Using the aforementioned *in vivo* crosslinking experiments, this time using cysteine residues in the hinge, they found that hinge engagement
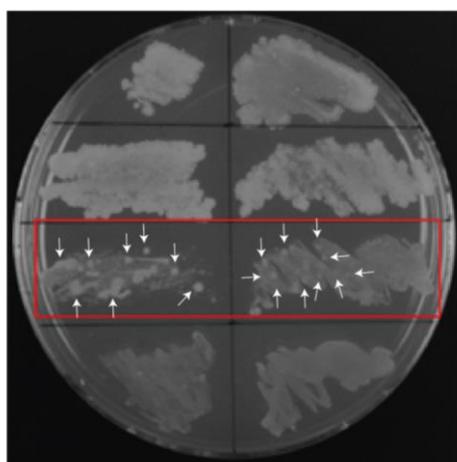
Figure 15. Example of *B. subtilis* patch with suppressor mutations
B. subtilis cells were streaked from -80°C stocks, the red rectangle indicates strains that obtained cells with suppressor mutations. The bigger colonies amongst the slower growing cells are presumably cells with suppressor mutations. The colonies are indicated with a white arrow. Strains within the red rectangle are BSG 1604 (left) and 1687 (right).

is slightly reduced when the flexible peptides are present. Endeavors were made by colleagues to insert these mutations into the native *B. subtilis* Smc protein. However, combining the flexible insertions below

the hinge with the E1118Q mutation resulted in strains that had highly decreased growth rates and were easily overgrown by cells that had made suppressor mutations (Fig. 15). This indicates that Smc proteins with flexible insertions below the hinge in combination with the E1118Q mutation are toxic for cells. The strains used for the crosslinking experiments (*smc(cysless, R643C, TEV-His12-HaloTag)* with the flexible insertions) did not show this strong phenotype. To test whether opening of the hinge domain indeed promotes localization to *parS* sites these strains were subjected to ChIP-qPCR (Fig. 16B). Smc(cysless, R643C, TEV-His12-HaloTag) proteins have a similar localization pattern compared to the wild-type Smc proteins (compare Fig. 13C with Fig. 16B). When any of the flexible insertions are present in Smc(cysless, R643C, TEV-His12-HaloTag), then these mutant proteins localized more to *parS*-359 than *dnaA* and the amount of localization to the *parS* site is higher than observed for wild type. The combination of the flexible insertions with the E1118Q mutation showed the same pattern of localization as Smc(cysless, R643C, E1118Q, TEV-His12-HaloTag), however localization to *parS*-359 may be slightly increased for two of the flexible insertion strains but this cannot be stated with clear confidence. Nevertheless, from this experiment it can be concluded that localization to *parS*-359 sites is promoted in Smc without the E1118Q mutation when flexible insertions are present just below the hinge. This correlates with decreased hinge engagement as measured by crosslinking. Whether this is also the case when the E1118Q mutation is present remains to be further validated.
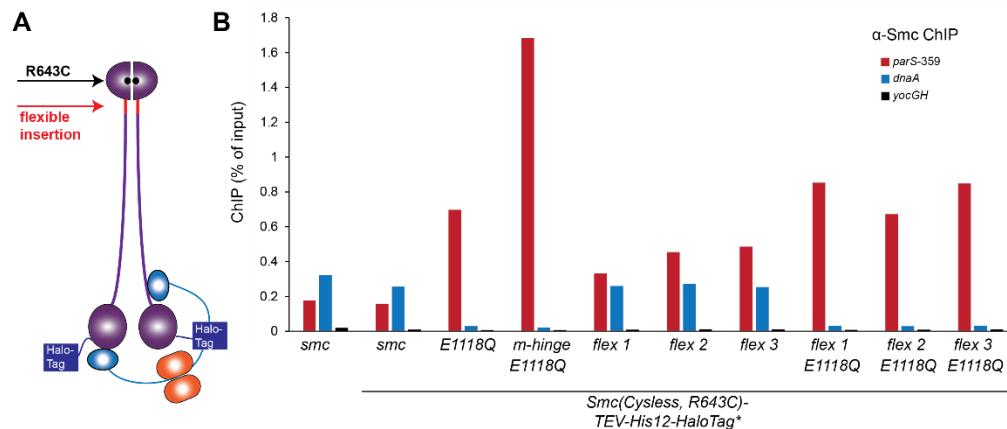
Figure 16. Flexible insertions below the hinge influences Smc localization
    A.   Schematic overview of the flexible insertion and R643C mutation in SMC.
    B.   ChIP-qPCR using α-Smc antiserum on strains BSG 1002, 1692, 1694, 1839, 1852, 1853, 1854, 1836, 1837 and 1838.

4.1.7 The Smc hinge is dispensable for localization to the chromosome

The results above show that mutations in the hinge that result in a monomeric hinge promote localization to the chromosome. It is however unclear whether it is the 'opening' of this hinge domain that promotes this localization or whether it is caused by other processes, such as DNA binding. A DNA binding site was proposed at the bottom surface of the hinge (Hirano & Hirano, 2006). Increased exposure of this DNA binding site could potentially also lead to increased localization to the chromosome. To test this, the hinge was removed from Smc by connecting residue 499 with 674 (Fig. 17A) with a flexible linker

(GGGSGGGSGGG). These residues were chosen on the basis of the crystal structure of the hinge of Smc from *T. maritima* (Fig. 5B) (Haering et al., 2002), such that these residues are in the hinge-proximal part of the coiled-coil and are adjacent to each other. The mutated proteins were expressed from the endogenous *smc* loci under their own promoter as the only copy of *smc*. *smc(Δhinge)* shows colony sizes comparable to *Δsmc*, indicating that it renders Smc non-functional (Fig. 17B). *smc(Δhinge, E1118Q)* displays colony sizes comparable to *smc(E1118Q)* although even slightly smaller colonies may be observed, indicating that the Smc(Δhinge, E1118Q) protein is possibly even somewhat more toxic to the cells than Smc(E1118Q) (Fig. 17B).
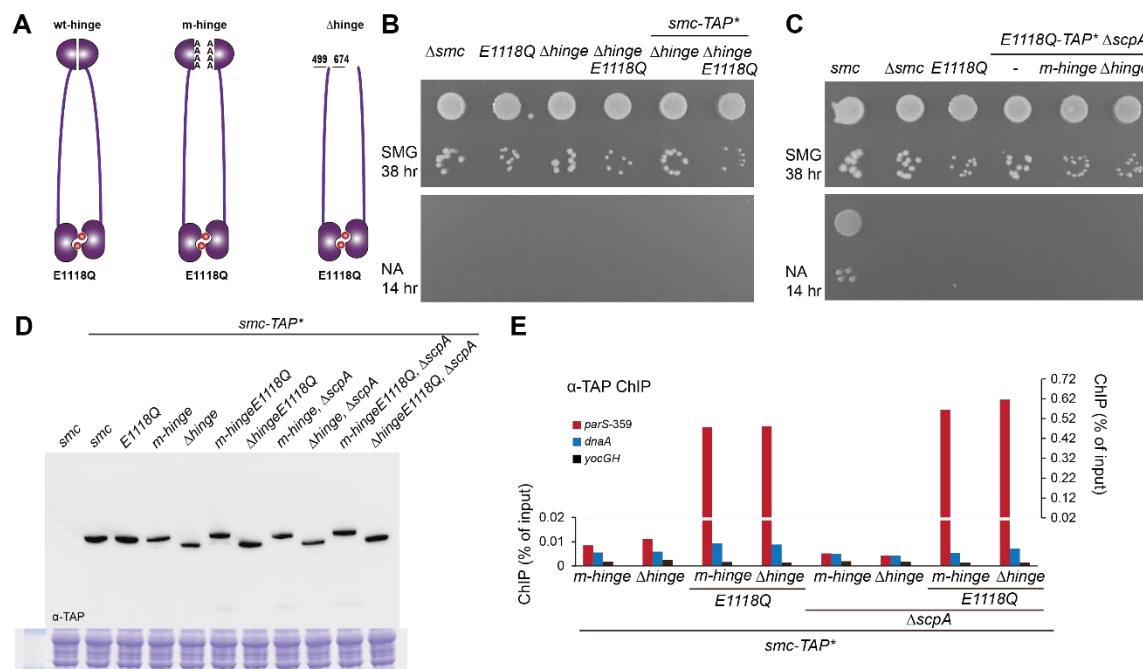
Figure 17. The Smc hinge is dispensable for localization to the chromosome
  A. Schematic representation of three different constructs used, wild-type Smc with the E1118Q mutation, Smc(m-hinge) with the E1118Q mutation and the Smc(Δhinge) with the E1118Q mutation.
  B. Colony formation assay using strains BSG 1007, 1008, 1626, 1619, 1896 and 1780.
  C. Colony formation assay using strains BSG 1002, 1007, 1008, 1520, 1689 and 1779.
  D. Western blot using PAP with strains BSG 1002, 1016, 1475, 1691, 1896, 1671, 1780, 1672, 1895, 1689 and 1779.
  E. ChIP-qPCR using IgG coupled beads of strains BSG 1691, 1896, 1671, 1780, 1672, 1895, 1689 and 1779. The data is plotted onto two different axes with different scales to be able to show the background (left axes) and real ChIP signals (right axes).

The construct was TAP-tagged on the C-terminus (without making changes in the other genetic make-up). A colony formation assay revealed no differences between TAP-tagged and non-tagged strains (Fig. 17C). Also, deletion of *scpA* resulted in growth comparable to *smc(E1118Q)* indicating that the Smc complex without a hinge and ScpA but with E1118Q is slightly toxic for cells (Fig. 17C). Western blot revealed similar expression levels of wild-type- and mutated TAP-tagged strains (Fig. 17D). ChIP-qPCR demonstrated that the Smc(Δhinge) proteins behaved very similar to the Smc(m-hinge) proteins. Smc(Δhinge) did not localize to the chromosome, whereas Smc(Δhinge, E1118Q) localized with similar levels to *parS*-359 as Smc(m-

hinge, E1118Q) (Fig. 17E). In addition, Smc*(*Δhinge, E1118Q), in the absence of ScpA localized to *parS*-359 in similar, or even slightly higher, levels than in the presence of ScpA (Fig. 17E). This demonstrates that the Smc hinge is not required for localization to loading sites on the chromosome.

4.1.8 Minimal requirement for the Smc complex to localize to the chromosome
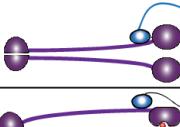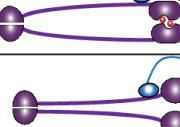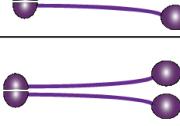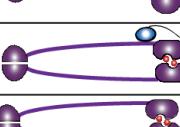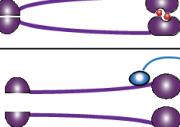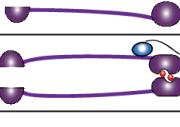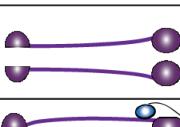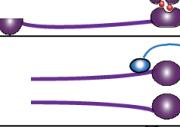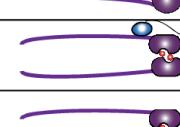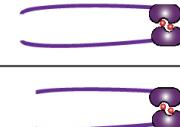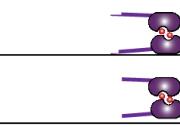
The results above show that efficient localization is obtained when the Smc hinge is in a monomeric state or absent and the heads are engaged, even in the absence of ScpA when ScpB also does not associate with the Smc complex. The recruitment of Smc(E1118Q) to the *parS* sites depends, however, on ParB. This suggests that Smc may have a binding site for ParB on the Smc head domain or between the head domain and the hinge-proximal part of the coiled-coil. To find the potential ParB binding site on Smc additional truncations of the coiled-coil were made (Fig. 18A). These truncations were constructed in the same way as the Smc(Δhinge) construct, all harbored the E1118Q mutation and were TAP-tagged at the C-terminus. In all truncated strains *scpA* was deleted. Surprisingly, when the coiled-coils were made only ~30 residues shorter than Smc(Δhinge) the colony sizes changed from the *smc(E1118Q)* type to the *Δsmc* type, indicating that these 30 residues have a role in the toxicity of Smc(E1118Q) (Fig. 18B). All other truncations also displayed colony sizes comparable to *Δsmc* (Fig. 18B-D). Western blot showed that all constructs are expressed to comparable levels (Fig. 18E-F). Next, the Smc truncation strains were subjected to ChIP-qPCR using rabbit IgG. In general, the shorter the constructs became the less localization was observed (Fig. 18G-H). However, there was a clear cut-off between constructs; Smc(Δ262-911) and Smc(Δ278-921) localized to *parS*-359 and Smc(*Δ262-942*) did not (Fig. 18G-H, Table 4). All other constructs that were shorter than Smc(Δ262-942) did not localize (Fig. 18G-H, Table 4). This shows that engaged heads with approximately one third of the coiled-coils are necessary for the Smc complex to be recruited to the *parS* sites.

The 21 residues between 922 and 943 on the C-terminal helix appear to be important for the Smc complex with engaged heads to be recruited to the *parS* sites. This may indicate that these residues might be part of an interaction site with ParB. An alignment of Smc proteins from different Firmicutes shows two valines and an arginine residue, within those 21 residues in the C-terminal coiled-coil, that are relatively conserved based on their properties between the Firmicutes (Fig. 19). These three residues are predicted to be located on the outer surface of the coiled-coils as based on the register of the coiled-coil. To test if this could be a binding site for recruitment to the chromosome, the arginine was mutated to glutamic acid to generate an opposite charge and the two valines were either mutated to serines to make them hydrophilic or to aspartic acids to give them a negative charge. The triple mutations (VS RE VS or VD RE VD) were introduced in the shortest localizing TAP tagged construct (*smc(Δ262-911)*) in the absence of *scpA* and were either named VS (valines to serines) or VD (valines to aspartic acids) (Fig. 18H). ChIP-qPCR showed that these mutants localized to the chromosome in similar levels as the non-mutated constructs (Fig. 18H). This demonstrates that these residues are not essential for localization.
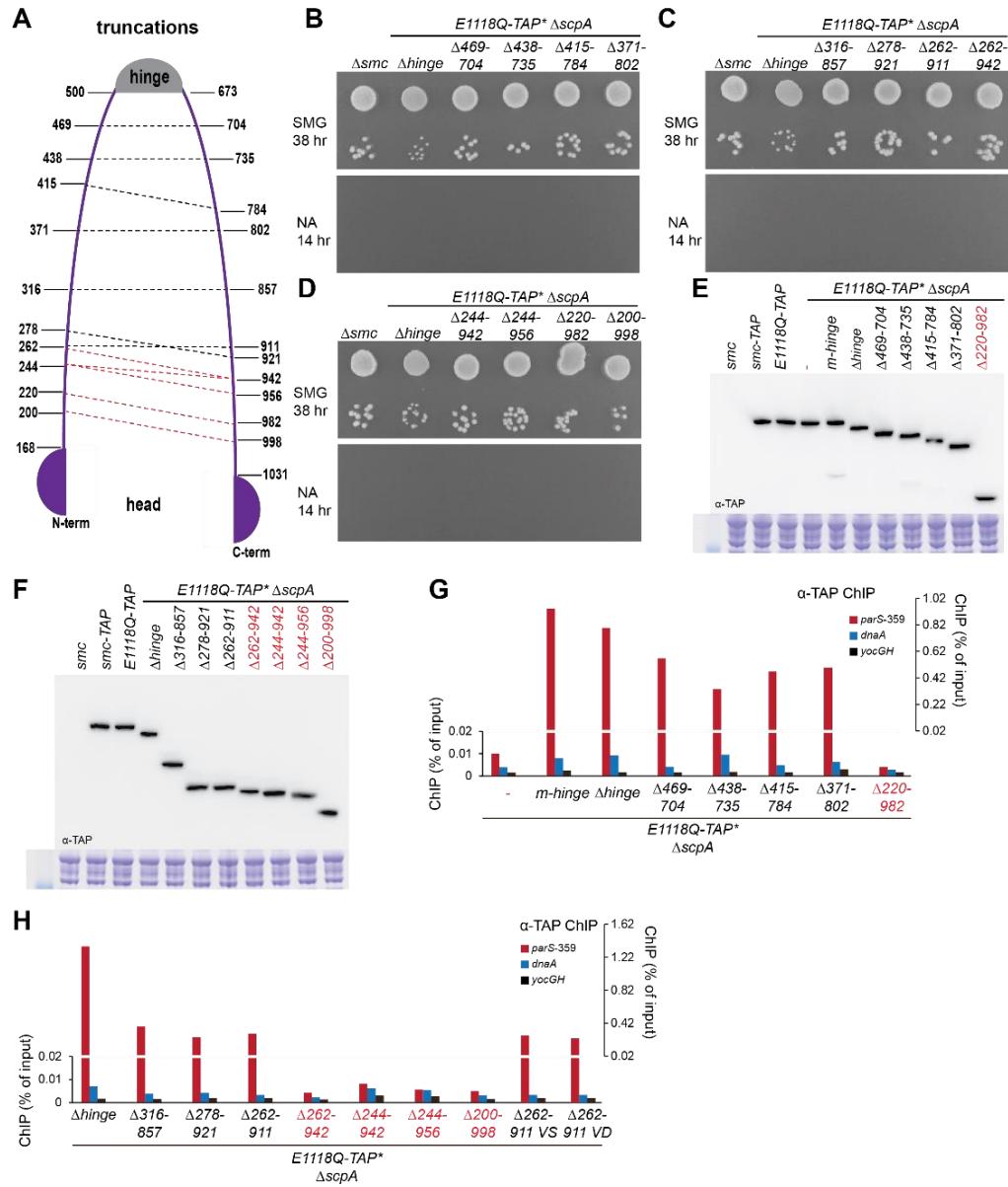
Figure 18. Minimal requirement for Smc to localize to the chromosome

A. Schematic overview of the introduced truncations into Smc. Displayed is one Smc monomer in which the indicated residues were connected with a flexible linker. The black dashed lines indicate truncations that localized to the chromosome, red dashed lines indicate truncations that did not localize.

B. Colony formation assay using strains BSG 1007, 1779, 1871, 1872, 1875 and 1874.

C. Colony formation assay using strains BSG 1007, 1779, 1873, 1830, 1829 and 1828.

D. Colony formation assay using strains BSG 1007, 1779, 1827, 1826, 1825 and 1824.

E. Western blot using PAP on strains BSG 1002, 1016, 1475, 1520, 1689, 1779, 1871, 1872, 1875, 1874 and 1825. Color coding as in A.

F. Western blot using PAP on strains BSG 1002, 1016, 1475, 1779, 1873, 1830, 1829, 1828, 1827, 1826 and 1824. Color coding as in A.

G. ChIP-qPCR using IgG-coupled beads of strains BSG 1520, 1689, 1779, 1871, 1872, 1875, 1874 and 1825. The data is plotted onto two different axes with different scales to be able to show the background (left axes) and real ChIP signals (right axes). Color coding as in A.

H. ChIP-qPCR using IgG-coupled beads of strains BSG 1779, 1873, 1830, 1829, 1828, 1827, 1826, 1824, 1876 and 1877. The data is plotted onto two different axes with different scales to be able to show the background (left axes) and real ChIP signals (right axes). Color coding as in A.

54

Table 4. Overview of localization of different constructs

The colored squares indicate that a construct localizes to the chromosome, dark green means strong localization to the indicated locus, light green indicates moderate localization to the indicated locus. Red squares indicate no localization to the indicated locus. Constructs listed without colored squares do not localize to the chromosome.

| Construct	Construct scheme	Localization to *parS*	Localization to *dnaA*	Colony formation phenotype
Smc		light green	dark green	*Wild-type*
Smc(E1118Q)		green	red	*Smc(E1118Q)*
Smc, ΔscpB		-	-	*Δsmc*
Smc, ΔscpA		-	-	*Δsmc*
Smc(E1118Q), ΔscpB		-	-	*Δsmc*
Smc(E1118Q), ΔscpA		-	-	*Δsmc*
Smc(m-hinge)		-	-	*Δsmc*
Smc(m-hinge, E1118Q)		green	red	*Smc(E1118Q)*
Smc(m-hinge), ΔscpA		-	-	*Δsmc*
Smc(m-hinge, E1118Q), ΔscpB		light green	red	*Δsmc*
Smc(m-hinge, E1118Q), ΔscpA		green	red	*Smc(E1118Q)/Δsmc*
Smc(Δhinge)		-	-	*Δsmc*
Smc(Δhinge, E1118Q)		green	red	*Smc(E1118Q)*
Smc(Δhinge, E1118Q), ΔscpA		green	red	*Smc(E1118Q)*
Smc(Δ469-704, E1118Q), ΔscpA		green	red	*Δsmc*
Smc(Δ438-735, E1118Q), ΔscpA		green	red	*Δsmc*
Smc(Δ415-784, E1118Q), ΔscpA		green	red	*Δsmc*
Smc(Δ371-802, E1118Q), ΔscpA		green	red	*Δsmc*
Smc(Δ316-857, E1118Q), ΔscpA		green	red	*Δsmc*
Smc(Δ278-921, E1118Q), ΔscpA		green	red	*Δsmc*
Smc(Δ262-911, E1118Q), ΔscpA		green	red	*Δsmc*
Smc(Δ262-942, E1118Q), ΔscpA		-	-	*Δsmc*

Figure 19. Alignment of Smc protein sequences among different Firmicutes

Alignment of *B. subtilis, Listeria monocytogenes, Staphylococcus aureus, Lactobacillus casei* and *S. pneumoniae* Smc protein sequence. The different colors indicate different conserved properties of the amino acid residues.

When T922 was present in the Smc(E1118Q) truncation, the construct localized to the chromosome, when the next 21 residues were removed (until Q943) localization was no longer present (Fig. 18), the two aforementioned residues are indicated. The stars indicate the three residues that were mutagenized in an attempt to identify a potential ParB binding site. Alignment was a courtesy of Dr. S. Gruber.
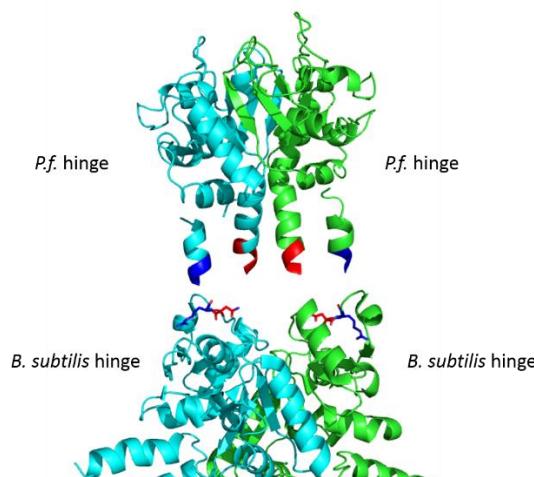

Figure 20. Schematic representation of the double hinge construct.

The *B. subtilis* hinge is connected to the *P. furiosis* (*P.f.*) hinge with a four amino acid long flexible linker. The connections are according to the indicated colors, blue and red.

Courtesy of Dr. Byong-Ha Oh and his lab members, Korea Advanced Institute of Science and Technology, Daejon, Korea.

4.1.9 Is hinge opening required for localization to *parS* sites?

The results above show that an open, or absent, hinge in the Smc complex promotes localization to *parS* sites. This suggests that a wild-type hinge domain in the Smc complex might hinder localization to *parS* sites and that the hinge might need to change its conformation for efficient recruitment to *parS* sites. This would imply that reducing the efficiency of conformationally changing the hinge domain will lead to decreased chromosomal localization. To test this, collaborators from the Oh lab in Korea placed an additional hinge 'above' the *B. subtilis* hinge (Fig. 20). The reasoning behind this was that dimerization of these two hinge domains would lead to a decrease in the efficiency of the conformational change in the hinge to occur. When these double hinge constructs were investigated in *B. subtilis* they localized similarly as open hinge proteins (Fig. 21A) and expression levels were slightly reduced (Fig. 21B), suggesting that protein folding may be affected in these double hinge mutants. Therefore, it was decided to not proceed with further experiments.
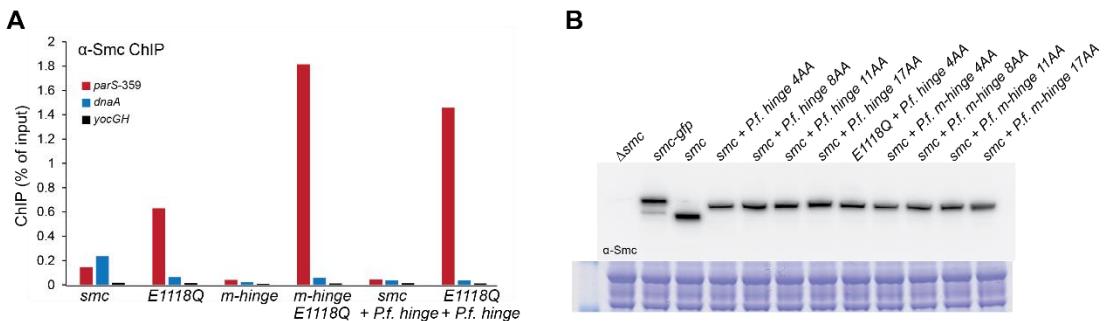

Figure 21. Smc with a double hinge and engaged heads localizes to the chromosome
    A.   ChIP-qPCR using α-Smc antiserum on strains BSG 1002, 1008, 1624, 1547, 1888 and 1900.
    B.   Western blot using α-Smc antiserum on strains BSG 1007, 1067, 1002, 1955, 1958, 1956, 1959, 1900, 1975, 1976, 1977 and 1978. Smc + p.f. hinge indicates the Smc(double hinge) proteins, AA stands for the amino acid length of the linker between the two hinges, see Chapter 7.1 for more details.

4.1.10 The level of ParB determines the level of Smc(E1118Q) recruitment to the chromosome

The Smc complex may have several modes of associating with the chromosome. For example, Smc may associate with the chromosome via a direct interaction with the DNA. Another possible association with the chromosome may be via an interaction with ParB. Little is known about the interaction between the Smc complex and ParB. This thesis work and previous studies (Gruber & Errington, 2009; Sullivan et al., 2009) suggest that the interaction of ParB with the Smc complex lies presumably within the Smc protein (Figs. 9, 12, 17 and 18). Figures 9C and D show that the amount of ParB that is present on a *parS* site roughly correlates with the amount of Smc(E1118Q) that localizes to those *parS* sites. This provides additional evidence that ParB and Smc may directly interact. However, it cannot be excluded that these levels of both proteins are influenced by the genomic surroundings, such as the presence of other proteins in those regions or DNA architecture.
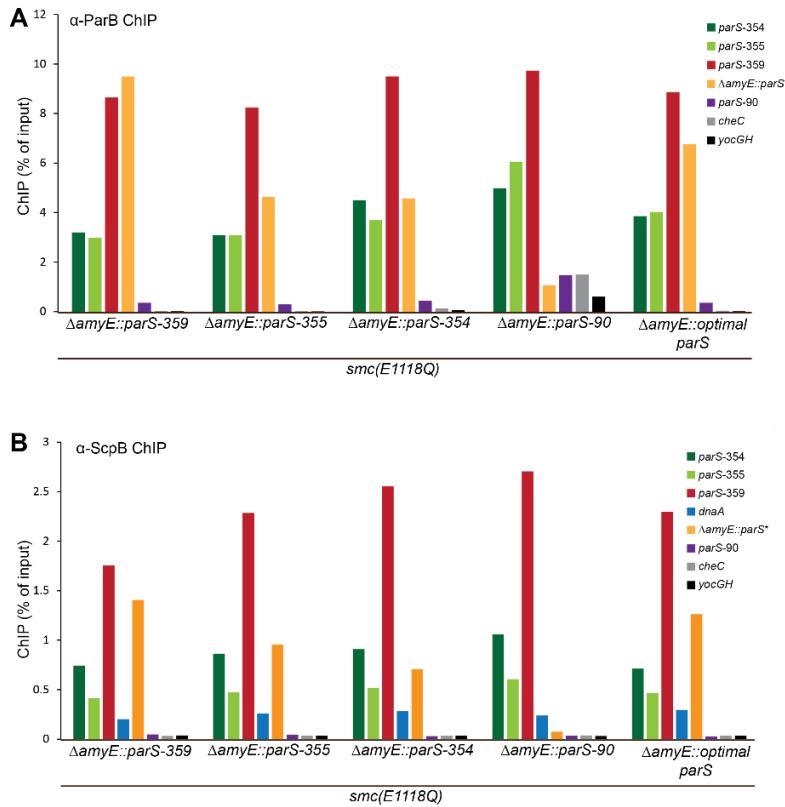
Figure 22. The level of ParB determines the level of Smc(E1118Q) recruitment to the chromosome
A.ChIP-qPCR using α-ParB antiserum of strains BSG 1471, 1541, 1542, 1543 and 1544. In the strain harboring *ΔamyE::parS*-90 a slight contamination is indicated by the increased enrichment of *cheC* and *yocGH*. However, since it is only minor the result is still reliable.
B. ChIP-qPCR using α-ScpB antiserum of strains BSG 1471, 1541, 1542, 1543 and 1544. The enrichment was normalized to the levels of *cheC* and *yocGH* of the strain harboring *parS*-355 at *amyE*.
Cells were grown in competence medium.

To get a deeper insight into this, in a strain harboring Smc(E1118Q), which localizes mostly to ParB binding sites on the chromosome (Fig. 9), different single ectopic *parS* sites were integrated at the non-essential *amyE* gene 328 kb away from the *oriC*, making strains that harbor 11 instead of 10 *parS* sites. Non-endogenous qPCR primer sequences were added at the *amyE* site in order to measure its ChIP enrichment by qPCR later on. Four different *parS* sites were tested, *parS*-359 which has high enrichment for ParB and Smc, *parS*-354 and -355 which have intermediate ParB enrichment and *parS*-90 which has low ParB enrichment (Fig. 9). In addition, a perfect palindromic sequence described as the optimal *parS* site with the most common nucleotide between the ten *parS* sites in *B. subtilis* at each position was inserted (Breier & Grossman, 2007). Whether or how much ParB localizes to this optimal *parS* site is unknown. ChIP-qPCR with α-ParB antiserum showed that ParB was enriched with the highest levels on the endogenous *parS*-359 in the tested strains except for the ectopic *parS*-359 which was enriched for ParB slightly more than the endogenous *parS*-359 sites (Fig. 22A). In all tested strains *parS*-354 and -355 showed intermediate ParB enrichment and *parS*-90 showed low ParB enrichment, as was previously observed (Breier & Grossman, 2007). At the ectopic *parS* sites at *amyE* this pattern of enrichment was also observed indicating that it is the actual *parS*-sequence that dictates the different levels of ParB. Surprisingly, the 'optimal' *parS* site did recruit more than intermediate levels of ParB (*parS*-354 and -355), but not to the levels of *parS*-359 showing that this palindromic sequence is not the most optimal sequence for ParB recruitment (Fig. 22A). This pattern of enrichment, high localization to *parS*-359, intermediate localization to *parS*-354 and -355,

low localization to *parS*-90 and suboptimal localization to the 'optimal' *parS* site, was also observed for ScpB in the presence of the Smc(E1118Q) protein (Fig. 22B). This shows that the *parS* sequence, and not the genomic surrounding, dictates the level of ParB at the *parS* site. Furthermore, this demonstrates that the levels of ParB determine the amount of ScpB in the presence of the Smc(E1118Q) protein and thus presumably the levels of the Smc(E1118Q) complex that localizes to the *parS* sites and is another indication towards a direct interaction of ParB with Smc.

4.1.11 ParB spreading appears to be required for Smc recruitment to the chromosome

Fluorescence microscopy data indicated that ParB spreading mutants (ParB(G77S)) and ParB(R80A)) no longer recruit the Smc complex to the chromosome (Graham et al., 2014). ChIP-seq data demonstrates that ParB(G77S) localizes to *parS* sites in sharp peaks and compacts DNA *in vitro*. ParB(R80A) does not compact DNA *in vitro,* it also localizes to *parS* sites in sharp peaks but the height of the peaks are reduced compared to wild type and ParB(G77S) (Autret et al., 2001; Breier & Grossman, 2007; Graham et al., 2014). Although wild-type Smc does not localize in these spreading mutants as judged by fluorescence microscopy (Graham et al., 2014), residual localization to the *parS* sites might still be observed by ChIP, especially for Smc mutant proteins that show strong localization to these sites. To test this, ChIP-qPCR was performed using α-Smc antiserum on strains harboring wild-type Smc or Smc(m-hinge, E1118Q) in the presence of ParB, ParB(G77S), ParB(R80A) or in the absence of ParB (Fig. 23A).
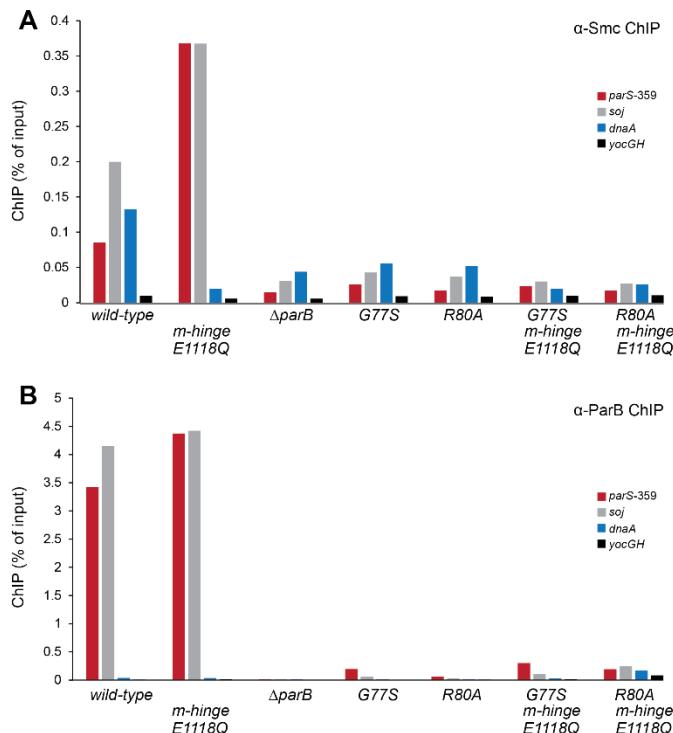
**Figure 23. Smc appears to not localize to ParB spreading mutants**
A.ChIP-qPCR using α-Smc antiserum on strains BSG 1051, 1974, 1050, 1943, 1944, 1972 and 1973.
B.ChIP-qPCR using α-ParB antiserum on strains BSG 1051, 1974, 1050, 1943, 1944, 1972 and 1973. Strain ParB(R80A), Smc(m-hinge, E1118Q) (BSG 1973) shows higher enrichment at the terminus locus (*yocGH*) and might be slightly contaminated.

Wild-type Smc in the presence of the ParB spreading mutants showed very little localization with levels similar to *ΔparB* (Fig. 23A). Enrichment for Smc(m-hinge, E1118Q) in combination with the ParB spreading mutants was similarly low. In addition, the observed enrichments, if at all, were not specific for the tested *parS* site, indicating that no recruitment of Smc takes place. Performing the same experiment using α-ParB antiserum showed only very little localization of the ParB spreading mutants to *parS*-359 (Fig. 23B). Enrichment at a locus directly adjacent (within 1.5 kb) to *pars*-359 (*soj*) was measured to test whether the localization was specific for this *parS* site. Wild type displayed similar levels of high enrichment to *parS*-359 and *soj*, presumably due to its spreading capabilities. ParB(G77S) showed decreased enrichment at the *soj* locus compared to the *parS*-359. This shows that ParB(G77S) has low but specific enrichment for the tested *parS* site in an ChIP protocol (Fig. 23B).

Previously, decreased but sharp localization of ParB(G77S) to *parS* sites was reported by using ChIP-on-chip (Breier & Grossman, 2007). On the contrary, Graham et al., 2014 reported for ParB(G77S) sharper peaks for all *parS* sites, similar levels for *parS*-354-355-356 and higher levels for *parS*-359 compared to wild type using ChIP-seq. For ParB(R80A) decreased localization in sharper peaks to *parS* sites was observed as compared to wild type using ChIP-seq (Graham et al., 2014). Although the observed distribution of ParB(G77S) in the ChIP-qPCR experiments presented here may correlate with the previously observed distribution (in sharper peaks at *parS* sites), the amount of localization compared to wild type does not correlate. The results for Smc(m-hinge, E1118Q) should therefore be very carefully interpreted. Nevertheless, these results are an additional minor indication that ParB spreading is indeed required for Smc recruitment to the chromosome.

4.2 Translocation of Smc on the chromosome in *B. subtilis*

The work performed in this thesis so far indicates that the Smc complex is recruited to the chromosome in a pre-hydrolysis state and that hydrolysis is required for wild type distribution over the chromosome. It was suggested for yeast cohesin that after initial loading of the SMC complex, the complexes translocate over the chromosome (Hu et al., 2011). For bacterial MukBEF it was also suggested that it was capable of translocating over the chromosome (Badrinarayanan et al., 2012b). For yeast cohesin it was proposed that it is aided in translocation by the transcription machinery (Lengronne et al., 2004; Schmidt et al., 2009). It is poorly understood whether translocation contributes to chromosome segregation. To be able to investigate this in the model organism *B. subtilis* it is important to know whether the Smc complex translocates in this organism.

4.2.1 The Smc complex translocates from loading sites to other parts of the chromosome

From the data above it is clear that the Smc complex does not need its hinge, nor its kleisin or additional subunits to localize to the chromosome. However, when the hinge or subunits are absent, localization only takes place if ATP hydrolysis is blocked. In that case, the observed localization is different from wild type. All Smc variants blocked in ATP hydrolysis localize to *parS* sites where presumably its loading onto the chromosome takes place. Only in the wild-type situation where ATP hydrolysis can take place the Smc complex seems to be capable of localizing to other proximal sites. It is however unclear how the Smc complex relocates from the loading sites to the other proximal sites. To deeper investigate whether the Smc complex in *B. subtilis* indeed translocates from its loadings sites to other sites on the chromosome an ectopic loading site (*parS*-359) was introduced in the wild-type *B. subtilis* genome at the *amyE* locus. In addition, a construct containing a mutant non-functional *parS* site (*mtparS*) (Murray et al., 2006) was also introduced into *B. subtilis*. To get a chromosome wide overview of the differences in localization of the Smc complex in the presence and absence of the ectopic *parS*-359 site, ChIP-seq was performed with an α-ScpB antiserum. The IP was normalized for the input by counting the mapped reads in 5000 bp sliding windows, the number of reads in a window for the IP sample was divided by the number of reads in the corresponding window of the input sample (Fig. 24A). In general, the distribution of ScpB on the chromosome for both strains look very similar and resemble the distribution obtained with the α-Smc antibody with occasional small differences (see Chapter 4.2.4). Comparing the strain with the *parS*-359 site at *amyE* to the strain with the *mtparS* at *amyE* in more detail reveals that there is more ScpB present around the *amyE* site when *parS*-359 is present. To more clearly distinguish the differences in distribution between the two strains a ratio was calculated between the two strains. First, the normalized number in each 5000 bp window of the ectopic *parS*-359 strain was divided by the normalized number in the corresponding 5000 bp window of the *mtparS* strain. Now, a number above 1 indicates that there were more reads in this window for *parS*-359 at *amyE*, a number below 1 indicates that there were more reads for *mtparS* at *amyE*. In order to show this on axes that have the same scaling for enriched and unenriched ratios, the ratio was converted
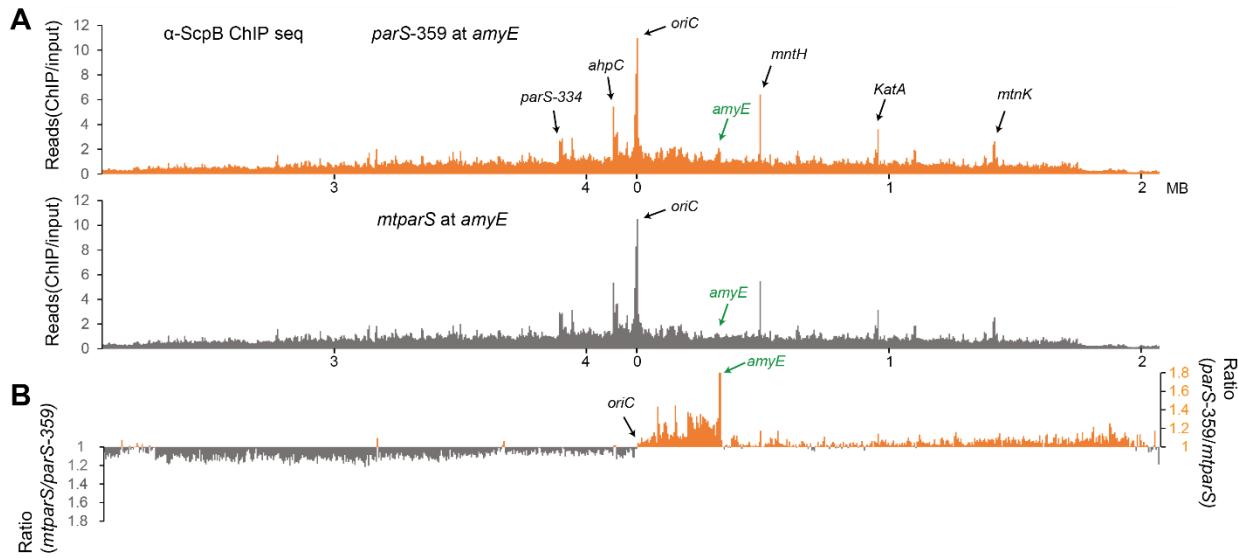
Figure 24. Smc translocates from loading sites to other parts of the chromosome

    A.   ChIP-seq using α-ScpB antiserum on BSG 1469 and 1470. Mapped reads were counted in 5000 bp windows, the amount of reads in the 5000 bp windows of the IP sample was divided by the amount of reads in the corresponding window of the input sample and plotted.

    B.   Ratio of the ChIP-seq signal that shows the difference in distribution of Smc of the two strains shown in A. The *amyE* locus is displayed in green, other genetic loci are in black.

as follows: If the number was above 1 the number stayed unchanged and this was plotted on one side of the x-axes, if the number was below 1 then the reciprocal value was used instead and plotted on the other side of the x-axes. The resulting graph shows values above the x-axes when more ScpB was present in the *parS*-359 at *amyE* strain and values below the x-axes when more ScpB was present in the *mtparS* at *amyE* strain, both on a linear scale (Fig. 24B). When *parS*-359 is present at the *amyE* locus more ScpB is localized between *oriC* and *amyE* than for the *mtparS*, with a clear cut off at *oriC*. Furthermore, more ScpB is present over the entire right arm of the chromosome. In contrast, on the left arm of the chromosome clearly less ScpB is present (Fig. 24B). This suggests that the Smc complex loaded at the *parS*-359 site at *amyE* is capable of translocating from its loading site to the region between *oriC* and *amyE* and to the entire right arm of the chromosome. The extra Smc complex that is localized there is likely depleted from the left arm of the chromosome.

4.2.2 The architecture of the Smc hinge and arrangement of the hinge-proximal coiled-coils may play a role in translocation

From the work described in this thesis it can be concluded that a functional hinge is necessary for wild-type distribution on the chromosome. What the hinge exactly does is, however, not exactly clear. Other members in the lab made different chimeric Smc proteins in *B. subtilis* Smc where the hinge and short stretches of the adjacent coiled-coil were replaced with the hinge domain of other Smc (or Rad50) proteins from other organisms. The chimeric Smc proteins were expressed from the endogenous *smc* locus as the only copy in the cell. When the *B. subtilis* hinge was substituted with hinges from the closely related species *Bacillus*
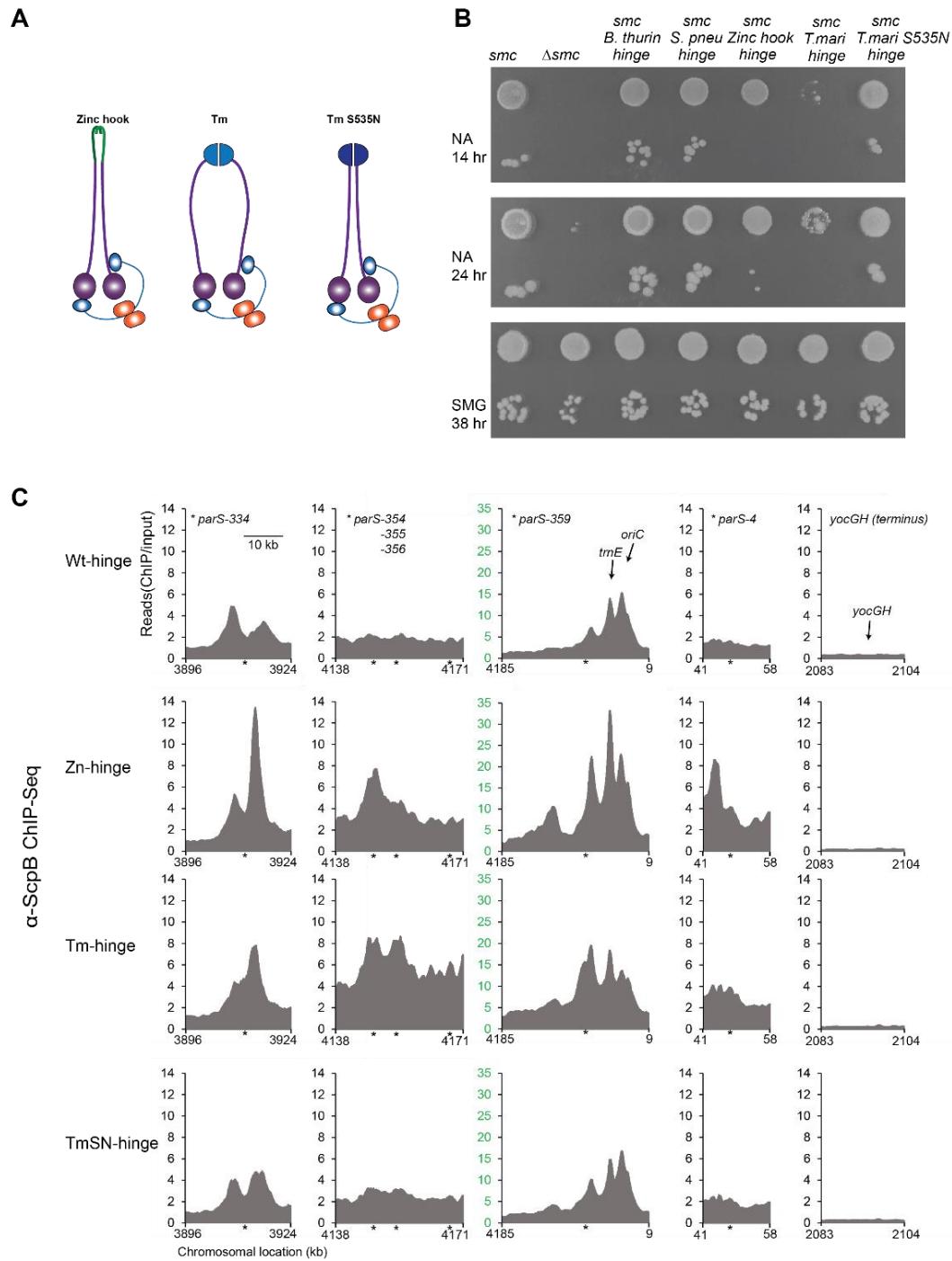
Figure 25. Properties of chimeric Smc proteins

A. Schematic overview of three chimeric hinge Smc proteins. Zinc hook shows the Smc chimera with the zinc hook dimerization domain from Rad50, the conformation of the hinge-proximal part of the coiled-coils is unknown. Tm stands for the *T. maritima* chimera which has the more ring like structure, Tm S535N stands for the suppressed *T. maritima* chimera which adopts to the more rod-like structure.

B. Colony formation assay using strains BSG 1002, 1007, 1017, 1018, 1075, 1592 and 1688.

C. ChIP-seq using α-ScpB antiserum on strains BSG 1470, 1997, 1999 and 2001. Reads were counted in 1000 bps every 100 bps and normalized as described in Chapter 3.7. Green axes indicate different scaling compared to the other graphs.

63

thuringiensis and *S. pneumoniae* viability was not impaired indicating wild-type functioning of these Smc proteins (Fig. 25B). When the hinge was substituted with the Rad50 zinc hook from *P. furiosis* (*smc(Zn hinge)*) (Fig. 25A) single colonies were formed on NA but slower than for wild-type Smc indicating a mild defect in this chimeric protein (Fig. 25B). Interestingly, this defect is partially restored when this chimeric protein is expressed from the *amyE* locus (Fig. 11B).

In the crystal structure of the *T. maritima* hinge domain the coiled-coils extend side-ways from the hinge domain (Haering et al., 2002) (Fig. 5B and 25A). In the recently obtained structure of the hinge domain of *P. furiosis* the coiled-coils extend downwards from the hinge and showed a rod-like conformation (Fig. 5C) (Soh et al., 2014). Soh and coworkers using *B. subtilis* Smc showed that upon DNA and ATP binding the hinge-proximal part of the coiled-coils changes from an aligned state into a more ring-like conformation (Soh et al., 2014). In addition, they made chimeras of *B. subtilis* Smc where the *B.subtilis* hinge was replaced with the *T. maritima* hinge domain. In *B. subtilis* this chimeric Smc is non-functional, however screening for suppressor mutations in the hinge that support growth on NA revealed several mutations close to the connection between the hinge and the coiled-coils (Soh et al., 2014). Testing the conformation of the hinge-proximal coiled-coils by crosslinking experiments showed that the non-suppressed *B. subtilis-T.maritima* chimeric protein has the more ring-like state (open coiled-coils) whereas the suppressed (S535N) *B. subtilis-T.maritima* chimeric protein adapted more frequently the rod-like conformation (Soh et al., 2014) (Fig. 25A), indicating that the rod-like conformation is important for *in vivo* functioning. The finding that the chimera with the *T. maritima* hinge (*Smc(Tm hinge)*) did not support growth on NA and that the suppressed (S535N) *T. maritima* hinge (*Smc(TmSN hinge)*) did support growth on NA to wild-type levels was confirmed (Fig. 25B).

To test whether the observed growth defects, presumably caused by differences in the conformation of the hinge-proximal coiled-coil had effects on chromosomal localization and/or translocation of the Smc complex, ChIP-seq was performed on wild-type Smc, Smc(Zn hinge), Smc(Tm hinge) and Smc(TmSN hinge). The α-ScpB antiserum was used for the IP to counteract for differences in moiety recognition of the different hinges of the α-Smc antiserum, for simplicity the Smc proteins are denoted. The growth impaired chimeras, Smc(Zn hinge) and Smc(Tm hinge), showed higher localization levels to the *parS* sites and its surroundings than wild type and Smc(TmSN hinge) (Fig. 25C). Also the distribution at and around the *parS* sites is different for Smc(Zn hinge) and Smc(Tm hinge) compared to wild type and Smc(TmSN hinge) with sharper peaks at or directly adjacent to the *parS* sites (Fig. 25C). Strikingly, the localization of Smc(TmSN hinge) resembled wild-type localization almost identically at the *parS* sites and *oriC* region (Fig. 25C). Investigating the distribution on a larger scale revealed that Smc(Zn hinge) and Smc(Tm hinge) localize much more around *oriC* and less on the extended arms of the chromosome compared to wild type (Fig. 26A). To better visualize the differences in distribution, ratios were calculated as in Figure 24B between the chimeric proteins and wild type. From the ratio it is clear that Smc(Zn hinge) and Smc(Tm hinge) do localize in higher levels around the *oriC* up to the region adjacent to *parS*-354 and to the right of *parS*-334 than wild type. Localization for these two chimeras is less on the arms of the chromosome compared to wild type

(Fig. 26B). In addition, Smc(TmSN hinge) also localizes to higher levels around the *oriC* than wild type but to a much lesser extent than the two non-functional chimeras (Fig. 26B).
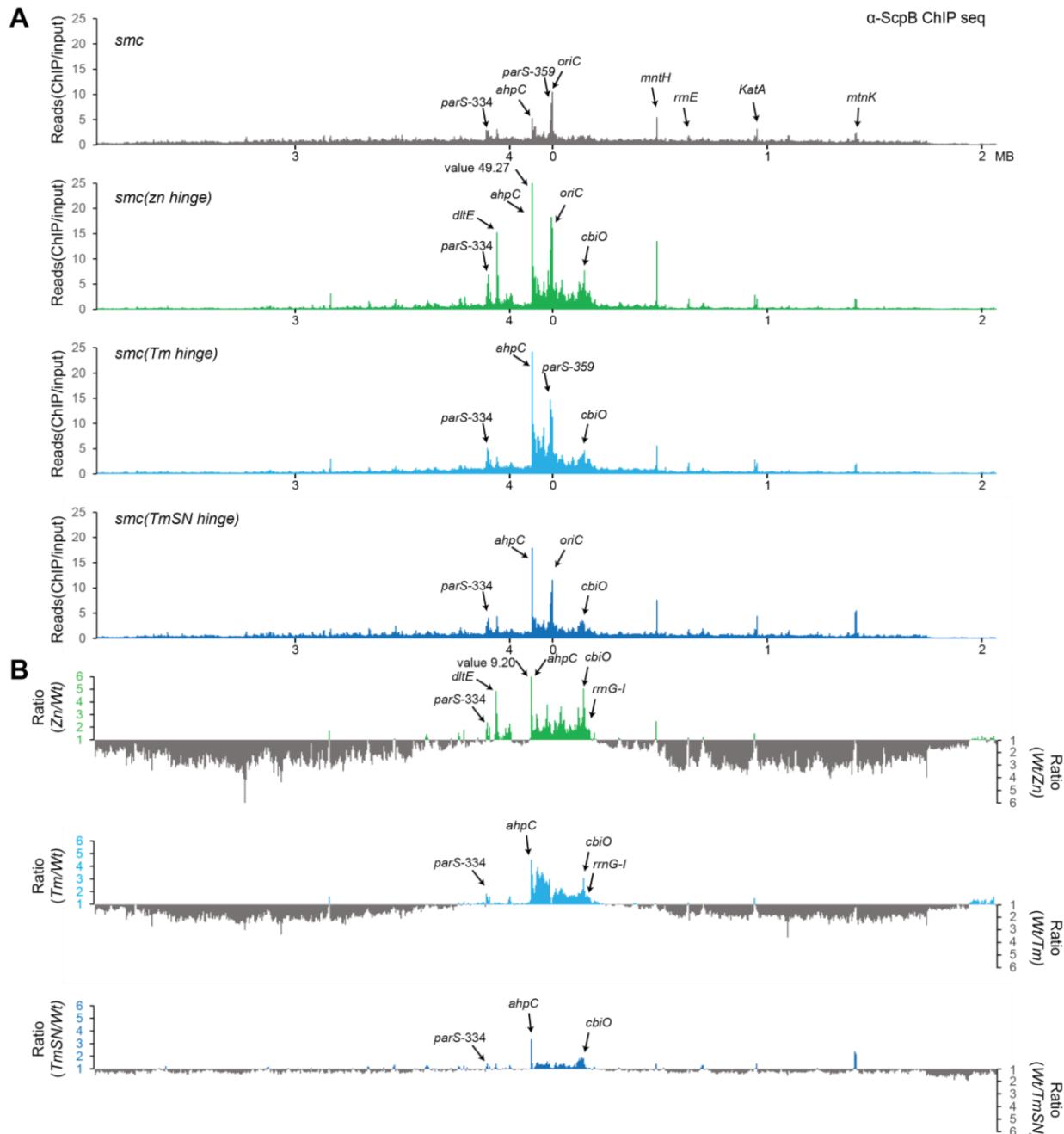
Figure 26. Genome-wide overview of chimeric Smc complex localization tested by α-ScpB ChIP
  A. ChIP-seq using α-ScpB antiserum on strains BSG 1470, 1997, 1999 and 2001.
  B. Ratio of the ChIP-seq signal that shows the difference in distribution of Smc of the strains shown in A.
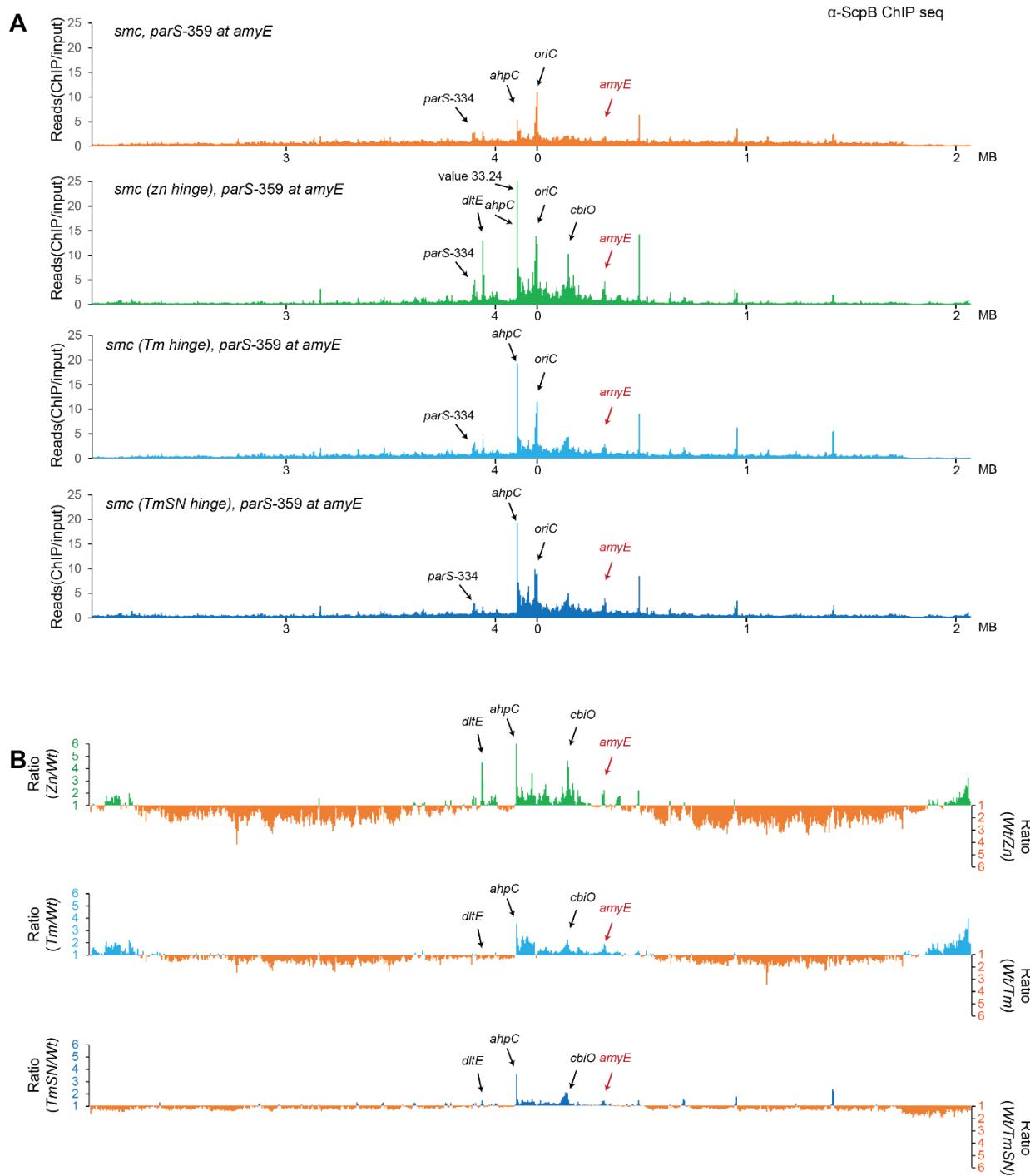
Figure 27. Genome-wide overview of chimeric Smc complex localization in the presence of an additional *parS* site
  A. ChIP-seq using α-ScpB antiserum on strains BSG 1469, 1996, 1998 and 2000.
  B. Ratio of the ChIP-seq signal that shows the difference in distribution of Smc of the strains shown in A.

To be able to observe differences in localization patterns that these chimeric proteins may have outside the *oriC* region experiments were performed with an additional *parS*-359 site at *amyE* (Fig. 27). The chimeric proteins localize more at the *parS*-359 site at *amyE* than wild type, with most localization for Smc(Zn hinge) and rather little for Smc(TmSN hinge) (Fig. 27A). To be able to observe the differences in this distribution better, ratios were calculated as in Figure 24B between the chimeric proteins and wild type. These ratios show that the amount of chimeric protein present at the ectopic *parS*-359 site is indeed increased, however the amount of chimeric proteins adjacent to this *parS*-359 site does not differ much from wild-type levels (Fig. 27B) implying that the chimeric proteins are capable of translocating from the loading site to proximal chromosomal regions. This is underlined when this experiment is compared to a similar experiment using wild-type Smc and Smc(E1118Q) in the presence of the additional *parS*-359. The levels of Smc(E1118Q)
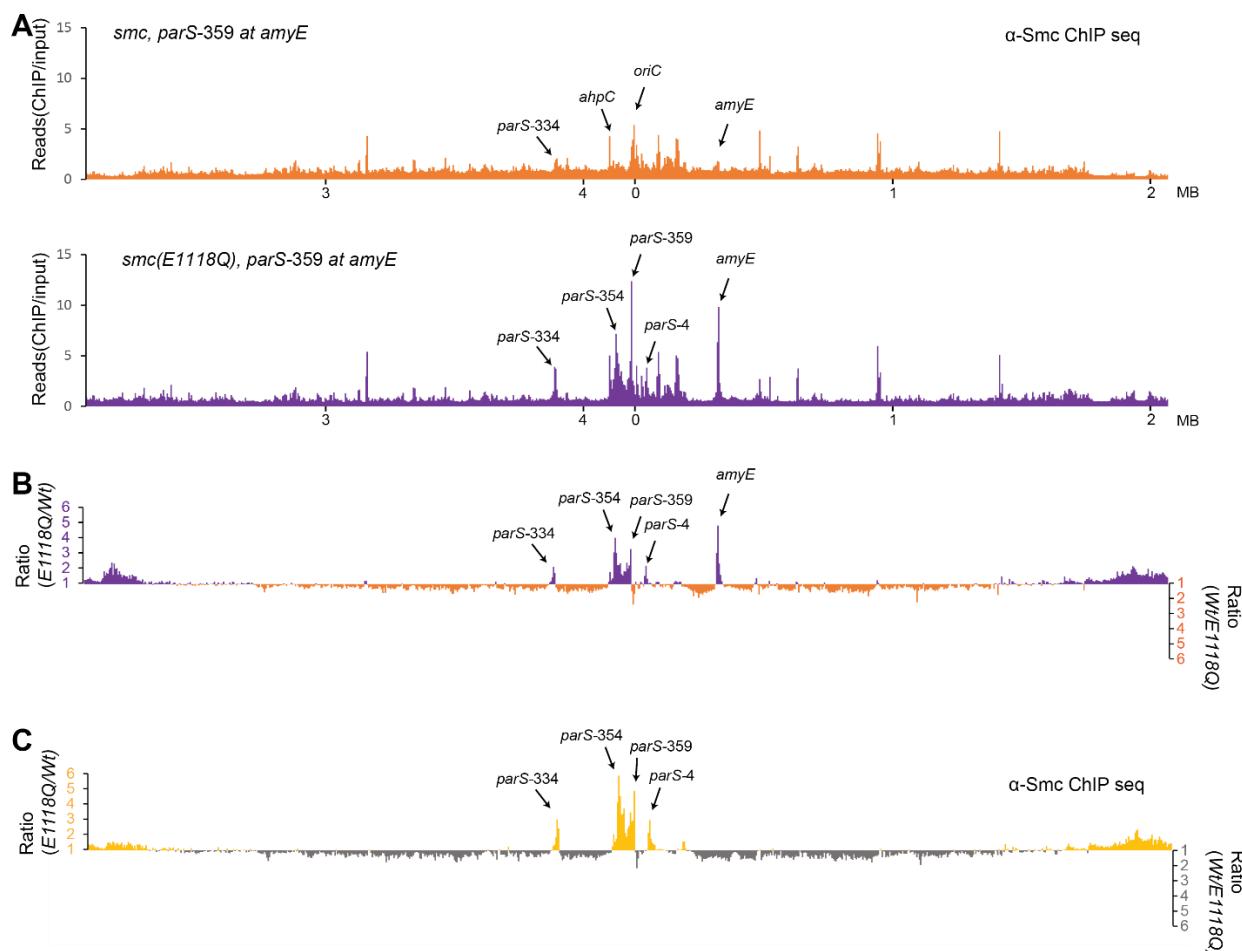
**Figure 28. Differences in distribution of wild-type Smc and Smc(E1118Q)**
    A. ChIP-seq using α-Smc antiserum on strains BSG 1469 and 1471.
    B. Ratio of the ChIP-seq signal that shows the difference in distribution of Smc and Smc(E1118Q) of the strains shown in A.
    C. Ratio of the ChIP-seq signal that shows the difference in distribution of Smc and Smc(E1118Q) of the strains shown in figure 9 (BSG 1002 and 1008).

at the additional *parS*-359 are clearly higher than for wild type, the levels around this *parS* site are, in contrast, clearly lower (Fig. 28A-B) suggesting that Smc(E1118Q) is not capable of translocating from its loading site. Furthermore, comparing the ratio of wild-type Smc to Smc(E1118Q) localization without the additional *parS* site with those ratios for the chimeric proteins (compare Fig. 28C with 26B) clearly shows a different pattern with sharper and thus less broad localization of Smc(E1118Q) to *parS* sites and *oriC* (Fig. 28C). This suggests that Smc(Zn hinge) and Smc(Tm hinge) localize to loading sites and are capable of translocating from there, however since accumulated levels in large regions around the loading sites are observed, translocation seems to be reduced compared to wild type. Smc(TmSN hinge) displays localization patterns much more similar to wild type but does seem to have a minor defect in translocation capabilities. This points towards a role of the capability to form a rod-like formation in the hinge-proximal coiled-coils (Smc(TmSN hinge)) for translocation on the chromosome.

4.2.3 TAP-tagged Smc displays a defect in translocating

Thus far most chromosomal localization studies of Smc complexes have used tagged Smc proteins (Gruber & Errington, 2009; Hu et al., 2011; Minnen et al., 2011). In *B. subtilis*, a deletion of *parB* does not result in impaired growth, however when *parB* was deleted in an *smc-Pk3* or *smc-GFP* strain, the cells were either not viable or very sick, respectively (Gruber & Errington, 2009) indicating that these tagged alleles do not function like wild-type Smc. A deletion of *parB* in the s*mc-TAP* background had no obvious effects on growth (Gruber & Errington, 2009). However, although Smc-TAP may be functional as judged by a growth assay, this does not exclude the possibility that it has some defects. One of these defects could be an altered chromosomal localization. To investigate whether a tag on Smc influences its chromosomal localization, ChIP-seq was carried out with rabbit IgG on an Smc-TAP strain, with an α-ScpB antiserum on a wild-type Smc strain and with an α-Smc serum on a wild-type Smc strain. The latter α-Smc ChIP-seq data was performed in a different experiment and therefore care should be taken in direct comparisons (Fig. 29). Overall, the pattern of localization of Smc, ScpB and Smc-TAP looks very similar with most enrichment around the *oriC* region and clear peaks at the *oriC* and highly transcribed genes (Fig. 29A). However, Smc-TAP localizes more to the *oriC* region, to the *parS* sites as well as to adjacent regions suggesting that Smc-TAP is capable of locally translocating (Fig. 29). In addition, Smc-TAP has decreased localization to the arms of the chromosome compared to Smc and ScpB, suggesting that this protein might have a defect in translocating over large distances on the chromosome.

4.2.4 Potential differences in localization of Smc and ScpB

Previously, differences in dynamics of ScpAB and Smc were reported (Kleine Borgmann et al., 2013b). In time-lapse imaging, Smc was found to have a mobile fraction (80%) and a static fraction (20%) on the chromosome, whereas ScpA and ScpB were found to be mostly static (87%) (Kleine Borgmann et al., 2013b). Other than this microscopy data not much is known about differences between Smc and Smc in complex with ScpAB. To investigate whether Smc and ScpB (presumably mostly in complex with Smc and

ScpA) localize differently on the chromosome, ChIP-seq was carried out once using the α-ScpB antiserum and once using the α-Smc antiserum (Fig. 30). The overall pattern of ScpB and Smc are not very different, however local differences can be observed. Calculating the ratios of differences in localization as in Figure 24B shows this more clearly (Fig. 30B). For example, a clear peak is visible of ScpB at the *oriC* (Fig. 30). Smc also localizes in a peak to the *oriC* but this peak is less pronounced compared to ScpB. ScpB localizes more to the left side of *oriC* in a general fashion and not specifically more to *parS* sites than Smc. Overall there is slightly more ScpB over the half of the chromosome that is surrounding the *oriC* whereas Smc seems more present around the terminus regions and highly transcribed genes. Thus, although the overall pattern of localization of ScpB and Smc is very similar distinct differences can also be observed. This suggests a (small) difference in localization for Smc in complex with ScpAB and Smc alone.
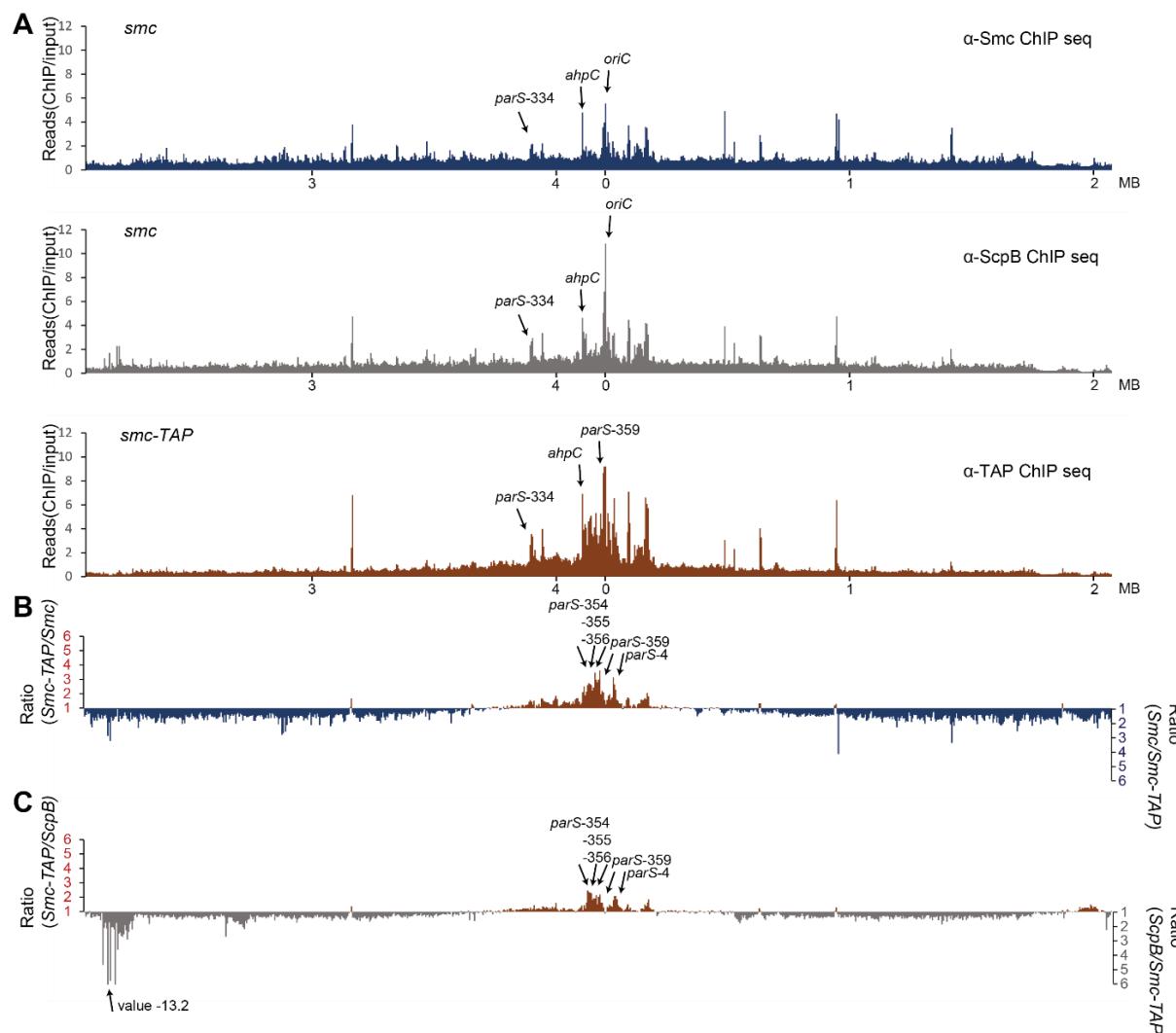
Figure 29. TAP-tagged Smc displays a defect in translocating
A. ChIP-seq with α-Smc antiserum on wild-type Smc, α-ScpB antiserum on wild-type Smc and rabbit IgG on an Smc-TAP strain. Used strains are BSG 1002 and 1016
B. Ratio of the ChIP-seq signal that shows the difference in distribution of Smc and Smc-TAP of the strains shown in A.
C. Ratio of the ChIP-seq signal that shows the difference in distribution of ScpB and Smc-TAP of the strains shown in A.
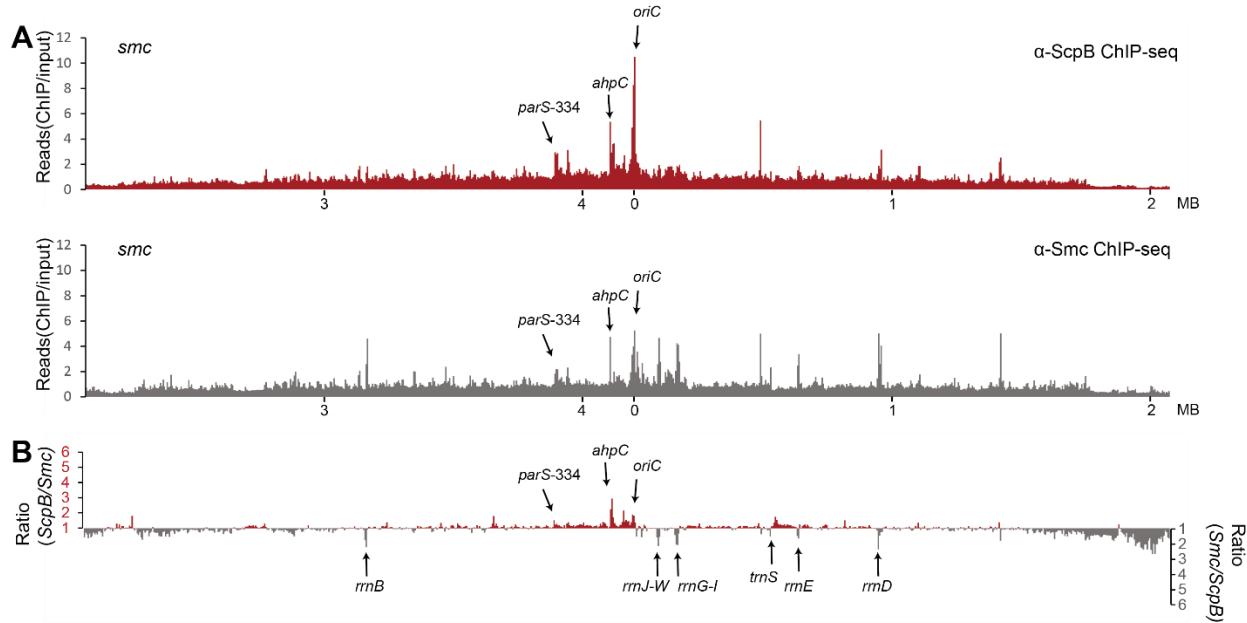
Figure 30. Differences in localization of Smc and ScpB

A. ChIP-seq with α-ScpB antiserum on wild-type Smc and α-Smc antiserum on wild-type Smc. Used strains are BSG 1470 and 1002.

B. Ratio of the ChIP-seq signal that shows the difference in distribution of ScpB and Smc of the strains shown in A.

4.3 Chromosomal interactions mediated by Smc

The work in this thesis suggests that after initial recruitment to the chromosome the wild-type Smc complex translocates over the chromosome and that this translocation is important for Smc functioning. However, it is not understood how exactly Smc achieves this translocation and how it contributes to faithful chromosome segregation. To get a deeper insight into these processes, it is important to understand what the specific association of the Smc complex is with the chromosome. MukBEF and cohesin were shown to be capable of bridging DNA *in vitro* (Petrushenko et al., 2010; Sun et al., 2013). The presumed topological associations of cohesin and condensin with DNA and chromosomal entrapment of Smc-ScpAB also suggest that it may be capable of bridging DNA *in vivo* (Ivanov & Nasmyth, 2005, 2007; Haering et al., 2008; Cuylen et al., 2011; Murayama & Uhlmann, 2013; Wilhelm et al., submitted). Therefore, a possible interaction of the Smc complex in *B. subtilis* with the chromosome may involve bridging of chromosomal loci.

4.3.1 Elucidating chromosomal interactions mediated by Smc one-by-one using ChIP-3C in *B. subtilis*

The emergence of 3C-techniques (Box 1) in the last decade makes it feasible to elucidate interactions within chromosomes. However, to determine loci specifically held together by Smc, 3C performed with wild type has to be compared to 3C performed in the absence of Smc. The absence of Smc in *B. subtilis* results in a strong defect including a reduced growth rate and aberrations in chromosome segregation and organization. Therefore, loci appearing to interact via Smc in a 3C experiment might be of indirect consequences from the severe defects rather than from direct interactions mediated by the Smc complex. The use of Smc mutants is omitted when 3C is preceded by ChIP. This enriches for the loci specific for Smc and gives a higher probability of elucidating the specific loci brought together by Smc. Therefore, ChIP-3C was the method of choice. Protocols specific for ChIP-3C were not available, therefore several adaptations to existing 3C and ChIP protocols were made. This included increased input material, reduced sonication to allow for larger DNA fragments, selecting and testing an appropriate restriction enzyme and ligation on beads as trying to elute the crosslinked DNA-protein complexes from the beads resulted in very low DNA yields. To quantify the ligation products, specific primers designed over potentially ligated DNA were used in Taqman PCR (Table 2). Since ParB binds to the ten *parS* sites in the *B. subtilis* genome and usually only one focus per *oriC* can be observed in fluorescence microscopy of live cells (Glaser et al., 1997), ParB may actually tether different *parS* sites. To test this, ChIP-3C experiments were also performed for ParB. In Figure 31, the ChIP enrichments and ChIP-3C results are shown. For ScpB, the general pattern suggests that the higher the ChIP enrichment, the higher the amount of DNA loci brought together between *parS*-359 and the other indicated loci (Fig. 31A). For ParB, the overall pattern looks similar with high ChIP-enriched loci showing higher ChIP-3C signals (Fig. 31B). In 3C derived methods, random ligations occurring during the proximity ligation step are considered background. However, abundant DNA have a higher
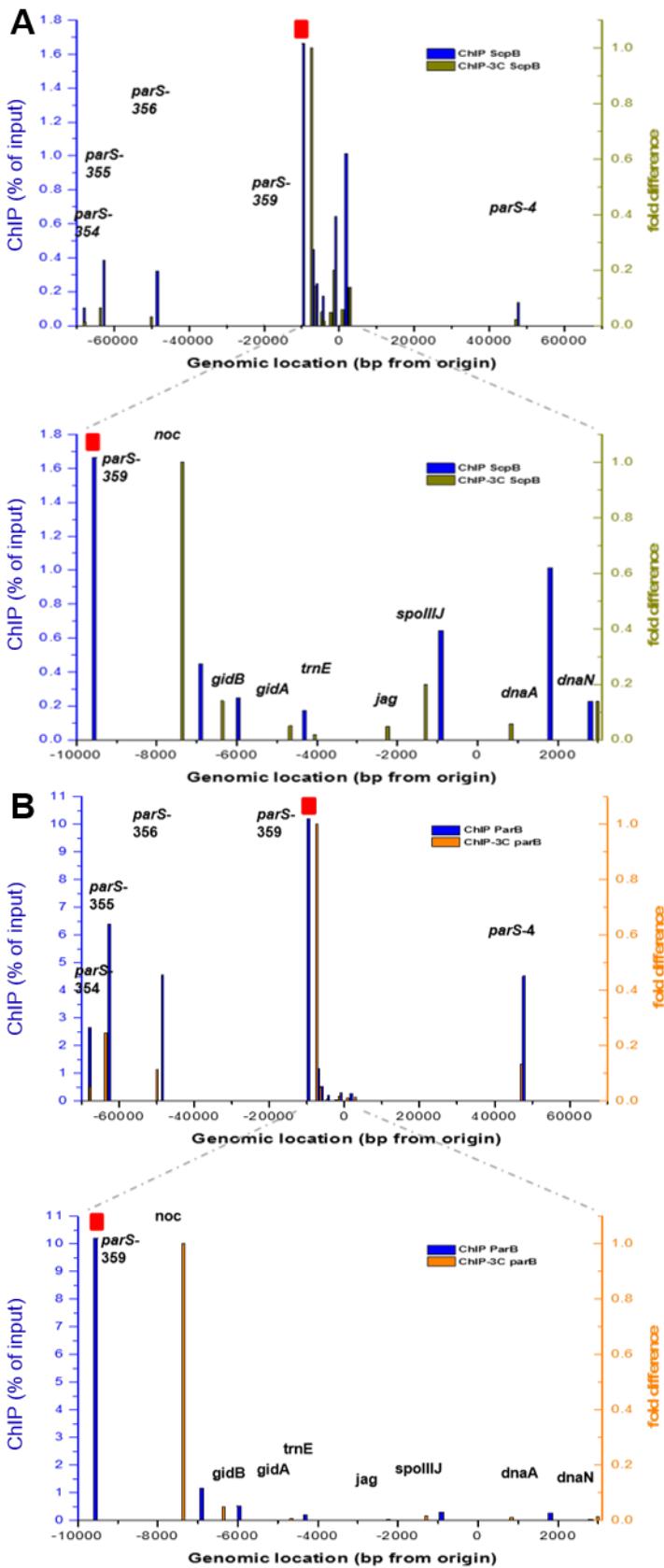
Figure 31. ChIP-3C on ScpB and ParB

A.ChIP-3C performed with α-ScpB antiserum on wild-type *B. subtilis* cells. In blue the ChIP enrichments are shown, in green the ChIP-3C measurements. The red square indicates where the used Taqman probe was positioned, and thus between which locus and other loci on the chromosome the interactions were measured. For ChIP-3C data the fold difference was calculated from the differences in Ct values in the Taqman qPCR compared to the *noc* locus.

B.ChIP-3C performed with α-ParB antiserum on wild-type cells. ChIP enrichments are shown in blue, the ChIP-3C measurements are shown in orange. Other features see A. Used strain for both samples was BSG 1001. Cells were grown in competence medium.

probability to ligate. Because 3C was preceded by ChIP, the DNA loci of interest are enriched and therefore have a higher probability to randomly ligate. To obtain specific ChIP-3C signals additional controls are needed. Other 3C derived methods account for the frequency of random ligations by internal controls, therefore one of these methods was chosen to elucidate chromosomal interactions mediated by Smc.

4.3.2 Elucidating chromosomal interactions mediated by Smc genome-wide using ChIA-PET in *B. subtilis*

The ChIA-PET method accounts for the frequency of random ligations by using an internal control of different linkers which can be distinguished and used for statistical analysis (Box 2). Furthermore, a genome-wide overview of the loci that are held together are given. Therefore, due to this advantage, ChIA-

---

Box 2. Overview of the ChIA-PET method

During the ChIP procedure DNA that is crosslinked to a protein of interest is coupled onto a bead via an antibody. These beads are split into two different aliquots, to each aliquot a different linker is ligated (A or B). The beads to which the different linkers were ligated are subsequently mixed again after which proximity ligation is performed. This results in differently ligated DNA, 1) self-ligations, occurring to a single DNA strand which are usually less than 5 kb in size, the linker composition is non-chimeric (AA or BB) 2) intra-molecular ligations, the ligations that is sought after in the 3C methods in which two DNA strands held together by a single protein (complex) ligate to each other also resulting in non-chimeric linker composition (AA or BB), 3) inter-molecular ligations where two DNAs that are held by two separated proteins attached to the same bead ligate, this produces a non-chimeric linker composition (AA or BB) or 4) inter-bead ligations where DNAs attached to proteins on different beads ligate this gives chimeric (AB or BA) and non-chimeric (AA or BB) linker compositions. The DNA is subsequently cleaved with *Mme*I which cleaves 20 bps away from its recognition site (which is present in the linkers). The DNA is purified with streptavidin coated beads (the linkers contain a biotin tag), purified and adapters necessary for high throughput sequencing are ligated to the fragment. The DNA is amplified by PCR after which the library can be sequenced.

PET was chosen, over ChIP-3C, to study the loci held together by Smc and ParB directly in a genome-wide manner. At the start of this project at the end of 2011, the ChIA-PET method was relatively new and had only been performed in mammalian cells (Fullwood *et al.*, 2010). Therefore, ChIA-PET needed to be adapted for use with *B. subtilis*. Optimizations were based on experience with the ChIP-3C protocol. These included adjusting the amount of input cells, performing proximity ligation on the beads, optimization of DNA purification and performing reactions in smaller volumes. After optimizing the PCR step a 166 bps ChIA-PET band could be detected (Fig. 32). This band was cut from gel, purified and cloned into a blunt end cloning vector. A total of 60 and 48 clones for ScpB and ParB, respectively, were analyzed for the ligated DNA fragments (Fig. 33AB). The ScpB library shows most ligation occurring between the same linkers (AA or BB), with slightly more ligations for the AA linkers. The localization of these non-chimeric ligations are well distributed over the half of the chromosome containing the *oriC* region as would be expected for the Smc complex. Only a small percentage of chimeric (AB) ligations were observed. This indicates that most ligated DNA fragments are derived from ligations on a single bead, suggesting that most ligation events are derived from DNA loci that were in close proximity. The ParB sample was poor with only 10 observed interactions, between only two locations on the chromosome. Also a PCR product that was used to initially test the linkers, adapters and all the enzymatic reactions for ChIA-PET was detected, presumably due to cross-contamination. BB or AB ligations were not observed. This suggests that ligated DNA fragments were mostly derived from DNA loci that were in close proximity. However, the low amount of observed DNA ligations implies that ParB is poor in bridging chromosomal DNA loci.
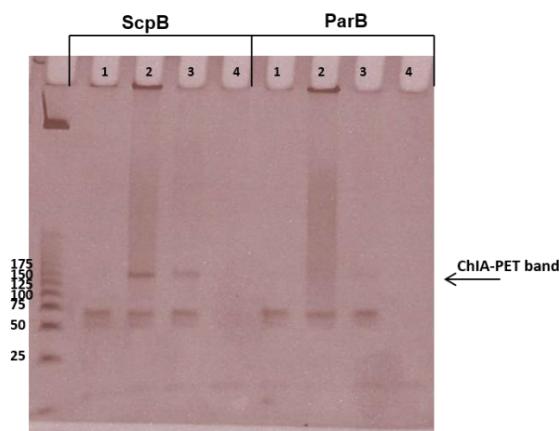
Figure 32. Example of a 6% PAGE gel after the ChIA-PET procedure.
Four different PCR conditions for each sample (ScpB and ParB) were used to optimize the amplification of the DNA after ChIA-PET. The 166 bps ChIA-PET band is visible in few of the PCR reactions. The ~60 bps band presumably represents ligated adapters.

The results above indicate that the ScpB library contained DNA fragments that consisted of correctly ligated fragments, i.e. the linkers, the genomic DNA and adapters. In addition, the results indicate that the ScpB library contained mostly the desired proximity ligated DNA fragments, therefore the aim was to sequence this library using high throughput sequencing. In the original ChIA-PET protocol 454 sequencing adapters were used but companies available locally used other 454 sequencing adapters and could therefore not directly sequence this library. Illumina sequencing was recommended because of the reduced cost and increased number of reads that could be obtained with this method. The ChIA-PET experiment was

therefore repeated using the forked Illumina® Truseq adapters or NEBNext® Multiplex Oligos for Illumina for ligation to the digested proximity ligated DNA. Unfortunately this resulted in mainly ligated adapters and was therefore not suited for high throughput sequencing. The previously obtained libraries could also be amplified by PCR after which the company would ligate the appropriate adapters to the DNA fragments, in this case much more DNA would be needed (3 µg instead of 100 ng). An approach was chosen in which the existing library with the 454 adapters was PCR amplified using short (20 bp) primers (Fig. 33C). The short length of the primers made it feasible to perform 100 bps single end (SE) sequencing.

A

Linker composition	Number of clones	Percentage of clones
AA	22	37%
BB	12	20%
AB or BA	4	7%
Non-analyzable	22	36%
Total	60	100%

B

Linker composition	Number of clones	Percentage of clones
AA	10	21%
BB	-	0%
AB or BA	-	0%
Non-analyzable	32	67%
PCR contamination	6	12%
Total	48	100%

C
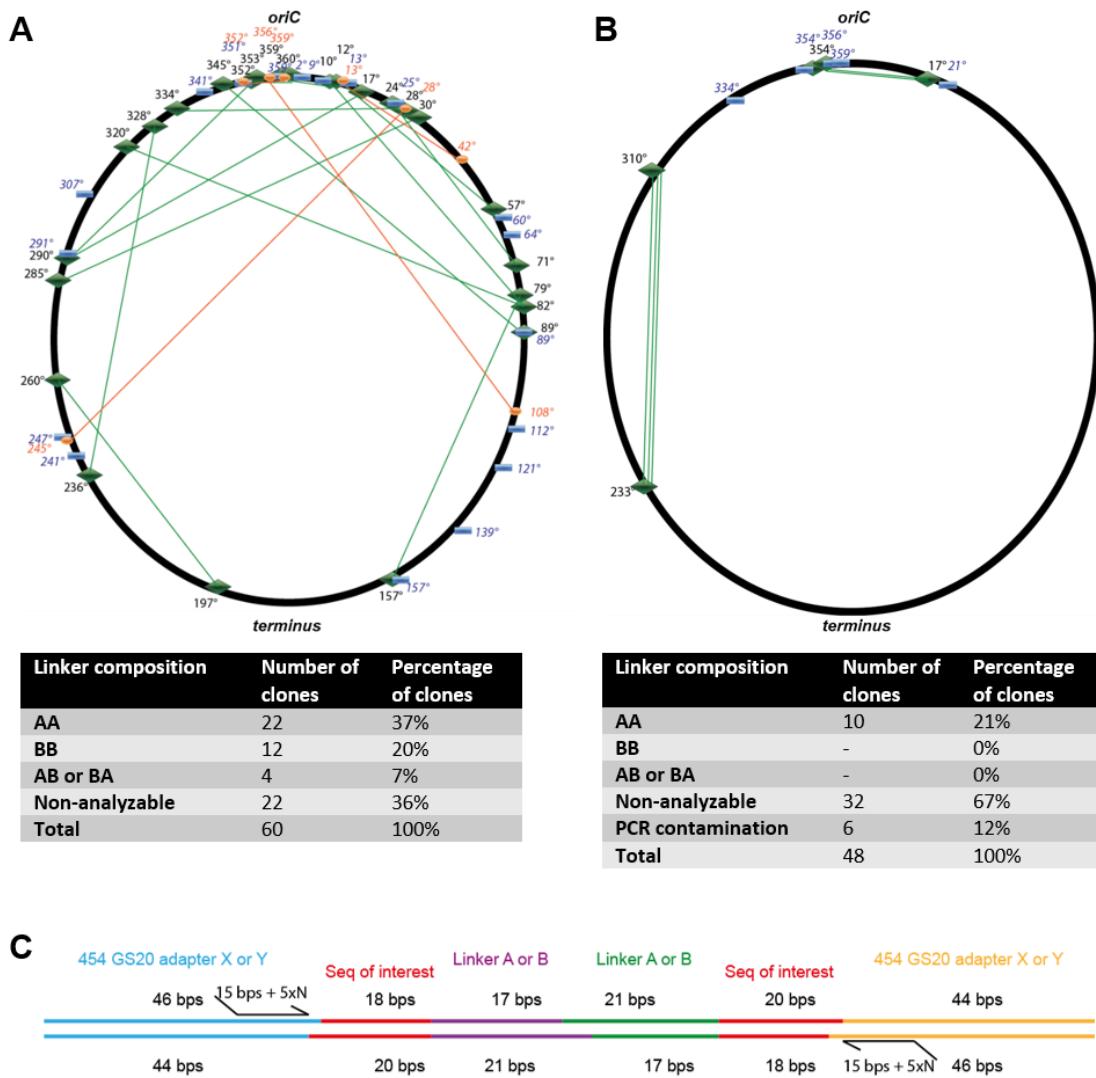
Figure 33. In house testing of the ChIA-PET library
  A. Analysis of clones which contain DNA fragments of obtained interactions in ChIA-PET using α-ScpB antiserum. Blue rectangles indicate self-ligations, green diamonds indicate AA or BB ligations, orange spheres indicate AB or BA ligations.
  B. Analysis of clones which contain DNA fragments of obtained interactions in ChIA-PET using α-ParB antiserum. See legend in A.
  C. Overview of a ChIA-PET fragment, the primers used with 15 bps homology and 5 random bases (5xN) are indicated.

For the ScpB and ParB libraries 71 and 82 million reads were obtained, respectively. Of these, 183 and 175 random reads, respectively, were initially manually analyzed (Fig. 34). This showed that the correct fragment was sequenced and that only little inter-bead ligation had occurred (<5%). For the ScpB sample, the AA and BB intra- or inter-molecular ligations were well distributed over the half of the chromosome containing the *oriC* region and no duplicates were observed. This suggest that most ligations were derived from proximity ligation events and that many different genomic loci brought together by the Smc complex are present in the library, suggesting that Smc is capable of mediating many different chromosomal loci. In the ParB sample duplicates were observed, these are presumably caused by the PCR amplification. This suggests that few DNA ligations occurred between different loci and implies that ParB either brings only a few loci together or that it is very poor in bridging chromosomal DNA.
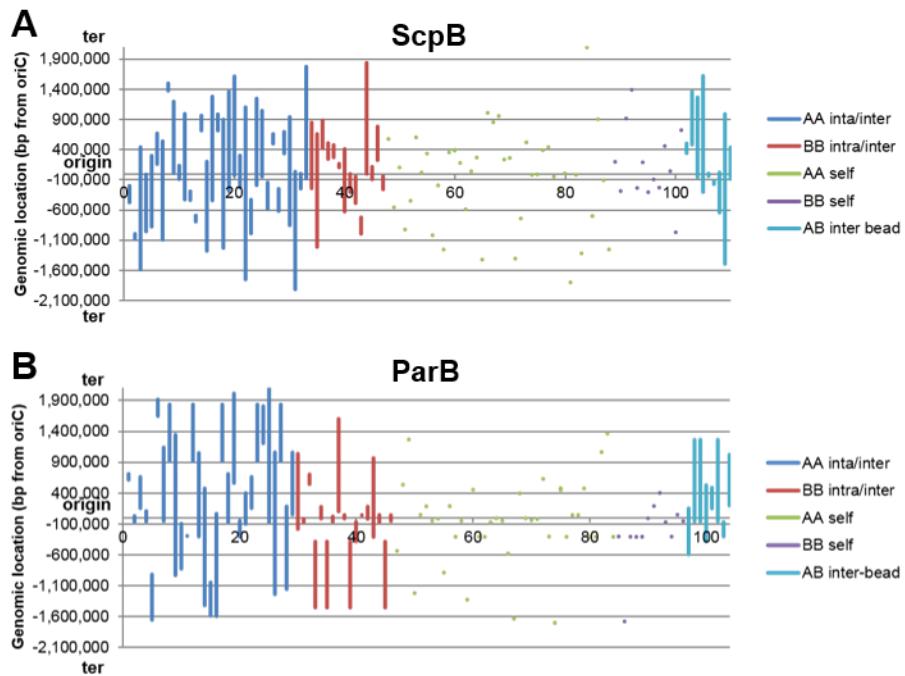

Figure 34. Overview of manually analyzed high throughput sequencing reads of ChIA-PET Observed interactions are indicated by the vertical lines and were plotted across the *oriC*. Ter stands for terminus. In A the ScpB sample is shown, in B the ParB sample. Lines on the same heights indicate in most cases duplicates. Used strain for both samples is BSG 1001. Cells were grown in competence medium.

A bioinformatics tool specifically designed to analyze ChIA-PET high throughput sequencing reads in a quantitative and statistical manner was published (Li et al., 2010) and this was the preferred choice to analyze the dataset. However, this required a collaboration with the Bioinformatics Core Facility of the Max Planck Institute (MPI) for Biochemistry (initially located at the MPI for Plant Breeding in Cologne). The collaboration was established in January 2013. However, up to now installation of the ChIA-PET tool proved to be difficult, mainly due to poor documentation. Therefore bioinformaticians manually treated the data by sorting the reads with non-chimeric linkers (AA and BB) from the chimeric (AB or BA) linkers. The linkers and adapters were removed and the remaining genomic sequences were uniquely mapped and analyzed for chromosomal interactions between 1000 bps windows. The proneness of random ligations occurring between enriched DNA loci still persisted. To identify interactions occurring with higher frequency
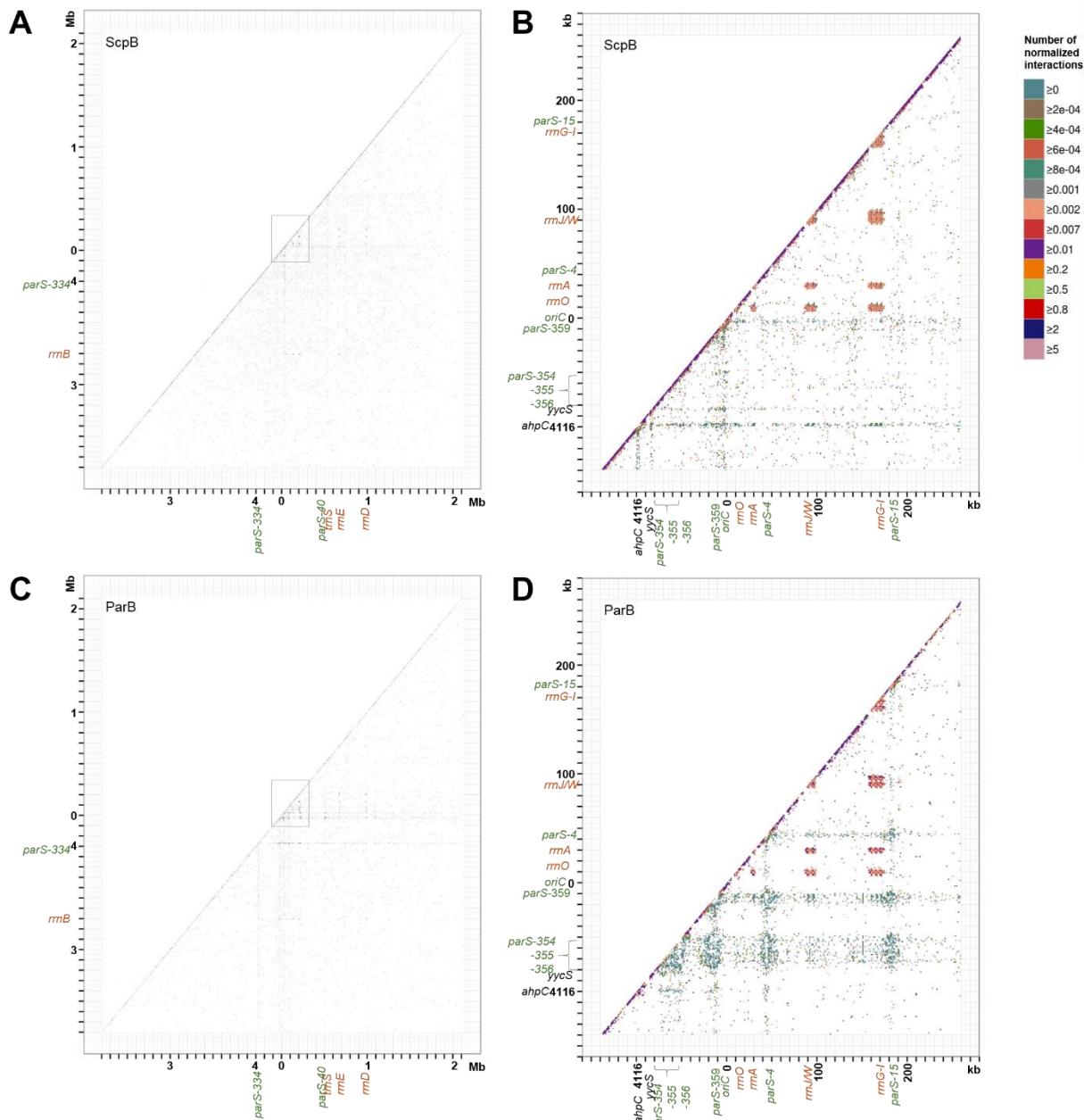
Figure 35. ChIA-PET interaction plots after manual treatment of the high throughput sequencing reads.

A. Genome-wide overview of chromosomal interactions induced by ScpB/the Smc complex, the grey box indicates the area used for the zoomed in overview in B.
B. Origin region overview of chromosomal interactions caused by ScpB/ the Smc complex.
C. Genome-wide overview of chromosomal interactions induced by ParB, the grey box indicates the area used for the zoomed in overview in D.
D. Origin region overview of chromosomal interactions caused by ParB.
Indicated *parS* sites are writen in green, highly transcribed genes are writen in red, other genetic loci are writen in black. Used strain in both samples is BSG 1001, cells were grown in competence medium.

77

than would be expected from their abundance, the observed interactions were normalized, see Table 3 and Chapter 3.9.2. The normalized values were plotted (Fig. 35). For both ScpB and ParB, a clear diagonal line of self-ligations can be observed, which is expected in a 3C derived experiment. For ScpB most interaction can be seen in the *oriC* region and there are a few lines that contain interactions between a single locus and many other loci on the chromosome (Fig. 35A). These lines show interactions of loci where Smc and ScpB are enriched in ChIP experiments (Fig. 9 and 24), and this is confirmed in a plot showing the *oriC* region with a higher resolution (Fig. 35B). For ParB the lines occurring between a single locus and many other loci on the chromosome are even more pronounced (Fig. 35CD). Interaction occurs between *parS* sites and *parS* sites with many other loci on the chromosome. In addition, interactions between highly transcribed genes were also observed (Fig. 35CD). This would imply that the Smc complex mediates chromosomal interactions mostly between regions where they are enriched in ChIP experiments such as the *oriC* region, *parS* sites and highly transcribed genes. In contrast to the findings of the manual analysis of the high throughput sequencing reads ParB seems to be capable of bridging several chromosomal loci for which it is enriched in ChIP experiments (Fig. 9), such as *parS* sites and highly transcribed genes.
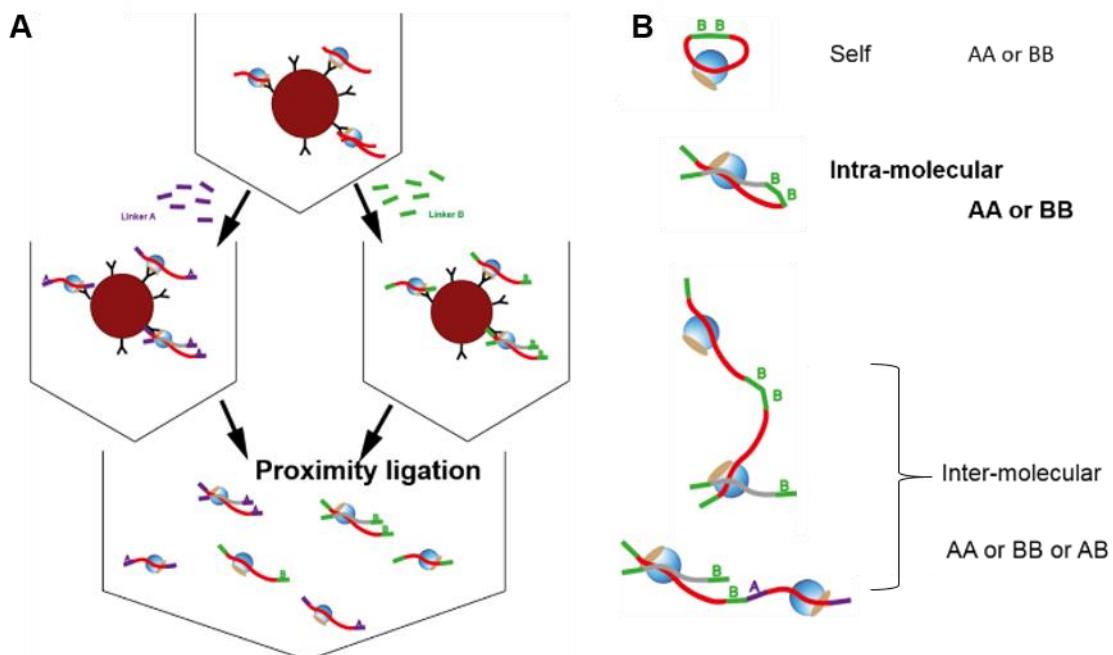
Figure 36. Overview of ligation in solution used in ChIA-PET
    A. After the linkers have been ligated to the DNA on the beads the crosslinked DNA-protein complexes are released from the beads into solution. The two different aliquots are mixed after which the proximity ligation step is performed.
    B. This results in DNAs that are differently ligated, 1) self-ligations resulting in non-chimeric linker composition (AA or BB) and within ~5 kb on the chromosome, 2) intra-molecular ligations, ligations occurring between two DNAs that are held together by one protein (complex) which gives non-chimeric linker compositions (AA or BB), 3) inter-molecular ligations which occur between two DNAs that are crosslinked to two separated proteins, this is the background in ChIA-PET and produces non-chimeric linker compositions (AA or BB) and in equal amounts chimeric compositions (AB or BA). The amount of AB and BA ligations shows half of the background (inter-molecular ligations) and together with the ChIP enrichment is used for statistical analysis in the ChIA-PET tool.

It may not be surprising that interactions on the chromosome as elucidated by ChIA-PET seem to take place between loci enriched in ChIP experiments for the Smc complex and ParB. However, although a normalization procedure to account for proneness of random ligations between enriched DNA loci was applied, it cannot be said with confidence that the interactions are statistically significant. Whether these interactions are indeed statistically significant remains to be tested for which the ChIA-PET tool would ideal. In addition, the identified interactions need to be verified by preferably using other techniques than 3C-derived methods.

In the adapted ChIA-PET protocol proximity ligation was performed with DNA attached to the beads. Thereby all DNA that is attached to one bead will ligate to the same linker. As such, the chimeric linker background observed with on bead proximity ligation reflects ligations between beads, but does not account for ligations between DNA fragments attached to two separate proteins on the same bead (Fig. 36). Therefore, the ChIA-PET protocol was further optimized by performing the proximity ligation in solution to distinguish ligations occurring between DNA crosslinked to two separate proteins based on chimeric linker composition (Fig. 36B). In addition, the proximity ligation step on beads was performed in a small volume (2 ml). However, the larger the volume used in the proximity ligation step, the less background ligations occur due to random collisions. Therefore, the protocol was adjusted to perform the proximity ligation in solution step in a larger volume (10 ml). To account for the observed bias in AA ligations, linker B was replaced with a newly designed and tested linker, D. Furthermore, to avoid the numerous rounds of PCR necessary to obtain enough DNA material for high throughput sequencing, new primers with the Illumina Truseq sequences were designed (Fig. 37) and tested on the 454 adapter library. However, it was chosen not to sequence these novel libraries until proper bioinformatic analysis could be performed.
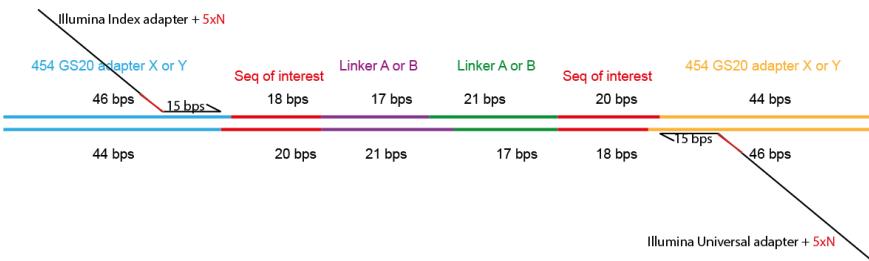

Figure 37. ChIA-PET fragment with primers generating Illumina adapters on the fragment after PCR.
The primers use 15 bps homology to the 454 adapters that are ligated onto the fragment, then five random base pairs that are needed to focus the lasers during Illumina high throughput sequencing and subsequently the sequence of the Illumina indexed or universal adapter.

5. Discussion

SMC complexes play pivotal roles in chromosome segregation, chromosome organization and DNA repair. To execute these roles, interactions between SMC complexes and chromosomes are required. However, the precise mechanisms of action of SMC complexes are poorly understood. To gain deeper insight into these mechanisms it is important to understand exactly how SMC complexes associate with the chromosome. A study in yeast suggested that cohesin blocked in ATP hydrolysis is capable of associating with the chromosome at loading sites and that wild-type cohesin may translocate over the chromosome (Hu et al., 2011). It was shown that Smc from *B. subtilis* undergoes a conformational change upon DNA binding in the presence of ATP (Soh et al., 2014) and that ScpAB may be important to drive ATP hydrolysis (Kamada et al., 2013). The work presented here gives new insights in the function of ATP hydrolysis and the loading mechanism for chromosomal association and translocation of the *B. subtilis* Smc complex.

5.1 Insights into the mechanism of Smc recruitment to the chromosome

5.1.1 A model for the molecular mechanism of Smc recruitment to the chromosome

The work presented in this thesis found that a mutant blocked in ATP hydrolysis (Smc(E1118Q)) localizes specifically to the binding sites of its loading factor (ParB) (Fig. 8-9). This chromosomal localization is dependent on both ParB and the kleisin/additional subunits of Smc (ScpA and ScpB) (Fig. 12). The level of ParB on the ParB binding sites determines the amount of localization of Smc(E1118Q) to these sites (Fig. 22). The specific localization of Smc(E1118Q) is not a result of impaired chromosome segregation of strains harboring Smc(E1118Q) (Fig. 11). In addition, when the Smc complex has a monomeric hinge or when the hinge is absent, localization of the ATP hydrolysis blocked mutant is strongly increased, even in the absence of ScpA (see Table 4 for an overview of localization of the different constructs, Fig. 13 and 17). Furthermore, the Smc heads in an engaged state with approximately one-third of the head-proximal coiled-coil are sufficient for localization to ParB loading sites (Table 4 and Fig. 18). Together, this data suggests that in the wild-type situation, where chromosomal localization depends on ScpAB, hinge dimerization hinders localization and that ScpAB is needed in this case to enable the complex to target to the loading sites. From experiments using mutants that have altered head-engaged states and/or differ in rod or ring-like conformations it could be derived that the Smc complex with engaged heads and a ring-like conformation targets more efficiently to loading sites (Fig. 14), suggesting that this conformational state is important for initial recruitment to the chromosome. Head-engagement (perhaps together with DNA binding) may be required to induce the complex to transition from the rod-like state to the more ring-like conformation. Speculatively, this particular conformation (engaged heads and ring-like conformation) could have consequences for the arrangement of the hinge as well and this different conformation of the hinge domain may be important for chromosomal association of Smc. It was previously suggested that ScpB binding to ScpA stimulates the ATPase activity of the Smc complex (Kamada et al., 2013), therefore ScpAB

may be required to promote head-engagement and thereby induce the aforepostulated conformational change in the complex required for targeting to loading sites (Fig. 38).

Together, this implies a model for the recruitment of the Smc complex to the chromosome in which upon binding of ATP and ScpAB to a dimer of Smc the Smc heads engage. This induces a conformational change in the hinge-proximal part of the complex going from a rod-like state to a more ring-like state and is presumably the state that interacts with ParB/*parS* sites by which the Smc complex is recruited to the chromosome (Fig. 38).
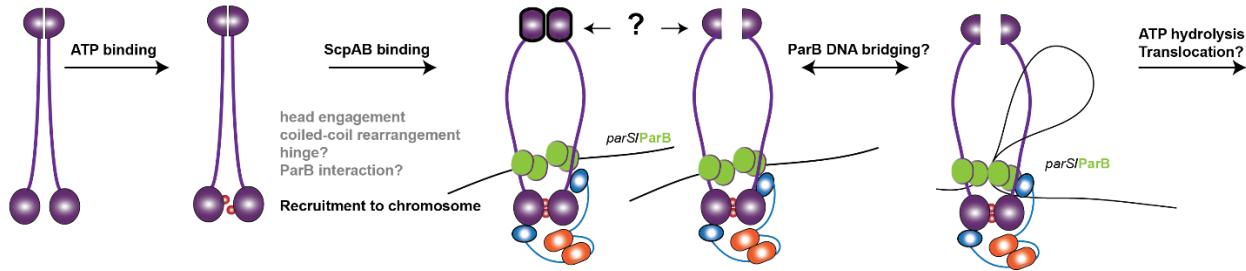

Figure 38. Model of the mechanism required for Smc recruitment to the chromosome
To a dimer of Smc ATP may bind, upon binding of ScpAB the heads may engage (perhaps in combination with DNA binding) inducing a conformational change in the hinge-proximal part of the complex going from a rod-like state to a more ring-like state. This conformation can interact with ParB by which recruitment to the chromosome takes place, the ParB interaction site presumably lies within the head-proximal one third of the coiled-coils. How ParB structures the DNA *in vivo* is unknown, but *in vitro* data shows it is capable of bridging and condensing DNA. Smc may load onto loops created by ParB and after ATP hydrolysis has occurred translocate over large distances on the chromosome from there. The exact conformation of the hinge domains of Smc in the ATP hydrolysis cycle remains to be further studied.

The work for this thesis demonstrates that in an Smc complex with engaged heads the hinge is dispensable for recruitment to the chromosome. In contrast, work in cohesin suggested that the hinge is required for recruitment to the chromosome also when the heads are engaged by introducing the EQ mutation (Hu et al., 2011). However, the work in cohesin did not include a clear monomeric or absent hinge but included a hinge replacement with an MP1-p14 dimerization domain which is known to tightly dimerize (Kurzbauer et al., 2004) or an introduction of a mutation in the hinge that destroys the hinge coiled-coil-proximal dimerization domain but did not make a full monomer (Mishra et al., 2010). The MP1-p14 dimerization domain might dimerize so tightly that it hinders localization to the chromosome and it is largely unclear what the effect of the introduced mutation is. In addition, the cohesin work was performed in yeast which, due to lethality of non-functional SMC proteins, requires simultaneous expression of wild-type and mutant SMC proteins which may influence the results. Thus, from the work in yeast cohesin it is not excluded that the basic mechanism of the initial recruitment found for *B. subtilis* Smc here is relevant for eukaryotes. For cohesin, evidence was found that hinge opening might be needed for chromosomal association (Gruber et al., 2006), which is consistent with the observations in this thesis. However, to clearly demonstrate whether the basic localization mechanism found for *B. subtilis* Smc here is also the localization mechanism for cohesin, ChIP experiments in strains in which the cohesin hinge is cleaved off in the presence of engaged heads should be performed. If this does not show similar localization patterns as was observed here in *B.*

subtilis this might imply that the situation is more complex in eukaryotes (e.g. requirement of additional loading factors that may need an interaction with the hinge) and this would ask for additional investigation. Nevertheless, the work in this thesis, together with work from colleagues in the lab, strongly suggests that the *B. subtilis* Smc complex with a ring-like conformation and engaged heads can be efficiently recruited to the chromosome.

5.1.2 An insertion into the coiled-coil may be part of a ParB binding site

In *B. subtilis* Smc the C-terminal coiled-coils contain ~26 more residues than the N-terminal coiled-coil. This suggests that the coiled-coil is non-continuous and may have insertions that extrude from the coiled-coils as was shown for *E. coli* MukB (Weitzel et al., 2011). This was confirmed by a very recent paper from the same lab. They found that in *B. subtilis* Smc the C-terminal coiled-coil was 3 residues longer than the N-terminal coiled-coil between residues 777 and 794 and 24 residues longer between residues 948 and 990 (Waldman et al., 2015). In the work shown here, this latter insertion lies close to the residues that determined the cut off between head-engaged constructs that localized (Smc(Δ278-921, E1118Q)) and did not localize (Smc(Δ262-942, E1118Q)) to loading sites (Fig. 18). This could imply that there may be an insertion in the coiled-coil that is important for Smc localization to loading sites. Localization of Smc(E1118Q) clearly depended on ParB (Fig. 12) which suggest that localization of (Smc(Δ278-921, E1118Q) also depends on ParB. As such, ParB may potentially interact with the region of the insertion.

5.1.3 ParB spreading appears to be required for Smc localization to the chromosome

Previously it was shown that ParB can spread several kilobases from its *parS* binding site *in vivo* (Murray et al., 2006). More recent *in vitro* data suggests that the actual mechanism of ParB spreading consists of DNA bridging activity of ParB by which it introduces DNA loops and condenses DNA (Graham et al., 2014; Taylor et al., 2015). Mutants impaired in ParB spreading were proposed to have defects in either the DNA bridging activity or interactions between ParB dimers (Graham et al., 2014). Previous microscopy data suggested that the Smc complex is not recruited to these ParB spreading mutants, implying that the ParB activity of condensing DNA might be required for Smc recruitment to the chromosome (Graham et al., 2014). However, these microscopy experiments do not exclude that there may be residual localization of Smc to the ParB spreading mutants which could not be observed by microscopy but which may be detected by ChIP. To get a deeper understanding of the requirements of initial recruitment of Smc localization to the chromosome, for which ParB is needed (Gruber & Errington, 2009; Sullivan et al., 2009), ChIP experiments were performed in this work using the ParB spreading mutants and wild-type Smc or Smc proteins that were shown to localize strongly (Smc(m-hinge, E1118Q)) to ParB binding sites (Fig. 23A). No specific localization of any of the Smc proteins in the presence of ParB spreading mutants was observed (Fig. 23A) suggesting that the ParB activity of DNA looping and thereby condensing is indeed required for the Smc complex to be recruited to the chromosome.

In this work the ParB spreading mutants showed reduced ParB localization to the chromosome than was previously observed (Fig. 23B) (Breier & Grossman, 2007; Graham et al., 2014). In the previous studies genome-wide methods were used (ChIP-on-chip and ChIP-seq) and the analysis of these methods is different than for ChIP-qPCR. For example, during ChIP-seq and its analysis same amounts of DNA are being sequenced and the same number of reads are being generated. The same number of reads are either obtained during the actual sequencing or by normalizing between different samples. In addition, if for one sample the localization to the chromosome was reduced, and thus less IP DNA was obtained, one has to either upscale the experiment for that particular sample or amplify the DNA of that sample. The normalization and differences in the amount of IP DNA between samples could generate artifacts such as an overestimation of the signal. These artifacts are absent in ChIP-qPCR because IP efficiencies are directly calculated as the percentage of the input material from the same sample (internal normalization), there is thus no need for a normalization or generating similar amounts of IP DNA between samples. In addition, DNA sizes for ChIP-seq experiments are typically 200-800 bps in length. The ChIP protocol used for this thesis uses DNA of 1500 bps on average. ParB spreads over several kbs on the DNA, therefore ParB that is actually located next to the *parS* site may be precipitated and increase the IP DNA of the tested *parS* site. Thereby wild-type ParB might show a higher localization at *parS*-359 in the used ChIP protocol for this thesis compared to the previous studies. It would require a change and optimization of the used sonication method, by e.g. waterbath sonication, and sequencing the ChIP-DNA to clarify whether the differences observed in localization of the ParB spreading mutants are due to differences in the used ChIP protocols or due to other factors such as the usage of different strains.

Although there are differences in observed enrichment of the ParB spreading mutants, both this thesis work and a previous study (Graham et al., 2014) support the notion that the activity of ParB in looping DNA is required for the Smc complex to be recruited to the chromosome. This would suggest that the Smc complex requires a certain DNA structure that is facilitated by ParB to be recruited to the chromosome (Fig. 38).

5.1.4 Why are strains harboring the E1118Q mutation so sick?

Strains that harbor the E1118Q mutation display smaller colonies than an *smc* deletion strain indicating that these cells are sicker than cells of an *smc* deletion strain. In addition, endeavors were made to construct strains which had chimeric Smc proteins (Smc(Zn hinge), Smc(Tm hinge) or flexible insertions below the hinge in combination with the E1118Q mutation, this resulted in strains that were 'super sick' and were easily overgrown by cells that had obtained suppressor mutations (Fig. 15). This suggests that the 'super sickness' is caused by a synthetic phenotype in which (a slight) sickness caused by alterations in the hinge in combination with the sickness of strains harboring the E1118Q in Smc results in a 'super sick' phenotype. Interestingly, all the Smc proteins with alterations in the hinge but without the E1118Q mutation localize more strongly to *parS* sites and *oriC* than wild type (Fig. 16, 25, 26). When these altered hinge mutants with the E1118Q mutation were generated in Smc(cysless, Tev-His12-Halotag) proteins their cells grew faster than cells of their native counterparts and were not overgrown with other cells. In addition,

Smc(cysless, Tev-His12-Halotag) proteins localize less to the chromosome than the corresponding native Smc proteins (Fig. 14 and 16). This suggests that Smc(cysless, Tev-His12-Halotag) proteins with alterations in the hinge combined with the E1118Q mutation may also localize less to the chromosome than their native counterparts. It may be that strains harboring native Smc proteins that have alterations in the hinge in combination with the E1118Q mutation have a 'super localization' to the chromosome and may thereby cause defects, for example in chromosome segregation, which reduces their growth drastically. This is however not experimentally confirmed. The toxicity observed in *smc(E1118Q)* strains may similarly be due to more continuous or more stable localization to the chromosome. When wild-type functioning Smc and Smc(E1118Q) were simultaneously expressed this toxicity was alleviated (Fig. 11B). The decreased difference in localization of Smc(E1118Q) over wild-type at the loading site compared to strains that harbor only Smc(E1118Q) (compare Fig. 8 and 11) suggests that both complexes compete for the same loading site, thereby the toxicity may be reduced.

5.1.5 Localization to highly transcribed genes?

Different SMC complexes have been reported to localize to highly transcribed genes in several organisms (Jeppsson et al., 2014a). This indicates that the observed localization to highly transcribed genes in this study may be a conserved feature of SMC complexes. However, surprisingly, in the ChIP experiments used in this thesis work ParB also localized to highly transcribed genes, a feature that was not observed in a previous ChIP-on-chip method probing ParB (Breier & Grossman, 2007). Furthermore, for budding yeast and bacteria it was reported that highly transcribed genes can give false positive signals in ChIP experiments (Teytelman et al., 2013; Waldminghaus & Skarstad, 2010). It can therefore not be excluded that the localization to highly transcribed genes is a specific artifact of the ChIP protocol used in the work for this thesis or any other protocol. This could apply to all studied organisms, the localization to highly transcribed genes should therefore be interpreted with great caution.

5.2 Insights into translocation of the Smc complex on the chromosome

5.2.1 The Smc complex seems to translocate from loading sites over large distances on the chromosome

Smc blocked in ATP hydrolysis (Smc(E1118Q)) localizes to ParB binding sites (Smc loading sites) on the chromosome (Fig. 8-9), in contrast, wild-type Smc has a wider distribution with strongest localization at and around *oriC* (Fig. 8-9). If Smc(E1118Q) represents a loading intermediate, this suggests that wild-type Smc is capable of translocating from loading sites over large distances on the genomic DNA. To gain additional knowledge about this presumed translocation an additional loading site (*parS*) was added in the genome of *B. subtilis*. The localization of ScpB in this strain was compared with the localization in the absence of the additional loading site and showed that the additional loading site altered the amount of ScpB globally

on the different arms of the chromosome (Fig. 24). In the presence of the additional loading site ScpB localizes more on the entire right arm of the chromosome and is particularly more enriched in the region between the *oriC* and the additional loading site. In addition it has reduced localization on the left arm of the chromosome. This strongly suggests that the Smc complex is capable of translocating over very large distances (Mb) on the chromosome, a feature not reported before on this scale. What the role of translocation of Smc complexes on the chromosome is, is unknown. However, since the Smc complex has such a major influence on chromosome segregation it is likely that translocation is important for that process. Smc complexes may be important for avoiding entanglements between newly replicated chromosomal DNA by structuring the DNA locally. Recently it was shown that ATP hydrolysis is required for chromosomal entrapment of DNA (Wilhelm et al., submitted). It is unknown whether chromosomal entrapment of Smc is required for Smc translocation and whether these processes occur sequentially and if so in what order. It may be that the actual entrapment is part of the presumed translocation, e.g. Smc may trap DNA into its ring after the initial recruitment at loading sites. Because distant loci may be entrapped, which occurs after the initial recruitment, this may be the observed translocation (in which Smc translocates from initial recruitment sites to more distant loci) which would thus require ATP hydrolysis, this is however very speculative. Another possible scenario is that Smc needs to be stably loaded onto chromosomes, which presumably requires ATP hydrolysis and chromosomal entrapment. After this loading step Smc may then translocate passively (i.e. ATP hydrolysis independently) or driven by other motor proteins.

The increased localization between *oriC* and the additional loading site prompts to speculate that there are factors that influence the supposed translocation. For example, Smc may be capable of translocating in two directions on the chromosome. It may be pushed by e.g. the replication or transcription machinery from the *oriC* into the direction of the terminus, as was suggested for yeast cohesin which was proposed to be pushed by the transcription machinery (Lengronne et al., 2004). Another possibility is that there are factors that recruit Smc after its initial loading towards the *oriC*, this possibility also fits well with the wild-type localization of Smc where the strongest localization is observed at the *oriC*. These two possibilities are not mutually exclusive.

Intriguingly, I found that Smc is enriched at at least three of the eight loci where DnaA, the DNA replication initiation protein, is mostly enriched in the *B. subtilis* genome (Ishikawa et al., 2007). These loci are *dnaA* located right next to the *oriC*, *ywcI-vpr* which lies 4 kb upstream of *parS*-334 and *yydA-yycA* which lies 28 kb downstream of *ahpC* and 12 kb upstream of *parS*-354 (Fig. 9C). The peak of Smc(E1118Q) at *parS*-334 is remarkably skewed to the upstream region, and to the left of *parS*-354 a large quantity of Smc(E1118Q) can be observed, features that are not present in the ParB localization (Fig. 9D). On other *parS* sites Smc(E1118Q) and ParB show a perfect overlap. This could suggest that DnaA, part of the replication machinery, influences Smc localization and that they may interact with each other (Fig. 9CD). In agreement with this speculation, it was reported for *X. laevis* that cohesin acetylation promotes sister chromatid

cohesion only in association with the replication machinery (Song et al., 2012), which may suggest that cohesin or factors regulating cohesin interact with the replication machinery.

To address the matter of translocation into more detail, further investigations should be performed by applying ChIP and (time lapse) microscopy using inducible promoters, temperature sensitive alleles of Smc or photo inducible Smc by which Smc can be depleted and subsequently induced in cells. This in combination with a time course in ChIP, as was previously reported (Poorey et al., 2013), to observe the loading and presumed translocation in a time course after Smc induction should be extremely useful in gaining more insight into the initial recruitment and perhaps translocation process of Smc. Inhibiting replication and transcription and investigating Smc translocation with the methods above should give more understanding of their roles in the presumed translocation of Smc.

5.2.2 The Smc hinge and arrangement of the hinge-proximal coiled-coil may play a role in translocation

Comparing the ratios of differences in localization of the chimeric Smc proteins (Smc(Zn hinge), Smc(Tm hinge), Smc(TmSN hinge) with wild type, with the ratio of differences in localization of Smc(E1118Q) with wild type, indicates that the chimeric proteins seem to be able to translocate because Smc(E1118Q) shows hardly any (if at all) translocation and the chimeric proteins do seem to show an amount of translocation (Fig. 26-28). The ChIP-seq experiments using the chimeric Smc proteins indicate towards a role of rod-formation (Smc(TmSN hinge)) in efficient translocation on the chromosome (Fig. 26-28). However, the localization differences with the non-functional proteins (Smc(Zn hinge) and Smc(Tm hinge), of which Smc(Tm hinge) was shown to have a more ring-like conformation, that localized more to *parS* sites/*oriC* region may not just be a result of a defect in translocation. The observed differences may come from an earlier step during the loading mechanism, such as chromosomal entrapment, which may occur after the initial recruitment to *parS*/ParB, and may be required for proper translocation. It remains to be tested whether these mutants are capable of entrapping chromosomal DNA. Nevertheless, the chimeric proteins, both the functional and non-functional ones do seem to translocate and when rod-formation can occur (Smc(TmSN hinge)) the translocation pattern resembles wild-type translocation more than when rod-formation cannot be achieved (Smc(Tm hinge)) (Fig. 25-28). This suggests that rod-formation is important either for chromosomal entrapment or that this is the conformational state that can translocate efficiently over the chromosome.

5.2.3 Potential differences in localization of Smc and ScpB

Comparing the localization of Smc and ScpB by calculating the ratio of the difference in localization displayed that ScpB has slightly increased presence over the half of the chromosome that surrounds the *oriC*. Smc on the other hand localized more to the terminus half and highly transcribed genes. A possible explanation may be that Smc in complex with ScpAB is loaded at the *parS* sites in the vicinity of the *oriC* as for recruitment and chromosomal entrapment in the presence of a wild-type hinge ScpAB are needed

(Fig. 12, Wilhelm et al., submitted). The Smc complex may then translocate away from its initial loading sites, an action for which ScpAB may not be needed and thus ScpAB dissociates from the complex and a reduced signal of ScpB from the *oriC* towards the terminus is observed. A previous study that suggested differences in dynamics for the Smc complex and Smc may fit with this. In this study ScpA and ScpB were observed to be mostly static on the chromosome (Kleine Borgmann et al., 2013b). This may imply that the Smc complex is static when it gets loaded onto the chromosome in the presence of ScpAB. The same study reported that the Smc protein was mostly mobile on the chromosome (Kleine Borgmann et al., 2013b), this may be the translocation of Smc, presumably as a dimer of Smc, and ScpAB may dissociate from the complex. However, the observed differences in localization of Smc and ScpB were very small, therefore another reasonable explanation is that Smc and ScpB do not differ in localization. The observed differences may be due to variations in formaldehyde crosslinking efficiencies of Smc and ScpB with the DNA or in antisera characteristics. It seems plausible that the α-Smc antiserum is less efficient than the α-ScpB antiserum. Thereby the signal obtained with α-ScpB is more specific and α-Smc contains more background compared to α-ScpB. This would explain why Smc seems more present at the terminus DNA (presumably background) and at highly transcribed genes (perhaps an artifact in this ChIP-protocol). Since the dynamics observed for the Smc complex are derived only from single-molecule fluorescence microscopy from a single lab and the ChIP-seq experiments performed here are not directly addressing dynamics of the Smc complex nothing can be concluded with confidence about the dynamics of Smc. In addition, the observed differences between Smc and ScpB in the ChIP-seq data are very small; it seems therefore most plausible that these observed differences are due to a difference in crosslinking or antisera specificities. Performing the proposed experiments to gain more insights into recruitment and translocation of the Smc complex (Chapter 5.2.1) might shine more light onto the dynamics of the Smc complex and its subunits.

5.3 Insights into chromosomal interactions mediated by Smc

The obtained genome-wide overview of interactions mediated by ScpB as observed in the ChIA-PET experiment are consistent with the notion that the Smc complex is capable of bringing many different chromosomal loci together (Fig. 35) (Jeppsson et al., 2014a). The loci that it seems to bridge are all loci that the Smc complex is enriched for in a typical ChIP experiment under the conditions used for this thesis work (Fig. 24A). This implies that the Smc complex holds all loci together where it is enriched in ChIP and that it is capable of bridging loci that are separated over large distances in the genome and suggests that the Smc complex has a very global influence on chromosomal architecture. For ParB similar results were obtained (Fig. 35), with ParB bridging the loci that are enriched in ChIP experiments (Fig. 9). This suggests that ParB is capable of tethering different *parS* sites. The observations made for the Smc complex and ParB could imply that ParB bridges different *parS* sites, when the Smc complex is recruited to these *parS* sites it may translocate from there and bridge loci in-between the p*arS* sites in a global fashion. Smc may obtain its distribution on the chromosome via translocation, perhaps via pushing of loops into the Smc ring.

The scale of translocation influences which loci can be bridged and as the work from this thesis suggest that Smc is capable of translocating over Mb in scale and can bridge very distant loci this implies that the loops that Smc can hold are very large. Smc is present globally over the half of the chromosome containing the *oriC* (Fig. 9 and Fig. 24) and bridged loci are also found most in this region (Fig. 35). This suggests that Smc bridges loci in a general manner. In addition, more pronounced bridging activity is seen between loci where Smc has peaks of enrichment in a ChIP experiment (Fig. 9, 24 and 35), this might imply that Smc translocation may be hindered at those sites and thus more Smc accumulates at those sites. If DNA loops are indeed going through the Smc ring then the DNA loci where Smc accumulates will be found more often in an Smc ring and would thereby be observed to be bridged more frequently. The observed data would also imply that Smc might be condensing DNA via its bridging activity, which might help in sister chromosome segregation, by for example creating rigidity within the chromosome as was proposed for condensin (Cuylen & Haering, 2011), or by avoiding entanglements between DNA from two sister chromosomes. In addition, the observed aberrations in chromosome organization in *smc* deletion cells (Britton et al., 1998) could be derived from the lack of DNA bridging activity of Smc in these cells. For both ScpB and ParB it was observed that they bridge regions containing highly transcribed genes (Fig. 35), implying that the Smc complex and ParB play a role in organizing those regions by holding them together in clusters. This might be related to the observation in eukaryotic chromosomes where regions with active genes are located more on the periphery of chromosomes (De Wit & De Laat, 2012), this might aid in efficient transcription of these regions.

However, although in these ChIA-PET experiments a normalization procedure was applied to account for proneness of random ligation between enriched DNA loci, no statistical tests were performed to test whether the observed interactions are significant. Therefore the results above should be interpreted very carefully and should be verified by statistical analysis and confirmed by techniques which are preferably not 3C derived.

5.4 Overall implications and outlook

Together, all this data implies a model for a molecular loading mechanism in which ScpAB promotes head engagement which (perhaps together with DNA binding) induces a conformational change from a rod-like state into a ring-like state, which may also influence the conformational state of the hinge (Fig. 38). This allows interaction of the Smc (engaged) heads with approximately one-third of the head-proximal coiled-coil and *parS* sites/ParB. After ATP hydrolysis, Smc translocates over large distances on the chromosome (Fig. 38), possibly in a rod-like state.

The Smc complex is found over large regions on the chromosome (Fig. 9 and 24) and seems to be capable of bridging different chromosomal loci (Fig. 35). How would this help in chromosome segregation? A few, not mutually exclusive, models in which the Smc complex would avoid entanglements between two sister chromosomes can be thought of; 1) Smc might hold sister chromosomes together in a cohesin like fashion

(Fig. 39A). This model is however not supported by studies showing that sister origins segregate quickly after replication and that replication and segregation occur sequentially (Wang et al., 2013). In addition, this model is also not supported by the observation from the ChIA-PET experiment that Smc can bridge DNA loci from different arms of the chromosome (Fig. 35). 2) The Hi-C experiment in *C. crescentus* (Le et al., 2013) might imply that Smc may hold the left and the right arm (inter-arm) of the chromosome together so that the two sister chromosomes do not get entangled (Fig. 39B). This model is however not supported by the finding that an additional loading site increased the amount of the Smc complex specifically on one arm of the chromosome (Fig. 24). This model would suggest that in that specific experiment more equal localization should be observed on both arms of the chromosome, it can however not be excluded that the Smc loading dynamics at the additional loading site is impaired because of the different chromosomal localization of this additional loading site. However, the observation that the Smc complex bridges DNA genome-wide (Fig. 35) does support this model. 3) Another alternative is that Smc holds smaller loops on the same arm of the chromosome (intra-arm) (Fig. 39C) and might thereby create rigidity in the chromosome that helps to segregate the two sisters as was proposed for condensin (Cuylen & Haering, 2011) (Fig. 39C). This model is supported by the observation that an additional loading site increases the amount of Smc complex on one arm of the chromosome (Fig. 24). However, this model is not supported by the observation that the Smc complex bridges DNA loci genome-wide (Fig. 35) as only interactions between loci on one arm would be expected.

The recent observations on the ParB DNA bridging activity, which was suggested to be required for Smc localization by (Graham et al., 2014) and in this thesis work, imply that Smc is loaded onto DNA loops generated by ParB. The observed translocation of Smc may consist of these DNA loops transporting into the Smc ring. The DNA may be pushed into the ring by other motor proteins or by Smc translocating actively onto the loops, the latter seems unlikely because of the low ATPase rate of Smc (<1 s^{-1}) (Kamada et al., 2013). The finding that an additional loading site increases the amount of Smc specifically on one arm of the chromosome (Fig. 24) strongly suggest that Smc hold loci together in an intra-arm fashion. The evidence arguing against this model comes from the observed loci that Smc may bridge (Fig. 35) which is derived from data that is not statistically tested. Therefore the data in this thesis work seems to supports the intra-arm model mostly. To elucidate with confidence which of the three models, or combination of which models, for bridging and or looping activities of Smc on the chromosome (Fig. 39) is correct, 3C derived methods that are analyzed statistically in combination with a deeper investigation of the translocation of Smc (See Chapter 5.2.1) are needed. In addition, this may tell us whether Smc is implicated in organizing the chromosome by, for example structuring the macrodomains similar to what was suggested for cohesin by maintaining chromosome territories and topologically associating domains (Phillips-Cremins et al., 2013; Seitan et al., 2013; Sofueva et al., 2013; Mizuguchi et al., 2014; Zuin et al., 2014). With the knowledge obtained about the initial recruitment and translocation of the Smc complex to the chromosome and the molecular procedures for ChIP-3C and ChIA-PET that are now established for *B. subtilis* the understanding

of the role of Smc in chromosome segregation and organization in *B. subtilis* should explicate in the years to come.

It remains to be tested whether the observed results in this thesis work and the model for Smc recruitment to the chromosome (Fig. 38) derived from it can be related to eukaryotic SMC complexes. The initial steps made with yeast cohesin (Hu et al., 2011) do not clarify this (Chapter 5.1.1), and it could well be that the proposed basic mechanism needed for Smc recruitment to the chromosome is a conserved feature. Alternatively the mechanism may only be conserved between SMC complexes that were shown to form the more rod-like conformations such as condensins and *B. subtilis* Smc (Soh et al., 2014), and not cohesins which presumably adopts to a more ring-like conformation (Haering et al., 2002).

Currently it cannot be excluded that prokaryotic Smc complexes exhibit a very basic mechanism, something evolution might have elaborated on for the more complicated situation in eukaryotes and may therefore have caused modifications in the very basic mechanism. However, with the knowledge obtained in this thesis it can be easily tested whether the here discovered basic mechanism of Smc recruitment is conserved in eukaryotes. And as such, this thesis may contribute to lay part of the foundation in understanding the molecular mechanisms of SMC functioning in life.
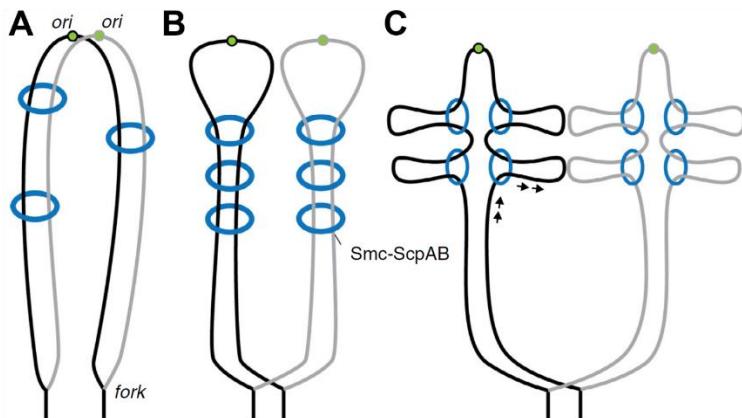
**Figure 39. Models of how SMC may associate with the chromosome and could potentially influence chromosome segregation.**
A. Smc could hold sister chromosomes together in a cohesin like fashion.
B. Smc may separate sisters holding the left and right arm of one chromosome (inter-arm).
C. Smc may hold intra-arms of the chromosome.
The Smc ring is shown in blue, green dots represent *oriCs*.
Taken from (Gruber, 2014).

6. References

Abe, S., Nagasaka, K., Hirayama, Y., Kozuka-Hata, H., Oyama, M., Aoyagi, Y., Obuse, C., et al. (2011). The initial phase of chromosome condensation requires Cdk1-mediated phosphorylation of the CAP-D3 subunit of condensin II. *Genes & Development*, *2*, 863–874. doi:10.1101/gad.2016411.substrates

Adachi, S., & Hiraga, S. (2003). Mutants suppressing novobiocin hypersensitivity of a mukB null mutation. *Journal of bacteriology*, *185*(13), 3690–3695. doi:10.1128/JB.185.13.3690

Akiyoshi, B., & Gull, K. (2013). Evolutionary cell biology of chromosome segregation: insights from trypanosomes. *Open biology*, (figure 1). Retrieved from http://rsob.royalsocietypublishing.org/content/3/5/130023.short

Almedawar, S., Colomina, N., Bermúdez-López, M., Pociño-Merino, I., & Torres-Rosell, J. (2012). A SUMO-dependent step during establishment of sister chromatid cohesion. *Current biology : CB*, *22*(17), 1576–81. doi:10.1016/j.cub.2012.06.046

Arumugam, P., Gruber, S., Tanaka, K., Haering, C. H., Mechtler, K., & Nasmyth, K. (2003). ATP Hydrolysis Is Required for Cohesin's Association with Chromosomes. *Current Biology*, *13*(22), 1941–1953. doi:10.1016/j.cub.2003.10.036

Autret, S., Nair, R., & Errington, J. (2001). Genetic analysis of the chromosome segregation protein Spo0J of Bacillus subtilis: evidence for separate domains involved in DNA binding and interactions. *Molecular microbiology*, *41*, 743–755. Retrieved from http://onlinelibrary.wiley.com/doi/10.1046/j.1365-2958.2001.02551.x/full

Badrinarayanan, A., Lesterlin, C., Reyes-Lamothe, R., & Sherratt, D. (2012a). The Escherichia coli SMC complex, MukBEF, shapes nucleoid organization independently of DNA replication. *Journal of bacteriology*, *194*(17), 4669–76. doi:10.1128/JB.00957-12

Badrinarayanan, A., Reyes-Lamothe, R., Uphoff, S., Leake, M. C., & Sherratt, D. J. (2012b). In Vivo Architecture and Action of Bacterial Structural Maintenance of Chromosome Proteins. *Science*, *338*(6106), 528–531. doi:10.1126/science.1227126

Belton, J.-M., McCord, R. P., Gibcus, J. H., Naumova, N., Zhan, Y., & Dekker, J. (2012). Hi-C: a comprehensive technique to capture the conformation of genomes. *Methods (San Diego, Calif.)*, *58*(3), 268–76. doi:10.1016/j.ymeth.2012.05.001

Ben-Shahar, T., Heeger, S., Lehane, C., & East, P. (2008). Eco1-dependent cohesin acetylation during establishment of sister chromatid cohesion. *Science*, (10). doi:10.1126/science.1157774

Besprozvannaya, M., & Burton, B. M. (2014). Do the same traffic rules apply? Directional chromosome segregation by SpoIIIE and FtsK. *Molecular microbiology*, *93*(4), 599–608. doi:10.1111/mmi.12708

Bhalla, N., Biggins, S., & Murray, A. (2002). Mutation of YCS4, a budding yeast condensin subunit, affects mitotic and nonmitotic chromosome behavior. *Molecular biology of the cell*, *13*(February), 632–645. doi:10.1091/mbc.01

Bouthier de la Tour, C., Toueille, M., Jolivet, E., Nguyen, H.-H., Servant, P., Vannier, F., & Sommer, S. (2009). The Deinococcus radiodurans SMC protein is dispensable for cell viability yet plays a role in DNA folding. *Extremophiles*, *13*(5), 827–837. doi:10.1007/s00792-009-0270-2

Breier, A. M., & Grossman, A. D. (2007). Whole-genome analysis of the chromosome partitioning and sporulation protein Spo0J (ParB) reveals spreading and origin-distal sites on the Bacillus subtilis chromosome. *Molecular microbiology*, *64*(3), 703–18. doi:10.1111/j.1365-2958.2007.05690.x

Brewer, B. (1988). When polymerases collide: replication and the transcriptional organization of the E. coli chromosome. *Cell*, *53*, 679–686. Retrieved from http://www.sciencedirect.com/science/article/pii/0092867488900864

Britton, R., Lin, D., & Grossman, A. (1998). Characterization of a prokaryotic SMC protein involved in chromosome partitioning. *Genes & Development*, 1254–1259. Retrieved from http://genesdev.cshlp.org/content/12/9/1254.short

Buheitel, J., & Stemmann, O. (2013). Prophase pathway-dependent removal of cohesin from human chromosomes requires opening of the Smc3-Scc1 gate. *The EMBO journal*, *32*(5), 666–76. doi:10.1038/emboj.2013.7

Bürmann, F., Shin, H.-C., Basquin, J., Soh, Y.-M., Giménez-Oya, V., Kim, Y.-G., Oh, B.-H., et al. (2013). An asymmetric SMC-kleisin bridge in prokaryotic condensin. *Nature structural & molecular biology*, *20*(3), 371–9. doi:10.1038/nsmb.2488

Chan, K., Roig, M., Hu, B., & Beckouët, F. (2012). Cohesin's DNA exit gate is distinct from its entrance gate and is regulated by acetylation. *Cell*, *150*(5), 961–74. doi:10.1016/j.cell.2012.07.028

Charbin, A., Bouchoux, C., & Uhlmann, F. (2013). Condensin aids sister chromatid decatenation by topoisomerase II. *Nucleic acids research*, *42*(1), 340–8. doi:10.1093/nar/gkt882

Chuang, P., Albertson, D., & Meyer, B. (1994). DPY-27: a chromosome condensation protein homolog that regulates C. elegans dosage compensation through association with the X chromosome. *Cell*, *79*, 459–474. Retrieved from http://www.sciencedirect.com/science/article/pii/0092867494902550

Cooper, S., & Helmstetter, C. E. (1968). Chromosome replication and the division cycle of Escherichia coli B/r. *Journal of molecular biology*, *31*, 519–540.

Csankovszki, G., Collette, K., Spahl, K., & Carey, J. (2009). Three distinct condensin complexes control C. elegans chromosome dynamics. *Current Biology*, *19*(1), 9–19. doi:10.1016/j.cub.2008.12.006

Cuylen, S., & Haering, C. (2011). Deciphering condensin action during chromosome segregation. *Trends in cell biology*, *21*(9), 552–9. doi:10.1016/j.tcb.2011.06.003

Cuylen, S., Metz, J., & Haering, C. H. (2011). Condensin structures chromosomal DNA through topological links. *Nature structural & molecular biology*, *18*(8), 894–901. doi:10.1038/nsmb.2087

D'Ambrosio, C., Kelly, G., Shirahige, K., & Uhlmann, F. (2008a). Condensin-dependent rDNA decatenation introduces a temporal pattern to chromosome segregation. *Current Biology*, *18*(14), 1084–9. doi:10.1016/j.cub.2008.06.058

D'Ambrosio, C., Schmidt, C. K., Katou, Y., Kelly, G., Itoh, T., Shirahige, K., & Uhlmann, F. (2008b). Identification of cis-acting sites for condensin loading onto budding yeast chromosomes. *Genes & development*, *22*(16), 2215–27. doi:10.1101/gad.1675708

Danilova, O., Reyes-Lamothe, R., Pinskaya, M., Sherratt, D., & Possoz, C. (2007). MukB colocalizes with the oriC region and is required for organization of the two Escherichia coli chromosome arms into separate cell halves. *Molecular microbiology*, *65*(6), 1485–92. doi:10.1111/j.1365-2958.2007.05881.x

De Wit, E., & De Laat, W. (2012). A decade of 3C technologies: insights into nuclear organization. *Genes & development*, *26*(1), 11–24. doi:10.1101/gad.179804.111

Dekker, J., Marti-Renom, M. a, & Mirny, L. a. (2013). Exploring the three-dimensional organization of genomes: interpreting chromatin interaction data. *Nature reviews. Genetics*, *14*(6), 390–403. doi:10.1038/nrg3454

DeMare, L. E., Leng, J., Cotney, J., Reilly, S. K., Yin, J., Sarro, R., & Noonan, J. P. (2013). The genomic landscape of cohesin-associated chromatin interactions. *Genome Research*. doi:10.1101/gr.156570.113

Dorsett, D., & Merkenschlager, M. (2013). Cohesin at active genes: a unifying theme for cohesin and gene expression from model organisms to humans. *Current opinion in cell biology*, *25*(3), 327–33. doi:10.1016/j.ceb.2013.02.003

Dowen, J. M., Fan, Z. P., Hnisz, D., Ren, G., Abraham, B. J., Zhang, L. N., Weintraub, A. S., et al. (2014). Control of Cell Identity Genes Occurs in Insulated Neighborhoods in Mammalian Chromosomes. *Cell*, *159*(2), 374–387. doi:10.1016/j.cell.2014.09.030

Duro, E., & Marston, A. (2015). From equator to pole: splitting chromosomes in mitosis and meiosis. *Genes & development*, 109–122. doi:10.1101/gad.255554.114.Freely

Dworkin, J., & Losick, R. (2002). Does RNA polymerase help drive chromosome segregation in bacteria? *Proceedings of the National Academy of Sciences of the United States of America*, *99*(22). Retrieved from http://www.pnas.org/content/99/22/14089.short

Ebersbach, G., & Gerdes, K. (2005). Plasmid segregation mechanisms. *Annual review of genetics*, *39*, 453–79. doi:10.1146/annurev.genet.38.072902.091252

Engler, C., Gruetzner, R., Kandzia, R., & Marillonnet, S. (2009). Golden gate shuffling: a one-pot DNA shuffling method based on type IIs restriction enzymes. *PloS one*, *4*(5), e5553. doi:10.1371/journal.pone.0005553

Espeli, O., Lee, C., & Marians, K. J. (2003). A physical and functional interaction between Escherichia coli FtsK and topoisomerase IV. *The Journal of biological chemistry*, *278*(45), 44639–44. doi:10.1074/jbc.M308926200

Ferraiuolo, M. a, Sanyal, A., Naumova, N., Dekker, J., & Dostie, J. (2012). From cells to chromatin: capturing snapshots of genome organization with 5C technology. *Methods (San Diego, Calif.)*, *58*(3), 255–67. doi:10.1016/j.ymeth.2012.10.011

Fogel, M., & Waldor, M. (2006). A dynamic, mitotic-like mechanism for bacterial chromosome segregation. *Genes & Development*, 3269–3282. doi:10.1101/gad.1496506.tion

Fullwood, M. J., Han, Y., Wei, C.-L., Ruan, X., & Ruan, Y. (2010). Chromatin interaction analysis using paired-end tag sequencing. *Current protocols in molecular biology*, *Chapter 21*, Unit 21.15.1–25. doi:10.1002/0471142727.mb2115s89

Fullwood, M. J., Liu, M. H., Pan, Y. F., Liu, J., Xu, H., Mohamed, Y. Bin, Orlov, Y. L., et al. (2009). An oestrogen-receptor-alpha-bound human chromatin interactome. *Nature*, *462*(7269), 58–64. doi:10.1038/nature08497

Gallego-Paez, L., & Tanaka, H. (2014). Smc5/6-mediated regulation of replication progression contributes to chromosome assembly during mitosis in human cells. *Molecular biology of the cell*, *25*(2), 302–17. doi:10.1091/mbc.E13-01-0020

Gard, S., Light, W., Xiong, B., Bose, T., McNairn, A. J., Harris, B., Fleharty, B., et al. (2009). Cohesinopathy mutations disrupt the subnuclear organization of chromatin. *The Journal of cell biology*, *187*(4), 455–62. doi:10.1083/jcb.200906075

Gerdes, K., Howard, M., & Szardenings, F. (2010). Pushing and pulling in prokaryotic DNA segregation. *Cell*, *141*(6), 927–42. doi:10.1016/j.cell.2010.05.033

Gerlich, D., Hirota, T., Koch, B., Peters, J., & Ellenberg, J. (2006). Condensin I stabilizes chromosomes mechanically through a dynamic interaction in live cells. *Current biology*, *16*(4), 333–44. doi:10.1016/j.cub.2005.12.040

Glaser, P., Sharpe, M., & Raether, B. (1997). Dynamic, mitotic-like behavior of a bacterial protein required for accurate chromosome partitioning. *Genes & Development*, 1160–1168. Retrieved from http://genesdev.cshlp.org/content/11/9/1160.short

Gligoris, T. G., Scheinost, J. C., Burmann, F., Petela, N., Chan, K.-L., Uluocak, P., Beckouet, F., et al. (2014). Closing the cohesin ring: Structure and function of its Smc3-kleisin interface. *Science*, *346*(6212), 963–967. doi:10.1126/science.1256917

Graham, T. G. W., Wang, X., Song, D., Etson, C. M., Van Oijen, A. M., Rudner, D. Z., & Loparo, J. J. (2014). ParB spreading requires DNA bridging. *Genes & development*, *28*(11), 1228–38. doi:10.1101/gad.242206.114

Green, M., & Sambrook, J. (2012). Molecular cloning: a laboratory manual. *Cold Spring Harbor Laboratory Press*. Retrieved from http://library.wur.nl/WebQuery/clc/2011050

Gruber, S. (2014). Multilayer chromosome organization through DNA bending, bridging and extrusion. *Current Opinion in Microbiology*, *22*, 102–110. doi:10.1016/j.mib.2014.09.018

Gruber, S., Arumugam, P., Katou, Y., Kuglitsch, D., Helmhart, W., Shirahige, K., & Nasmyth, K. (2006). Evidence that loading of cohesin onto chromosomes involves opening of its SMC hinge. *Cell*, *127*(3), 523–37. doi:10.1016/j.cell.2006.08.048

Gruber, S., & Errington, J. (2009). Recruitment of condensin to replication origin regions by ParB/SpoOJ promotes chromosome segregation in B. subtilis. *Cell*, *137*(4), 685–96. doi:10.1016/j.cell.2009.02.035

Gruber, S., Haering, C., & Nasmyth, K. (2003). Chromosomal cohesin forms a ring. *Cell*, *112*, 765–777. Retrieved from http://www.sciencedirect.com/science/article/pii/S0092867403001624

Gruber, S., Veening, J.-W., Bach, J., Blettinger, M., Bramkamp, M., & Errington, J. (2014). Interlinked sister chromosomes arise in the absence of condensin during fast replication in B. subtilis. *Current biology*, *24*(3), 293–8. doi:10.1016/j.cub.2013.12.049

Guacci, V., Koshland, D., & Strunnikov, A. (1997). A direct link between sister chromatid cohesion and chromosome condensation revealed through the analysis of MCD1 in S. cerevisiae. *Cell*, *91*(1), 47–57. Retrieved from http://www.sciencedirect.com/science/article/pii/S0092867401800088

Hadjur, S., Williams, L., Ryan, N., & Cobb, B. (2009). Cohesins form chromosomal cis-interactions at the developmentally regulated IFNG locus. *Nature*, *460*(7253), 410–3. doi:10.1038/nature08079

Haering, C. H., Farcas, A.-M., Arumugam, P., Metson, J., & Nasmyth, K. (2008). The cohesin ring concatenates sister DNA molecules. *Nature*, *454*(7202), 297–301. doi:10.1038/nature07098

Haering, C., Löwe, J., Hochwagen, A., & Nasmyth, K. (2002). Molecular architecture of SMC proteins and the yeast cohesin complex. *Molecular cell*, *9*, 773–788. Retrieved from http://www.sciencedirect.com/science/article/pii/S1097276502005154

Haering, C., Schoffnegger, D., & Nishino, T. (2004). Structure and stability of cohesin's Smc1-kleisin interaction. *Molecular cell*, *15*, 951–964. Retrieved from http://www.sciencedirect.com/science/article/pii/S1097276504005179

Haeusler, R., & Pratt-Hyatt, M. (2008). Clustering of yeast tRNA genes is mediated by specific association of condensin with tRNA gene transcription complexes. *Genes & Development*, 2204–2214. doi:10.1101/gad.1675908.Garrard

Hauf, S., Waizenegger, I., & Peters, J. (2001). Cohesin cleavage by separase required for anaphase and cytokinesis in human cells. *Science*, (18). Retrieved from http://www.sciencemag.org/content/293/5533/1320.short

Hayama, R., & Marians, K. J. (2010). Physical and functional interaction between the condensin MukB and the decatenase topoisomerase IV in Escherichia coli. *Proceedings of the National Academy of Sciences of the United States of America*, *107*(44), 18826–31. doi:10.1073/pnas.1008140107

Heidari, N., Phanstiel, D., & He, C. (2014). Genome-wide map of regulatory interactions in the human genome. *Genome Research*, 1905–1917. doi:10.1101/gr.176586.114.Freely

Hiraga, S., Niki, H., Ogura, T., & Ichinose, C. (1989). Chromosome partitioning in Escherichia coli: novel mutants producing anucleate cells. *Journal of Bacteriology*, *171*(3), 1496–1505. Retrieved from http://jb.asm.org/content/171/3/1496.short

Hirano, M, & Hirano, T. (1998). ATP-dependent aggregation of single-stranded DNA by a bacterial SMC homodimer. *The EMBO Journal*, *17*(23), 7139–7148. Retrieved from http://onlinelibrary.wiley.com/doi/10.1093/emboj/17.23.7139/full

Hirano, M., Anderson, D. E., Erickson, H. P., & Hirano, T. (2001). Bimodal activation of SMC ATPase by intra- and inter-molecular interactions, *20*(12).

Hirano, M., & Hirano, T. (2002). Hinge-mediated dimerization of SMC protein is essential for its dynamic interaction with DNA. *The EMBO journal*, *21*(21), 5733–44. Retrieved from http://www.pubmedcentral.nih.gov/articlerender.fcgi?artid=131072&tool=pmcentrez&rendertype=abstract

Hirano, M., & Hirano, T. (2004). Positive and negative regulation of SMC-DNA interactions by ATP and accessory proteins. *The EMBO journal*, *23*(13), 2664–73. doi:10.1038/sj.emboj.7600264

Hirano, M., & Hirano, T. (2006). Opening closed arms: long-distance activation of SMC ATPase by hinge-DNA interactions. *Molecular cell*, *21*(2), 175–86. doi:10.1016/j.molcel.2005.11.026

Hirano, T. (2012). Condensins: universal organizers of chromosomes with diverse functions. *Genes & development*, *26*(15), 1659–78. doi:10.1101/gad.194746.112

Hopfner, K., Craig, L., Moncalian, G., & Zinkel, R. (2002). The Rad50 zinc-hook is a structure joining Mre11 complexes in DNA recombination and repair. *Nature*, *418*(August), 562–566. Retrieved from http://www.nature.com/nature/journal/v418/n6897/abs/nature00922.html

Hopfner, K., Karcher, A., Shin, D., & Craig, L. (2000). Structural biology of Rad50 ATPase: ATP-driven conformational control in DNA double-strand break repair and the ABC-ATPase superfamily. *Cell*, *101*, 789–800. Retrieved from http://www.sciencedirect.com/science/article/pii/S0092867400808909

Hu, B., Itoh, T., Mishra, A., Katoh, Y., Chan, K.-L., Upcher, W., Godlee, C., et al. (2011). ATP hydrolysis is required for relocating cohesin from sites occupied by its Scc2/4 loading complex. *Current biology : CB*, *21*(1), 12–24. doi:10.1016/j.cub.2010.12.004

Ireton, K., Gunther, N. W., & Grossman, A. D. (1994). spoOJ Is Required for Normal Chromosome Segregation as well as the Initiation of Sporulation in Bacillus subtilis. *Journal of bacteriology*, *176*(17), 5320–5329.

Ishikawa, S., Ogura, Y., Yoshimura, M., Okumura, H., Cho, E., Kawai, Y., Kurokawa, K., et al. (2007). Distribution of stable DnaA-binding sites on the Bacillus subtilis genome detected using a modified ChIP-chip method. *DNA research*, *14*(4), 155–68. doi:10.1093/dnares/dsm017

Ivanov, D., & Nasmyth, K. (2005). A topological interaction between cohesin rings and a circular minichromosome. *Cell*, *122*(6), 849–60. doi:10.1016/j.cell.2005.07.018

Ivanov, D., & Nasmyth, K. (2007). A physical assay for sister chromatid cohesion in vitro. *Molecular cell*, *27*(2), 300–10. doi:10.1016/j.molcel.2007.07.002

Jensen, R., & Shapiro, L. (1999). The Caulobacter crescentus smc gene is required for cell cycle progression and chromosome segregation. *Proceedings of the National Academy of Sciences of the United States of America*, *96*(September), 10661–10666.

Jeppsson, K., Kanno, T., Shirahige, K., & Sjögren, C. (2014a). The maintenance of chromosome structure: positioning and functioning of SMC complexes. *Nature Reviews Molecular Cell Biology, 15*(9), 601–14. doi:10.1038/nrm3857

Jeppsson, K., Carlborg, K. K., Nakato, R., Berta, D. G., Lilienthal, I., Kanno, T., Lindqvist, A., Shirahige, K., & Sjögren, C. (2014b). The chromosomal association of the Smc5/6 complex depends on cohesion and predicts the level of sister chromatid entanglement. *PLoS genetics*, *10*(10), e1004680. doi:10.1371/journal.pgen.1004680

Jones, P., & George, A. (1999). Subunit interactions in ABC transporters: towards a functional architecture. *FEMS microbiology letters*, *179*(1999), 187–202. Retrieved from http://femsle.oxfordjournals.org/content/179/2/187.abstract

Kagey, M., Newman, J., & Bilodeau, S. (2010). Mediator and cohesin connect gene expression and chromatin architecture. *Nature*, *467*(7314), 430–5. doi:10.1038/nature09380

Kaimer, C., González-Pastor, J. E., & Graumann, P. L. (2009). SpoIIIE and a novel type of DNA translocase, SftA, couple chromosome segregation with cell division in Bacillus subtilis. *Molecular microbiology*, *74*(4), 810–25. doi:10.1111/j.1365-2958.2009.06894.x

Kaimer, C., Schenk, K., & Graumann, P. L. (2011). Two DNA translocases synergistically affect chromosome dimer resolution in Bacillus subtilis. *Journal of bacteriology*, *193*(6), 1334–40. doi:10.1128/JB.00918-10

Kamada, K., Miyata, M., & Hirano, T. (2013). Molecular basis of SMC ATPase activation: role of internal structural changes of the regulatory subcomplex ScpAB. *Structure*, *21*(4), 581–94. doi:10.1016/j.str.2013.02.016

Kegel, A, & Sjögren, C. (2011). The Smc5/6 complex: more than repair? *Cold Spring Harbor symposia on quantitative biology*, *LXXV*(75), 179–187. Retrieved from http://symposium.cshlp.org/content/early/2011/04/01/sqb.2010.75.047.short

Kegel, Andreas, Betts-Lindroos, H., & Kanno, T. (2011). Chromosome length influences replication-induced topological stress. *Nature*, *471*(7338), 392–6. doi:10.1038/nature09791

Kjos, M., & Veening, J.-W. (2014). Tracking of chromosome dynamics in live Streptococcus pneumoniae reveals that transcription promotes chromosome segregation. *Molecular microbiology*, *91*(6), 1088–105. doi:10.1111/mmi.12517

Kleine Borgmann, L. A. K., Hummel, H., Ulbrich, M. H., & Graumann, P. L. (2013a). SMC Condensation Centers in Bacillus subtilis Are Dynamic Structures. *Journal of bacteriology*, *195*(10), 2136–45. doi:10.1128/JB.02097-12

Kleine Borgmann, L. A. K., Ries, J., Ewers, H., Ulbrich, M. H., & Graumann, P. L. (2013b). The Bacterial SMC Complex Displays Two Distinct Modes of Interaction with the Chromosome. *Cell reports*, *3*, 1–10. doi:10.1016/j.celrep.2013.04.005

Kranz, A., Jiao, C., & Winterkorn, L. (2013). Genome-wide analysis of condensin binding in Caenorhabditis elegans. *Genome biology*, *14*(10), R112. doi:10.1186/gb-2013-14-10-r112

Kurzbauer, R., Teis, D., Araujo, M. E. G. De, Maurer-stroh, S., Eisenhaber, F., Bourenkov, G. P., Bartunik, H. D., et al. (2004). Crystal structure of the p14 ̄MP1 scaffolding complex : How a twin couple attaches mitogen- activated protein kinase signaling to late endosomes. *Proceedings of the National Academy of Sciences of the United States of America*, *101*(30), 10984–10989.

Laloraya, S., Guacci, V., & Koshland, D. (2000). Chromosomal addresses of the cohesin component Mcd1p. *The Journal of cell biology*, *151*(5), 1047–1056. Retrieved from http://jcb.rupress.org/content/151/5/1047.abstract

Lammens, A., Schele, A., & Hopfner, K. (2004). Structural Biochemistry of ATP-Driven Dimerization and DNA-Stimulated Activation of SMC ATPases. *Current Biology*, *14*, 1778–1782. doi:10.1016/j

Lammens, K., Bemeleit, D., & Möckel, C. (2011). The Mre11: Rad50 structure shows an ATP-dependent molecular clamp in DNA double-strand break repair. *Cell*, *145*(1), 54–66. doi:10.1016/j.cell.2011.02.038

Le, T. B. K., Imakaev, M. V, Mirny, L. & Laub, M. T. (2013). High-resolution mapping of the spatial organization of a bacterial chromosome. *Science*, *342*(6159), 731–4. doi:10.1126/science.1242059

Lee, P., Lin, D., Moriya, S., & Grossman, A. (2003). Effects of the chromosome partitioning protein Spo0J (ParB) on oriC positioning and replication initiation in Bacillus subtilis. *Journal of bacteriology*, *185*(4), 1326–1337. doi:10.1128/JB.185.4.1326

Lengronne, A., Katou, Y., & Mori, S. (2004). Cohesin relocation from sites of chromosomal loading to places of convergent transcription. *Nature*, *1040*(2002), 550–553. Retrieved from http://www.nature.com/nature/journal/v430/n6999/abs/nature02742.html

Li, G., Fullwood, M. J., Xu, H., Mulawadi, F. H., Velkov, S., Vega, V., Ariyaratne, P. N., et al. (2010). ChIA-PET tool for comprehensive chromatin interaction analysis with paired-end tag sequencing. *Genome biology*, *11*(2), R22. doi:10.1186/gb-2010-11-2-r22

Li, Y., Stewart, N., & Berger, A. (2010). Escherichia coli condensin MukB stimulates topoisomerase IV activity by a direct physical interaction. *Proceedings of the National Academy of Sciences of the United States of America*, *107*(44), 18832–18837. doi:10.1073/pnas.1008678107/-/DCSupplemental.www.pnas.org/cgi/doi/10.1073/pnas.1008678107

Lim, H. C., Surovtsev, I. V., Beltran, B. G., Huang, F., Bewersdorf, J., & Jacobs-Wagner, C. (2014). Evidence for a DNA-relay mechanism in ParABS-mediated chromosome segregation. *eLife*, *3*, e02758. doi:10.7554/eLife.02758

Lim, H., Kim, J., & Park, Y. (2011). Crystal structure of the Mre11–Rad50–ATPγS complex: understanding the interplay between Mre11 and Rad50. *Genes & Development*, *25*, 1091–1104. doi:10.1101/gad.2037811.

Lindow, J. C., Kuwano, M., Moriya, S., & Grossman, A. D. (2002a). Subcellular localization of the Bacillus subtilis structural maintenance of chromosomes (SMC) protein. *Molecular microbiology*, *46*(4), 997–1009. Retrieved from http://www.ncbi.nlm.nih.gov/pubmed/12421306

Lindow, J. C., Britton, R. A., & Grossman, A. D. (2002b). Structural Maintenance of Chromosomes Protein of Bacillus subtilis Affects Supercoiling In Vivo, *184*(19), 5317–5322. doi:10.1128/JB.184.19.5317

Lindroos, H., Ström, L., Itoh, T., & Katou, Y. (2006). Chromosomal association of the Smc5/6 complex reveals that it functions in differently regulated pathways. *Molecular cell*, *22*(6), 755–67. doi:10.1016/j.molcel.2006.05.014

Locher, K. P. (2009). Review. Structure and mechanism of ATP-binding cassette transporters. *Philosophical transactions of the Royal Society of London. Series B, Biological sciences*, *364*(1514), 239–45. doi:10.1098/rstb.2008.0125

Löwe, J., Cordell, S. C., & Van den Ent, F. (2001). Crystal structure of the SMC head domain: an ABC ATPase with 900 residues antiparallel coiled-coil inserted. *Journal of molecular biology*, *306*(1), 25–35. doi:10.1006/jmbi.2000.4379

Marko, J. (2009). Linking topology of tethered polymer rings with applications to chromosome segregation and estimation of the knotting length. *Physical Review E*, *79*(5), 051905. doi:10.1103/PhysRevE.79.051905

Marston, A. L. (2014). Chromosome segregation in budding yeast: sister chromatid cohesion and related mechanisms. *Genetics*, *196*(1), 31–63. doi:10.1534/genetics.112.145144

Mascarenhas, J., Soppa, J., Strunnikov, A. V, & Graumann, P. L. (2002). Cell cycle-dependent localization of two novel prokaryotic chromosome segregation and condensation proteins in Bacillus

subtilis that interact with SMC protein. *The EMBO journal*, *21*(12), 3108–18. doi:10.1093/emboj/cdf314

Mascarenhas, J., Volkov, A. V, Rinn, C., Schiener, J., Guckenberger, R., & Graumann, P. L. (2005). Dynamic assembly, localization and proteolysis of the Bacillus subtilis SMC complex. *BMC cell biology*, *6*, 28. doi:10.1186/1471-2121-6-28

McGlynn, P., Savery, N. J., & Dillingham, M. S. (2012). The conflict between DNA replication and transcription. *Molecular microbiology*, *85*(1), 12–20. doi:10.1111/j.1365-2958.2012.08102.x

Mehta, G., Kumar, R., Srivastava, S., & Ghosh, S. (2013). Cohesin: functions beyond sister chromatid cohesion. *FEBS letters*, *587*(15), 2299–312. doi:10.1016/j.febslet.2013.06.035

Minnen, A., Attaiech, L., Thon, M., Gruber, S., & Veening, J.-W. (2011). SMC is recruited to oriC by ParB and promotes chromosome segregation in Streptococcus pneumoniae. *Molecular microbiology*, *81*(3), 676–88. doi:10.1111/j.1365-2958.2011.07722.x

Mishra, A., Hu, B., Kurze, A., Beckouët, F., Farcas, A.-M., Dixon, S. E., Katou, Y., et al. (2010). Both interaction surfaces within cohesin's hinge domain are essential for its stable chromosomal association. *Current biology*, *20*(4), 279–89. doi:10.1016/j.cub.2009.12.059

Misulovin, Z., Schwartz, Y., Li, X., & Kahn, T. (2008). Association of cohesin and Nipped-B with transcriptionally active regions of the Drosophila melanogaster genome. *Chromosoma*, *117*(1), 89–102. doi:10.1007/s00412-007-0129-1

Mizuguchi, T., Fudenberg, G., Mehta, S., Belton, J.-M., Taneja, N., Folco, H. D., FitzGerald, P., et al. (2014). Cohesin-dependent globules and heterochromatin shape 3D genome architecture in S. pombe. *Nature*, *516*(7531), 432–435. doi:10.1038/nature13833

Möckel, C., & Lammens, K. (2012). ATP driven structural changes of the bacterial Mre11: Rad50 catalytic head complex. *Nucleic acids research*, *40*(2), 914–27. doi:10.1093/nar/gkr749

Moriya, S., Tsujikawa, E., Hassan, A. K. M., Asai, K., Kodama, T., & Ogasawara, N. (1998). A Bacillus subtilis gene-encoding protein homologous to eukaryotic SMC motor protein is necessary for chromosome partition. *Molecular Microbiology, 29*, 179–187. Retrieved from http://onlinelibrary.wiley.com/doi/10.1046/j.1365-2958.1998.00919.x/abstract

Murayama, Y., & Uhlmann, F. (2013). Biochemical reconstitution of topological DNA binding by the cohesin ring. *Nature*, *4*. doi:10.1038/nature12867

Murray, H., Ferreira, H., & Errington, J. (2006). The bacterial chromosome segregation protein Spo0J spreads along DNA from parS nucleation sites. *Molecular microbiology*, *61*(5), 1352–61. doi:10.1111/j.1365-2958.2006.05316.x

Nasmyth, K. (2011). Cohesin: a catenase with separate entry and exit gates? *Nature cell biology*, *13*(10), 1170–7. doi:10.1038/ncb2349

Nasmyth, K., & Haering, C. H. (2005). The structure and function of SMC and kleisin complexes. *Annual review of biochemistry*, *74*, 595–648. doi:10.1146/annurev.biochem.74.082803.133219

Nasmyth, K., & Haering, C. H. (2009). Cohesin: its roles and mechanisms. *Annual review of genetics*, *43*, 525–58. doi:10.1146/annurev-genet-102108-134233

Nicolas, P., Mäder, U., Dervyn, E., Rochat, T., Leduc, A., Pigeonneau, N., Bidnenko, E., et al. (2012). Condition-dependent transcriptome reveals high-level regulatory architecture in Bacillus subtilis. *Science*, *335*(6072), 1103–6. doi:10.1126/science.1206848

Nielsen, H. J., Youngren, B., Hansen, F. G., & Austin, S. (2007). Dynamics of Escherichia coli chromosome segregation during multifork replication. *Journal of bacteriology*, *189*(23), 8660–6. doi:10.1128/JB.01212-07

Niki, H., & Hiraga, S. (1998). Polar localization of the replication origin and terminus in Escherichia coli nucleoids during chromosome partitioning. *Genes & development*, 1036–1045. Retrieved from http://genesdev.cshlp.org/content/12/7/1036.short

Niki, H., Imamura, R., & Kitaoka, M. (1992). E. coli MukB protein involved in chromosome partition forms a homodimer with a rod-and-hinge structure having DNA binding and ATP/GTP binding activities. *The EMBO Journal*, *1*(1), 5101–5109. Retrieved from http://www.ncbi.nlm.nih.gov/pmc/articles/PMC556988/

Niki, H., Jaffe, A., Imamura, R., Ogura, T., & Hiraga, S. (1991). The new gene mukB codes for a 177 kd protein with coiled-coil domains involved in chromosome partitioning of E. coli. *The EMBO journal*, *1*(1), 183–193. Retrieved from http://www.ncbi.nlm.nih.gov/pmc/articles/PMC452628/

Nishiyama, T., Ladurner, R., & Schmitz, J. (2010). Sororin mediates sister chromatid cohesion by antagonizing Wapl. *Cell*, *143*(5), 737–49. doi:10.1016/j.cell.2010.10.031

Nolivos, S., & Sherratt, D. (2014). The bacterial chromosome: architecture and action of bacterial SMC and SMC-like complexes. *FEMS microbiology reviews*, *38*(3), 380–92. doi:10.1111/1574-6976.12045

Parelho, V., Hadjur, S., Spivakov, M., & Leleu, M. (2008). Cohesins functionally associate with CTCF on mammalian chromosome arms. *Cell*, *132*(3), 422–33. doi:10.1016/j.cell.2008.01.011

Pebernard, S., Schaffer, L., Campbell, D., Head, S. R., & N, B. M. (2008). Localization of Smc5/6 to centromeres and telomeres requires heterochromatin and SUMO, respectively. *The EMBO Journal*, *27*(22), 3011–23. doi:10.1038/emboj.2008.220

Pellegrino, S., Radzimanowski, J., & Sanctis, D. de. (2012). Structural and functional characterization of an SMC-like protein RecN: new insights into double-strand break repair. *Structure*, *20*(12), 2076–89. doi:10.1016/j.str.2012.09.010

Petrushenko, Z. M., Cui, Y., She, W., & Rybenkov, V. V. (2010). Mechanics of DNA bridging by bacterial condensin MukBEF in vitro and in singulo. *The EMBO journal*, *29*(6), 1126–35. doi:10.1038/emboj.2009.414

Petrushenko, Z., She, W., & Rybenkov, V. V. (2011). A new family of bacterial condensins. *Molecular microbiology*, *81*(July), 881–896. doi:10.1111/j.1365-2958.2011.07763.x

Phillips-Cremins, J. E., Sauria, M. E. G., Sanyal, A., Gerasimova, T. I., Lajoie, B. R., Bell, J. S. K., Ong, C.-T., et al. (2013). Architectural protein subclasses shape 3D organization of genomes during lineage commitment. *Cell*, *153*(6), 1281–95. doi:10.1016/j.cell.2013.04.053

Piccoli, G. De, Torres-Rosell, J., & Aragón, L. (2009). The unnamed complex: what do we know about Smc5-Smc6? *Chromosome research*, *17*(2), 251–63. doi:10.1007/s10577-008-9016-8

Poorey, K., Viswanathan, R., & Carver, M. (2013). Measuring chromatin interaction dynamics on the second time scale at single-copy genes. *Science*, *342*(23), 369–372. Retrieved from http://www.sciencemag.org/content/342/6156/369.short

Potts, P. R. (2009). The Yin and Yang of the MMS21-SMC5/6 SUMO ligase complex in homologous recombination. *DNA repair*, *8*(4), 499–506. doi:10.1016/j.dnarep.2009.01.009

Ptacin, J. L., Lee, S. F., Garner, E. C., Toro, E., Eckart, M., Comolli, L. R., Moerner, W. E., et al. (2010). A spindle-like apparatus guides bacterial chromosome segregation. *Nature cell biology*, *12*(8), 791–8. doi:10.1038/ncb2083

Rankin, S., Ayad, N. G., & Kirschner, M. W. (2005). Sororin, a substrate of the anaphase-promoting complex, is required for sister chromatid cohesion in vertebrates. *Molecular cell*, *18*(2), 185–200. doi:10.1016/j.molcel.2005.03.017

Rao, R., Pagan, J., & Senior, A. (1988). Directed mutagenesis of the strongly conserved lysine 175 in the proposed nucleotide-binding domain of alpha-subunit from Escherichia coli F1-ATPase. *Journal of Biological Chemistry*, (31), 15957–15963. Retrieved from http://www.jbc.org/content/263/31/15957.short

Rees, D. C., Johnson, E., & Lewinson, O. (2009). ABC transporters: the power to change. *Nature reviews. Molecular cell biology*, *10*(3), 218–27. doi:10.1038/nrm2646

Rimsky, S., & Travers, A. (2011). Pervasive regulation of nucleoid structure and function by nucleoid-associated proteins. *Current opinion in microbiology*, *14*(2), 136–41. doi:10.1016/j.mib.2011.01.003

Rowland, B. D., Roig, M. B., Nishino, T., Kurze, A., Uluocak, P., Mishra, A., Beckouët, F., et al. (2009). Building sister chromatid cohesion: smc3 acetylation counteracts an antiestablishment activity. *Molecular cell*, *33*(6), 763–74. doi:10.1016/j.molcel.2009.02.028

Rubio, E., & Reiss, D. (2008). CTCF physically links cohesin to chromatin. *Proceedings of the National Academy of Sciences of the United States of America*, *105*(24), 8309–8314. Retrieved from http://www.pnas.org/content/105/24/8309.short

Sawitzke, J., & Austin, S. (2000). Suppression of chromosome segregation defects of Escherichia coli muk mutants by mutations in topoisomerase I. *Proceedings of the National Academy of Sciences of the United States of America*, *97*(4), 1671–1676. Retrieved from http://www.pnas.org/content/97/4/1671.short

Schindelin, J., Arganda-Carreras, A., Frise, E., Kaynig, V., Longair, M., Pietzch, T., Preibisch, S., Rueden, C., et al. (2012) Fiji: an open-source platfrom for biological-image analysis. *Nature Methods,* 9(7), 676-682. doi: 10.1039/NMETH.2019

Schleiffer, A., Kaitna, S., Maurer-Stroh, S., Glotzner, M., Nasmyth, K., & Eisenhaber, F. (2003). Kleisins : A Superfamily of Bacterial and Eukaryotic. *Molecular cell*, *11*, 571–575.

Schmidt, C. K., Brookes, N., & Uhlmann, F. (2009). Conserved features of cohesin binding along fission yeast chromosomes. *Genome biology*, *10*(5), R52. doi:10.1186/gb-2009-10-5-r52

Schwartz, M. A., & Shapiro, L. (2011). An SMC ATPase mutant disrupts chromosome segregation in Caulobacter. *Molecular microbiology*, *82*(6), 1359–74. doi:10.1111/j.1365-2958.2011.07836.x

Seitan, V., Faure, A., & Zhan, Y. (2013). Cohesin-based chromatin interactions enable regulated gene expression within preexisting architectural compartments. *Genome research*, *23*, 2066–2077. doi:10.1101/gr.161620.113.

Sherratt, D. J., Søballe, B., Barre, F.-X., Filipe, S., Lau, I., Massey, T., & Yates, J. (2004). Recombination and chromosome segregation. *Philosophical transactions of the Royal Society of London. Series B, Biological sciences*, *359*(1441), 61–9. doi:10.1098/rstb.2003.1365

Shintomi, K., & Hirano, T. (2011). The relative ratio of condensin I to II determines chromosome shapes. *Genes & development*, *25*, 1464–1469. doi:10.1101/gad.2060311.1464

Sofueva, S., Yaffe, E., Chan, W.-C., Georgopoulou, D., Vietri Rudan, M., Mira-Bontenbal, H., Pollard, S. M., et al. (2013). Cohesin-mediated interactions organize chromosomal domain architecture. *The EMBO journal*, *32*(24), 3119–29. doi:10.1038/emboj.2013.237

Soh, Y.-M., Bürmann, F., Shin, H.-C., Oda, T., Jin, K. S., Toseland, C. P., Kim, C., et al. (2014). Molecular Basis for SMC Rod Formation and Its Dissolution upon DNA Binding. *Molecular Cell*, 290–303. doi:10.1016/j.molcel.2014.11.023

Song, J., Lafont, A., Chen, J., Wu, F. M., Shirahige, K., & Rankin, S. (2012). Cohesin acetylation promotes sister chromatid cohesion only in association with the replication machinery. *The Journal of biological chemistry*, *287*(41), 34325–36. doi:10.1074/jbc.M112.400192

Stephan, A. K., Kliszczak, M., Dodson, H., Cooley, C., & Morrison, C. G. (2011). Roles of vertebrate Smc5 in sister chromatid cohesion and homologous recombinational repair. *Molecular and cellular biology*, *31*(7), 1369–81. doi:10.1128/MCB.00786-10

Stouf, M., Meile, J.-C., & Cornet, F. (2013). FtsK actively segregates sister chromosomes in Escherichia coli. *Proceedings of the National Academy of Sciences of the United States of America*, *110*(27), 11157–62. doi:10.1073/pnas.1304080110

St-Pierre, J., Douziech, M., Bazile, F., Pascariu, M., Bonneil, E., Sauvé, V., Ratsima, H., et al. (2009). Polo kinase regulates mitotic chromosome condensation by hyperactivation of condensin DNA supercoiling activity. *Molecular cell*, *34*(4), 416–26. doi:10.1016/j.molcel.2009.04.013

Strick, T., Kawaguchi, T., & Hirano, T. (2004). Real-time detection of single-molecule DNA compaction by condensin I. *Current biology*, *14*, 874–880. doi:10.1016/j

Ström, L., Lindroos, H., Shirahige, K., & Sjögren, C. (2004). Postreplicative recruitment of cohesin to double-strand breaks is required for DNA repair. *Molecular cell*, *16*, 1003–1015. Retrieved from http://www.sciencedirect.com/science/article/pii/S1097276504007178

Sullivan, M., Higuchi, T., Katis, V. L., & Uhlmann, F. (2004). Cdc14 phosphatase induces rDNA condensation and resolves cohesin-independent cohesion during budding yeast anaphase. *Cell*, *117*(4), 471–82. Retrieved from http://www.ncbi.nlm.nih.gov/pubmed/15137940

Sullivan, N. L., Marquis, K. a, & Rudner, D. Z. (2009). Recruitment of SMC by ParB-parS organizes the origin region and promotes efficient chromosome segregation. *Cell*, *137*(4), 697–707. doi:10.1016/j.cell.2009.04.044

Sun, M., Nishino, T., & Marko, J. F. (2013). The SMC1-SMC3 cohesin heterodimer structures DNA through supercoiling-dependent loop formation. *Nucleic acids research*, (17), 1–12. doi:10.1093/nar/gkt303

Sutani, T., Kawaguchi, T., Kanno, R., Itoh, T., & Shirahige, K. (2009). Budding yeast Wpl1(Rad61)-Pds5 complex counteracts sister chromatid cohesion-establishing reaction. *Current biology*, *19*(6), 492–7. doi:10.1016/j.cub.2009.01.062

Tada, K., Susumu, H., Sakuno, T., & Watanabe, Y. (2011). Condensin association with histone H2A shapes mitotic chromosomes. *Nature*, *474*(7352), 477–83. doi:10.1038/nature10179

Tanaka, K., Hao, Z., Kai, M., & Okayama, H. (2001). Establishment and maintenance of sister chromatid cohesion in fission yeast by a unique mechanism. *The EMBO Journal*, *20*(20), 5779–5790. Retrieved from http://onlinelibrary.wiley.com/doi/10.1093/emboj/20.20.5779/full

Tanaka, T., Cosma, M., Wirth, K., & Nasmyth, K. (1999). Identification of cohesin association sites at centromeres and along chromosome arms. *Cell*, *98*, 847–858. Retrieved from http://www.sciencedirect.com/science/article/pii/S0092867400815184

Taylor, J. A., Pastrana, C. L., Butterer, A., Pernstich, C., Gwynn, E. J., Sobott, F., Moreno-Herrero, F., et al. (2015). Specific and non-specific interactions of ParB with DNA: implications for chromosome segregation. *Nucleic acids research*, *43*(2), 719–731. doi:10.1093/nar/gku1295

Teif, V. B., & Bohinc, K. (2011). Condensed DNA: condensing the concepts. *Progress in biophysics and molecular biology*, *105*(3), 208–22. doi:10.1016/j.pbiomolbio.2010.07.002

Ter Beek, J., Guskov, A., & Slotboom, D. J. (2014). Structural diversity of ABC transporters. *The Journal of general physiology*, *143*(4), 419–35. doi:10.1085/jgp.201411164

Teytelman, L., Thurtle, D., Rine, J., & Oudenaarden, A. van. (2013). Highly expressed loci are vulnerable to misleading ChIP localization of multiple unrelated proteins. *Proceedings of the National Academy of Sciences of the United States of America*, *110*(46), 18602–18607. doi:10.1073/pnas.1316064110/-/DCSupplemental.www.pnas.org/cgi/doi/10.1073/pnas.1316064110

Thanbichler, M. (2010). Synchronization of chromosome dynamics and cell division in bacteria. *Cold Spring Harbor perspectives in biology*, *2*(1), 1–15. doi:10.1101/cshperspect.a000331

Thanbichler, M., & Shapiro, L. (2006). Chromosome organization and segregation in bacteria. *Journal of structural biology*, *156*(2), 292–303. doi:10.1016/j.jsb.2006.05.007

Toro, E., & Hong, S. (2008). Caulobacter requires a dedicated mechanism to initiate chromosome segregation. *Proceedings of the National Academy of Sciences of the United States of America*, *105*(40), 15435–15440. Retrieved from http://www.pnas.org/content/105/40/15435.short

Toro, E., & Shapiro, L. (2010). Bacterial chromosome organization and segregation. *Cold Spring Harbor perspectives in biology*, *2*(2), 1–15. doi:10.1101/cshperspect.a000349

Torres-Rosell, J, Piccoli, G. De, Cordon-Preciado, V., Farmer, S., Jarmuz, A., Machin, F., Pasero, P., et al. (2007). Anaphase onset before complete DNA replication with intact checkpoint responses. *Science*, *315*, 1411–1416. Retrieved from http://sciencepubs.org/content/152/3729/1619.full.pdf

Torres-Rosell, Jordi, Machín, F., Farmer, S., Jarmuz, A., Eydmann, T., Dalgaard, J. Z., & Aragón, L. (2005). SMC5 and SMC6 genes are required for the segregation of repetitive chromosome regions. *Nature cell biology*, *7*(4), 412–9. doi:10.1038/ncb1239

Uhlmann, F., Lottspeich, F., & Nasmyth, K. (1999). Sister-chromatid separation at anaphase onset is promoted by cleavage of the cohesin subunit Scc1. *Nature*, 37–42. Retrieved from http://www.nature.com/articles/doi:10.1038%2F21831

Uhlmann, F., Wernic, D., & Poupart, M. (2000). Cleavage of cohesin by the CD clan protease separin triggers anaphase in yeast. *Cell, 103*, 375–386. Retrieved from http://www.sciencedirect.com/science/article/pii/S0092867400001306

Ünal, E., Arbel-Eden, A., Sattler, U., & Shroff, R. (2004). DNA damage response pathway uses histone modification to assemble a double-strand break-specific cohesin domain. *Molecular cell*, *16*, 991–1002. Retrieved from http://www.sciencedirect.com/science/article/pii/S1097276504007191

Upton, A. L., & Sherratt, D. J. (2013). Breaking symmetry in SMCs. *Nature structural & molecular biology*, *20*(3), 246–9. doi:10.1038/nsmb.2525

Van Bortle, K., Nichols, M. H., Li, L., Ong, C.-T., Takenaka, N., Qin, Z. S., & Corces, V. G. (2014). Insulator function and topological domain border strength scale with architectural protein occupancy. *Genome biology*, *15*(6), 1–18. doi:10.1186/gb-2014-15-5-r82

Viollier, P., Thanbichler, M., McGrath, P., West, L., Meewan, M., McAdams, H., & Shapiro, L. (2004). Rapid and sequential movement of individual chromosomal loci to specific subcellular locations during bacterial DNA replication. *Proceedings of the National Academy of Sciences of the United States of America*, *101*(25), 9257–9262. Retrieved from http://www.pnas.org/content/101/25/9257.short

Volkov, A. (2003). A prokaryotic condensin/cohesin-like complex can actively compact chromosomes from a single position on the nucleoid and binds to DNA as a ring-like structure. *Molecular and cellular biologyand cellular biology*, *23*(16), 5638–5650. doi:10.1128/MCB.23.16.5638

Waldman, V. M., Stanage, T. H., Mims, A., Norden, I. S., & Oakley, M. G. (2015). Structural mapping of the coiled-coil domain of a bacterial condensin and comparative analyses across all domains of life suggest conserved features of SMC proteins. *Proteins*. doi:10.1002/prot.24778

Waldminghaus, T., & Skarstad, K. (2010). ChIP on Chip: surprising results are often artifacts. *BMC genomics*, *11*, 414. doi:10.1186/1471-2164-11-414

Wang, W., Li, G.-W., Chen, C., Xie, X. S., & Zhuang, X. (2011). Chromosome organization by a nucleoid-associated protein in live bacteria. *Science (New York, N.Y.)*, *333*(6048), 1445–9. doi:10.1126/science.1204697

Wang, X., Montero Llopis, P., & Rudner, D. Z. (2013). Organization and segregation of bacterial chromosomes. *Nature reviews. Genetics, 14*(3), 191–203. doi:10.1038/nrg3375

Wang, X., & Sherratt, D. J. (2010). Independent segregation of the two arms of the Escherichia coli ori region requires neither RNA synthesis nor MreB dynamics. *Journal of bacteriology*, *192*(23), 6143–53. doi:10.1128/JB.00861-10

Wang, X., Tang, O. W., Riley, E. P., & Rudner, D. Z. (2014). The SMC condensin complex is required for origin segregation in Bacillus subtilis. *Current biology*, *24*(3), 287–92. doi:10.1016/j.cub.2013.11.050

Webb, C., Teleman, A., Gordon, S., & Straight, A. (1997). Bipolar localization of the replication origin regions of chromosomes in vegetative and sporulating cells of B. subtilis. *Cell*, *88*(1963), 667–674. Retrieved from http://www.sciencedirect.com/science/article/pii/S0092867400819091

Weitzel, C. S., Waldman, V. M., Graham, T. a, & Oakley, M. G. (2011). A repeated coiled-coil interruption in the Escherichia coli condensin MukB. *Journal of molecular biology*, *414*(4), 578–95. doi:10.1016/j.jmb.2011.10.028

Weitzer, S., Lehane, C., & Uhlmann, F. (2003). A Model for ATP Hydrolysis-Dependent Binding of Cohesin to DNA. *Current Biology*, *13*(22), 1930–1940. doi:10.1016/j.cub.2003.10.030

Wendt, K., Yoshida, K., Itoh, T., & Bando, M. (2008). Cohesin mediates transcriptional insulation by CCCTC-binding factor. *Nature*, *451*(7180), 796–801. doi:10.1038/nature06634

Wiggins, P. a, Cheveralls, K. C., Martin, J. S., Lintner, R., & Kondev, J. (2010). Strong intranucleoid interactions organize the Escherichia coli chromosome into a nucleoid filament. *Proceedings of the National Academy of Sciences of the United States of America*, *107*(11), 4991–5. doi:10.1073/pnas.0912062107

Wilhelm, L., Bürmann, F., Minnen, A., Shin, H.-C., Toseland, C.P., Oh, B.-H. & Gruber, S. SMC condensin entraps chromosomal DNA by an ATP hydrolysis dependent loading mechanism in *Bacillus subtilis.* Submitted to eLife.

Woldringh, C. (2002). The role of co-transcriptional translation and protein translocation (transertion) in bacterial chromosome segregation. *Molecular microbiology*, *45*, 17–29. Retrieved from http://onlinelibrary.wiley.com/doi/10.1046/j.1365-2958.2002.02993.x/full

Wolters, S., Ermolaeva, M. a, Bickel, J. S., Fingerhut, J. M., Khanikar, J., Chan, R. C., & Schumacher, B. (2014). Loss of Caenorhabditis elegans BRCA1 promotes genome stability during replication in smc-5 mutants. *Genetics*, *196*(4), 985–99. doi:10.1534/genetics.113.158295

Woo, J.-S., Lim, J.-H., Shin, H.-C., Suh, M.-K., Ku, B., Lee, K.-H., Joo, K., et al. (2009). Structural studies of a bacterial condensin complex reveal ATP-dependent disruption of intersubunit interactions. *Cell*, *136*(1), 85–96. doi:10.1016/j.cell.2008.10.050

Yan, J., Magnasco, M., & Marko, J. (1999). A kinetic proofreading mechanism for disentanglement of DNA by topoisomerases. *Nature*, *401*(October). Retrieved from http://www.nature.com/nature/journal/v401/n6756/abs/401932a0.html

Yanagida, M. (2005). Basic mechanism of eukaryotic chromosome segregation. *Philosophical transactions of the Royal Society of London. Series B, Biological sciences*, *360*(1455), 609–21. doi:10.1098/rstb.2004.1615

Zhao, S., & Fernald, R. (2005). Comprehensive algorithm for quantitative real-time polymerase chain reaction. *Journal of computational biology*, *12*(8), 1047–1064. Retrieved from http://online.liebertpub.com/doi/abs/10.1089/cmb.2005.12.1047

Zhao, X., & Blobel, G. (2005). A SUMO ligase is part of a nuclear multiprotein complex that affects DNA repair and chromosomal organization. *Proceedings of the National Academy of Sciences of the United States of America*, *102*(25). Retrieved from http://www.pnas.org/content/102/13/4777.short

Zuin, J., Dixon, J. R., Van der Reijden, M. I. J. a, Ye, Z., Kolovos, P., Brouwer, R. W. W., Van de Corput, M. P. C., et al. (2014). Cohesin and CTCF differentially affect chromatin architecture and gene expression in human cells. *Proceedings of the National Academy of Sciences of the United States of America*, *111*(3), 996–1001. doi:10.1073/pnas.1317788111

7. Appendix – Additional work performed

7.1 Additional work on Chapter 4.1.9 'Is hinge opening required for localization to *parS* sites?'

The question asked in this Chapter was whether a reduction in the efficiency of conformationally changing the hinge domain would lead to decreased chromosomal localization. This was addressed by placing another hinge dimerization domain 'above' the *B. subtilis* hinge in Smc, the reasoning being that dimerization of these two hinge domains would lead to a decrease in the efficiency of the conformational change in the hinge. The results obtained with Smc(double hinge) proteins suggested that these proteins had defects in protein folding. Both double hinge constructs do not form colonies on NA, indicating that these proteins do not support fast growth. This suggests that the double hinge is indeed not capable of forming the correct conformational change to be recruited to the chromosome. The Smc(double hinge) without E1118Q displays slightly larger colonies than a Δ*smc* strain on SMG implying that the double hinge Smc might still be partially functional (Fig. 40A). The smc(*double hinge, E1118Q)* strain shows colony sizes similar to an *smc(E1118Q)* strain (Fig. 40A). However, endeavors were made to understand what the defect of the Smc(double hinge) proteins was so that they could be modified. For example, a cause of the impaired folding may be the short four amino-acid linker that connects the *B. subtilis* hinge domain with the *P. furiosis* hinge domain which would not allow both hinges to dimerize simultaneously. To address this, constructs were made in which the linker length was increased to 8, 11 and 17 amino acids, respectively. These proteins were made in the absence and presence of E1118Q and displayed a similar effect on growth as the double hinge with the short linker (Table 5). Also the localization patterns of all these constructs were very similar to the constructs with the short linkers (Fig. 40B). Thus, the linker length does not have a major influence on the double hinge proteins.

Table 5. Overview of the colony formation phenotypes of the double hinge constructs.

Construct	Growth on NA	Colony formation phenotype
wild-type smc	Yes	*wild-type*
Δsmc	No	*Δsmc*
smc(E1118Q)	No	*smc(E1118Q)*
double hinge, 4 aa linker	No	*Δsmc*
double hinge, 8 aa linker	No	*Δsmc*
double hinge, 11 aa linker	No	*Δsmc*
double hinge, 17 aa linker	No	*Δsmc*
double hinge, 4 aa linker, E1118Q	No	*smc(E1118Q)*
double hinge, 8 aa linker, E1118Q	No	*smc(E1118Q)*
double hinge, 11 aa linker, E1118Q	No	*smc(E1118Q)*
double hinge, 17 aa linker, E1118Q	No	*smc(E1118Q)*
double hinge, 4 aa linker, P.f. m-hinge	No	*Δsmc*
double hinge, 8 aa linker, P.f. m-hinge	No	*Δsmc*
double hinge, 11 aa linker, P.f. m-hinge	No	*Δsmc*
double hinge, 17 aa linker, P.f. m-hinge	No	*Δsmc*

To understand why these proteins localize in a similar pattern as the monomeric hinge proteins it was then crucial to investigate what the cause of the defect of the Smc(double hinge) was. If the *B. subtilis* hinge in the double hinge proteins was capable of folding and dimerizing properly, then making the *P. furiosis* hinge monomeric should restore wild-type behavior of these double hinge proteins. The corresponding glycine residues that were mutated in the *B. subtilis* Smc to make the hinge monomeric were therefore mutated in the *P. furiosis* hinge. However, this resulted in cells that were still incapable of forming colonies on NA (Table 5) indicating that Smc remained non-functional. In addition, the expression levels were reduced compared to wild-type Smc (Fig. 21B). This indicated that protein folding is affected in all Smc(double hinge) proteins and that they thus do not fold as expected. Therefore, no further experiments were pursued in this direction and no conclusions can be drawn about the involvement hinge opening in chromosomal loading.
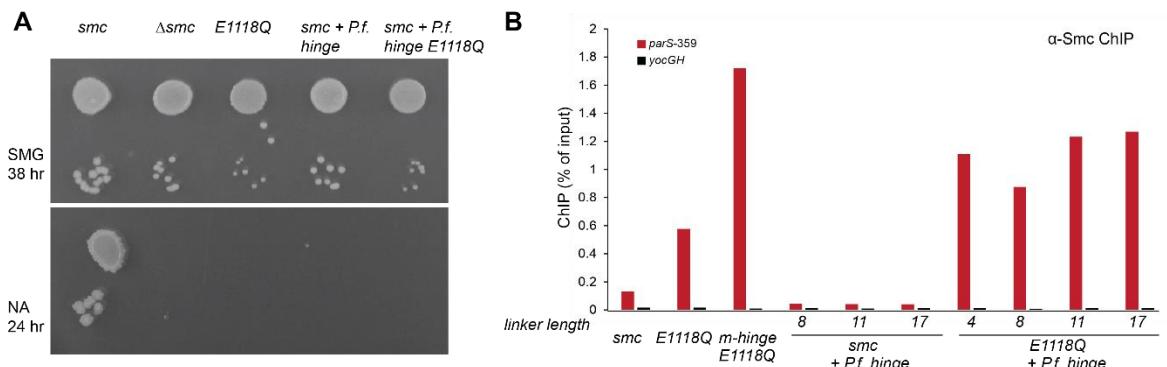
Figure 40. Smc with a double hinge and engaged heads localizes to the chromosome
A.   Colony formation assay using strains BSG 1002, 1007, 1008, 1888 and 1900.
B.   ChIP-qPCR using α-Smc antiserum on strains BSG 1002, 1008, 1547, 1982, 1984, 1986, 1981, 1983, 1985 and 1987.

7.2 Collaboration with Prof. Dr. Jan-Willem Veening, University of Groningen

One of the studied topics in the lab of Prof. Dr. Jan-Willem Veening at the University of Groningen, Netherlands is competence in *S. pneumoniae*. Members of his lab found that deleting or moving *parS* sites has an influence on competence in this organism. To confirm that this influence is a result of the changed localization of ParB and perhaps Smc I performed several ChIP-qPCR experiments on fixed *S. pneumoniae* cells that were sent from Groningen. Hereby it was confirmed that ParB localization has an influence on competence, presumably by spreading onto the competence genes, and a new *parS* site was identified.

7.3 Supervision of Master Thesis

I supervised a Master thesis entitled 'Detection of interaction partners of the β-sliding clamp DnaN from *B. subtilis* via label-free LC-MS'. In this Master thesis DnaN, Smc and ParB were His-tagged in *B. subtilis* and characterized for their growth. A label-free immunoprecipitation protocol for proteins from *B. subtilis* was established and optimized. Also, different steps before Liquid-Chromatography Mass Spectrometry (LC-MS), such as on beads proteolytic digests, protein denaturation steps and in gel digestion were tested.

After statistical analysis, amongst others, ScpA and ScpB were identified as interaction partners for Smc, also possible interaction partners were identified for DnaN. The master thesis was awarded with the grade 1.0 on a scale of 1.0 – 6.0 with 1.0 being the best grade.

7.4 Supervision of an eight week internship

In this eight week internship a master student tried to set up protein DNA crosslinking *in vivo* using a psoralen compound. Various methods were applied such as ChIP with formaldehyde crosslinking, ChIP with UV psoralen crosslinking and colony formation assays to test UV psoralen crosslinking.

7.5 Supervision of various bachelor and master students on projects related to my thesis work

Various bachelor and master students conducted research projects under my supervision varying from six weeks to three months. Their work involved cloning of plasmids, construction of *B. subtilis* strains, fluorescence microscopy and ChIP.

8. Acknowledgements

I cannot thank my mother enough for her unconditional love and support throughout all the stages in my life – including this PhD work.

My thanks also goes to all the friends, family and relatives all across the world.

And last, but certainly not least, I am grateful to my partner Wouter Koolhaas who stood by my side and gave me his unwavering support throughout the time of this PhD and beyond.

9. Curriculum Vitae

Personal details

Family name: Minnen   Place of birth: Amersfoort, the Netherlands
Given name: Anita   Nationality: Dutch
Date of birth: 15 March 1984   Gender: Female
                                                      Email: AnitaMinnen@gmail.com

Education

Dec.2011 – present   : **PhD candidate** at the Max Planck Institute for Biochemistry in Martinsried, Germany. Under supervision of Dr. S. Gruber.

Feb. 2010 – Dec. 2011 : **Master's degree** (Graduated with distinction/cum laude) in **Molecular Biology and Biotechnology** at University of Groningen, Groningen, The Netherlands

Sept. 2010   : Certificate 5B in **radiation protection**, permits working with radio isotopes in a laboratory, University of Groningen, Groningen, The Netherlands

Dec. 2009   : EDI level 4 certificate in **Teaching English as a Foreign Language** (TEFL) Eton institute of languages, Dubai, United Arab Emirates in cooperation with London Teacher Training College, London, United Kingdom

Sep. 2006 – Aug. 2009 : **Bachelor's degree** (graduated) in Life Science & Technology (LS&T), major in Molecular Life sciences, minor in Psychology, University of Groningen, Groningen, The Netherlands. Propaedeutic examination in August 2007.

Nov. 2007   : **VMT certificate** (Save Microbial Techniques), University of Groningen, Groningen, The Netherlands

Sept. 1996 - Jun. 2003 : **Graduation in Voorbereidend Wetenschappelijke Onderwijs** (pre-university education), 't Atrium, Amersfoort, The Netherlands

Research projects

Second **master's research project** of six and a half months in Evanston in the **United States**: The ER and stress in *Caenorhabditis elegans*. Supervised by Dr. J. Kirstein-Miles, Prof. Dr. R.I. Morimoto (Northwestern University) and Prof. Dr. I.J. van der Klei (University of Groningen).

First **master's research project** of six and a half months: Localisation and functional analysis of the SMC complex and ParBS system in *Streptococcus pneumoniae*. Supervised by Dr. J.W. Veening and Prof. Dr. O.P. Kuipers. Insight in the chromosome segregation machinery of *S. pneumoniae* was gained using DNA modifying techniques, ChIP, qPCR and fluorescence microscopy.

Bachelor's project of seven weeks; Screening the *Rhodococcus* sp. RHA1 genome for strong inducible promoters, supervised by Dr. E. Takano. An improved promoter-probe vector was constructed to obtain a genomic DNA expression library. The *Rhodococcus* sp. RHA1 genome was screened for inducible promoters by fluorescence assays and high throughput analysis.

Molecular cell biology research (seven weeks within Bachelor's degree), the role of peroxisome fission in viability in *Hansenula polymorpha* supervised by Prof. Dr. I.J. Van der Klei. Mutants differing in their peroxisomal and mitochondrial phenotype were studied on viability. Several techniques have been used in this research, fluorescence microscopy, cloning, vitality assays and ROS staining.

Microbiology and genetics research and **Biophysical chemistry and Biochemical research** were both research courses (Bachelor's degree) with four weeks of practical experience in which familiarising with the basics of the field were the main aim.

Bachelor's Essay (literature study) on combinatorial biosynthesis on polyketide synthase type I, supervised by Dr. E. Takano.

Master's Essay (literature study) on molecular understanding of temperature compensation in circadian clocks, supervised by Prof. Dr. M. Merrow.

Publications

Wilhelm, L., Bürmann, F., **Minnen, A.,** Shin, H.-C., Toseland, C.P., Oh, B.-H. & Gruber, S. SMC condensin entraps chromosomal DNA by an ATP hydrolysis dependent loading mechanism in *Bacillus subtilis.* Submitted to eLife.

Minnen, A.*, Attaiech, L.*, Thon, M., Gruber, S. and Veening, J.W. SMC is recruited to *oriC* by ParB and promotes chromosome segregation in *Streptococcus pneumoniae. Molecular Microbiology* 2011, **81**(3):676-688.

Awards and conferences

Gordon Research Conference on Chromosome Dynamics, May 2013, Lucca (Barga), Italy

Vereinigung für Allgemeine und Angewandte Mikrobiologie (VAAM) (Association for General and Applied Microbiology) **conference**, March 2012, Tübingen, Germany

Unilever Research prize, November 2011

Teaching experience

Supervision of practical course **Genetics for freshmen** at the University of Groningen, four weeks, October 2011

Supervision of several Master and Bachelor students during my PhD, 2011-2015

Work experience

2009   : Southwest technical Works L.L.C., Dubai, United Arab Emirates
                          Position: General Manager (part-time job)
                          Main tasks: Management, scheduling, logistics and marketing
2007 – 2009   : University of Groningen, Groningen, The Netherlands
                          Position: Coach (secondary job)
                          Main tasks: Coaching and supporting first year students in LS&T, inform on information
                          days about the degrees in Biology and LS&T
2006   : De Amersfoortse verzekeringen, Amersfoort, The Netherlands
                          Position: Administrative employee/call agent department of business connections,
                          employee department of claims.
                          Main tasks: administration of novel collectives for health insurances, inform brokers
                          about novel health insurances. Process health insurance claims.
2005   : Herritsch Bar und Restaurant, Velden, Austria
                          Position: managing ice cream shop, part of a cafe
                          Main tasks: Keeping stocks supplied, managing daily activities in the shop.
2004   : Bom Dia, Lagos, Portugal
                          Position: Assistant manager/Desk manager
                          Main tasks: Coordination of sales and bookings. Manage sellers, mediate complaints,
                          costumer care, key figure between all employees.
2003   :Teaching and Projects abroad, Brasov, Romania
                          Position: Volunteer
                          Main tasks: Helping in a historical museum and an orphanage, writing and taking
                          photographs for an English magazine in Brasov.

Sideline 2006-2011: member of the event committee and member of the lustre and yearbook committee (several positions within these committees) of the Groninger Studenten Duikclub Ad Fundum (Student scuba diving association in Groningen, The Netherlands).

Languages:

Dutch (native) and English fluent in speaking, reading and writing
German fluent in speaking and reading, good writing
Basic level of Portuguese, Spanish, French and Arabic